"Man's flight through life is sustained by the power of his knowledge."
Monument, US Air Force Academy

Part One: Introduction and Fundamentals

Anyone desiring to effectively *practice* catalysis, the science of catalytic reactions and catalysts, must have a firm grasp of the *fundamentals*. This is not accomplished on a whim; rather it requires significant expenditures of time and effort. Regardless of discipline, be it teaching, research, industrial practice, or management, intensive study, leading to understanding, is the key to success.

What are fundamentals? They include basic, underlying definitions, rules, principles, relationships, methods, models, and laws of science. They comprise the essence of the subject.

What are the fundamentals of catalysis for the practitioner? They include (1) definitions and models of catalysis, catalyst, and catalytic reaction; (2) the basic molecular processes in a catalytic reaction; (3) catalytic materials and properties; (4) methods of preparing and characterizing catalysts; (5) methods for measuring catalytic activity, selectivity, and longevity; and (6) design of reactors for studying and implementing catalytic reactions.

Of course, the above topics relating to fundamentals of catalysis might be ordered in many different ways. Based on our experience in teaching, we have chosen the following approach:

Chapter 1 provides important background and definitions of catalysis; it describes basic molecular processes in a catalytic reaction; quantitative definitions of rate and adsorption; and the roles of surface structure and support in catalysis.

Chapter 2 treats fundamentals of the structure and chemistry of catalytic materials; outlines important catalyst properties; and summarizes methods and principles involved in catalyst preparation.

Chapter 3 addresses methods and tools for determining catalyst properties with an emphasis on the study of catalytic surfaces.

Chapter 4 develops the basic equations for reactor design and illustrates their application; it addresses methods for collecting, analyzing, and reporting rate data for catalytic reactions.

Chapter 5 addresses the basic causes and mechanisms for catalyst decay as well as methods for avoiding deactivation; rate equations for different decay networks; collection of rate data; and design of reactors for a reaction involving a deactivating catalyst.

We think that your careful study of this material will prepare you well to fully appreciate and understand the information in the Practice section of this book and to more efficiently and successfully work in your own practice, whatever that may be.

Chapter 1

CATALYSIS: INTRODUCTION AND FUNDAMENTAL CATALYTIC PHENOMENA

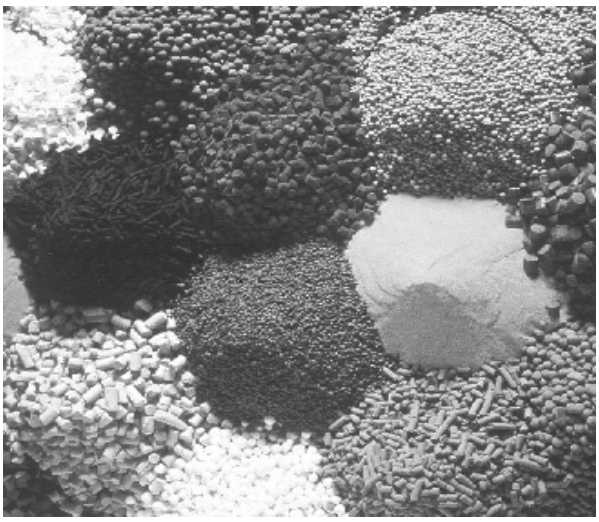

Commercial catalyst powders, pellets, and extrudates (courtesy of *Chem. & Eng. News*, Stinson, 1986).

"Chemistry without catalysis would be a sword without a handle, a light without brilliance, a bell without sound."

- A. Mittasch

1.1 Emergence of Catalyst Technology, A Brief History

1.1.1 Basic Variables for Control of Chemical Reactions

Since the beginning of time, man has been concerned about the control of chemical reactions. There are presently four basic variables available to us to control chemical reactions: (1) temperature, (2) pressure, (3) concentration, and (4) contact time.

In the 19th and early 20th centuries most industrial reactions were run at high temperatures and pressures in order to achieve reasonable rates of production. This is the *sledgehammer approach*. Unfortunately, these severe conditions are (1) energy intensive, (2) corrosive or otherwise damaging to equipment and materials, and (3) nonselective—that is, they result in undesirable side reactions and side products.

However, in the last 4–5 decades, two important technological developments have enabled us to run most chemical reactions under less severe conditions:

1. First, extensive use of catalysts, substances which speed up reaction rate, has enabled us to operate at lower pressures and temperatures. We call this the *feather approach*.
2. Second, improved methods of contacting, such as packed and fluidized catalyst beds, have enabled us to operate under continuous flow conditions at much higher efficiencies.

1.1.2 A Brief History of Catalyst Technology Development

Let's briefly trace the historical developments leading to the present extensive use of catalytic processes.[1] Catalyst technology was practiced on a small scale for centuries in inorganic form to make soap and in the form of enzymes to produce wines, cheeses, and other foods and beverages (Heinemann, 1981). The word 'catalysis' was coined by Berzelius in 1836; moreover, catalysts were identified and studied by Berzelius, Davy, Faraday, and other scientists in the early 1800s. However, industrial catalyst technology had its real beginning about 1875 with large-scale production of sulfuric acid on platinum catalysts, although sadly the inventor of this catalyst, Peregrin Philips (British Patent No. 6096, 1831), did not live to see the first contact sulfuric acid plant constructed (Burwell, 1983).

In the ensuing 100 years, catalyst technology expanded exponentially, although the timeline can be highlighted with several major breakthroughs (summarized in Table 1.1). The first of these was ammonia oxidation on Pt gauze developed by Ostwald and leading to the production of nitric acid in 1903. The discovery of promoted iron for ammonia synthesis by Mittasch, and the subsequent development of the ammonia synthesis process by Bosch and Haber occurred in the period of about 1908 to 1914; however, this important advance was no accident, since Mittasch, with typical German thoroughness, investigated over 2500 catalyst compositions in his search for the optimum. Ninety years later, it is still the most widely used catalyst for this reaction. Consider what impact this single discovery has had on agriculture and our ability to feed the masses of the world.

In the early 1900s (1920–1940), catalytic processes for hydrogenation of CO to methanol or liquid hydrocarbons paved the way for using synthesis gas from natural gas or coal to produce liquid fuels and chemicals.

---

[1] The history of catalytic technology has been reviewed by Heinemann (1981), while Davis and Hettinger (1983) have edited a volume that reviews selected histories of developments in heterogeneous catalysis with emphasis on those in the United States. Laidler's text on kinetics (1987) includes biographical sketches of important contributors to the fields of kinetics and catalysis research and technology.

Table 1.1 The Development of Important Industrial Catalytic Processes

Year of First Commercialization	Process/Reaction	Catalyst	Area of Industry
1875	Sulfuric acid mfg. $SO_2 + 1/2\ O_2 \rightarrow SO_3$	Pt, V_2O_5	Chemicals
1903	Nitric acid mfg. $2NH_3 + 5/2\ O_2 \rightarrow 2NO + 3H_2O$	Pt gauze	Chemicals
1913	Ammonia synthesis $N_2 + 3H_2 \rightarrow 2NH_3$	$Fe/Al_2O_3/K_2O$	Chemicals Fertilizers
1923	Methanol synthesis $CO + 2H_2 \rightarrow CH_3OH$	CuZnO	Chemicals
1930	Fischer-Tropsch synthesis $CO + 2H_2 \rightarrow C_1\text{-}C_{30}$ HCs	Fe/K/CuO, Co/Kieselguhr	Petroleum
1920–40	Hydrogenation reactions Hydrogenation of food oils	Ni/Kieselguhr, Raney	Petrochemicals Foods
1936–42	Catalytic Cracking $C_{20}\text{-}C_{30} \rightarrow C_8\text{-}C_{16}$ HCs	SiO_2 - Al_2O_3	Petroleum
1937	Ethylene oxidation $C_2H_4 + O_2 \rightarrow C_2H_4O$	Ag/Al_2O_3	Chemicals
1942	Paraffin alkylation $C_3H_6 + C_4H_{10} \rightarrow C_7H_{16}$	H_2SO_4, HF	Petroleum
1938–46	Oxo Process alkene + $CO/H_2 \rightarrow$ aldehydes	Co carbonyls (homogeneous)	Chemicals
1950	Catalytic Naphtha Reforming Dehydrogenation, isomerization	Pt/Al_2O_3	Petroleum
1955	Stereospecific Polymerization $n(C_2H_4) \rightarrow$ polyethylene	$TiCl_3/Al(R)_3$	Chemicals
1960	Wacker Process $C_2H_4 + H_2O \rightarrow CH_3CHO$	$PdCl_2$ (homogeneous)	Chemicals
1963	Ammoxidation $C_3H_6 + NH_3 + 3/2\ O_2 \rightarrow CH_2{=}CHCN + 3H_2O$	Bismuth Phosphomolybdate Sb/U oxide	Chemicals
1964–69	Oxychlorination $C_2H_2 + HCl \rightarrow C_2H_3Cl$	$CuCl_2$ (homogeneous)	Petrochemicals
1964–8	Zeolitic catalytic cracking Hydrocracking	Exchanged X, Y zeolites	Petroleum
1967	Multimetallic reforming	Pt-Re, Pt-Ir-Cu	Petroleum
1960s	Hydrodesulphurization $R\text{-}S + 2H_2 \rightarrow H_2S + RH_2$	$CoMo/Al_2O_3$	Petroleum
1976, 1981	Auto Emissions Control CO and HC oxidations NO reduction	Pt, Pd/Al_2O_3, Rh/Al_2O_3	Automotive Environmental Control
1980–95	Selective catalytic reduction of NO $4NH_3 + 4NO + O_2 \rightarrow 4N_2 + 6H_2O$	VO_xTiO_2, zeolites	Environmental Control
1980–95	Shape selective reactions e.g. mfg. of ethylbenzene	New zeolites, e.g. ZSM-5	Petrochemicals

Germany used this technology during World War II to provide synthetic fuels for operating their war machinery when petroleum supplies had been cut off. The development of efficient Ni catalysts for hydrogenation of organic compounds provided new synthesis routes to chemicals and foodstuffs, including low cholesterol vegetable oils. Catalytic cracking, which began between 1935 and 1940, was the first

significant use of solid catalysts in the petroleum industry—a very important development, which allowed refiners to increase gasoline yield and thereby use petroleum crude feedstock more efficiently. This was followed in 1950 by the development of catalytic naphtha reforming involving dehydrogenation of cyclohexane to benzene and isomerization of straight chain alkanes to increase gasoline octane rating. Around 1960 marked the beginning of hydrotreating catalyst technology at refineries to remove sulfur, nitrogen, and metals from petroleum feedstocks, a technology, which has continued to expand as petroleum feedstocks have become increasingly 'sour' with organic sulfur and nitrogen compounds.

Around 1955, Ziegler-Natta discovered that $AlCl_3$ catalysts could be used for production of polypropylene at low pressures. This and later discoveries of catalysts for making important monomer building blocks such as acrylonitrile and acrolein (beginning around 1963) revolutionized the chemical and polymer industries.

One of the first large-scale industrial processes to utilize a homogeneous catalyst was the Wacker Process for making acetaldehyde from ethylene. The use of this 'feather approach' (around 1960) enabled reduction of the temperature and pressure from 375–500°C and ten's of atmospheres to 100°C and 7 atm. Since then more than a dozen large-scale commercial processes (exceeding 100,000 metric tons per year) have been developed based on homogeneous catalysis, including olefin hydrogenation and disproportionation, carbonylation, oxidation, and polymerization (Heinemann, 1981).

Several decades ago, Weisz and Frilette (1960) coined the word 'shape-selective catalysis' to describe the unique selectivity properties of crystalline molecular sieves or zeolites in cracking *n*-alkanes to exclusively straight chain products. The 'shape-selectivity' of zeolites is based on their unique ability to selectively admit or reject molecules of a characteristic size and/or shape at the entrance to molecular-size pores containing active sites. Aluminosilicate zeolites are further characterized by a high density of strong acid sites. Because of their high activities and selectivities for acid-catalyzed reactions, zeolites quickly (1964–8) found application to catalytic cracking and hydrocracking of petroleum feedstocks. In the subsequent three decades, zeolites have found numerous applications to shape-selective petroleum processing and production of chemicals and fuels (Chen *et al*., 1989; Bhatia, 1990; Chon *et al*., 1996; Guisnet and Gilson, 2002; Auerbach *et al*., 2003), e.g. catalytic reforming to produce octane boosters, dewaxing of distillate fuels and lubebase feedstocks, oligomerization of light olefins to distillates, xylene synthesis and isomerization, ethylbenzene and paraethyltoluene synthesis, and gasoline or light olefin production from methanol.

During the late 1970s and early 1980s, noble metal catalysts were developed for control of CO, hydrocarbon and NO emissions from automobiles. Increased emphasis on environmental control in the United States and Europe during the 1980s and 1990s led to the development of vanadium titania and zeolite catalysts for selective reduction of nitrogen oxides with ammonia. Catalysts for removal of volatile organic hydrocarbons (VOCs) and hazardous organics such as chlorohydrocarbons were also developed during this period. Developments since 1990 will be addressed later in the chapter.

1.2 Importance of Catalysis and Catalyst Technology

1.2.1 Impact on Society and Life Forms

How important is catalysis? Without it our modern technological society would not have happened! Our worldwide economy is based on catalytic production of chemicals and fuels. Much of the food you eat is preprocessed catalytically and the clothes you wear are made of fabrics produced in catalytic processes (see Figure 1.1). The fuels that powered the vehicles that brought you to school or work today were produced in catalytic processes. Four of the largest sectors of our world economy, i.e. the petroleum, power, chemicals, and food industries, which account for more than 10 trillion dollars of gross world product, are largely dependent on catalytic processes.

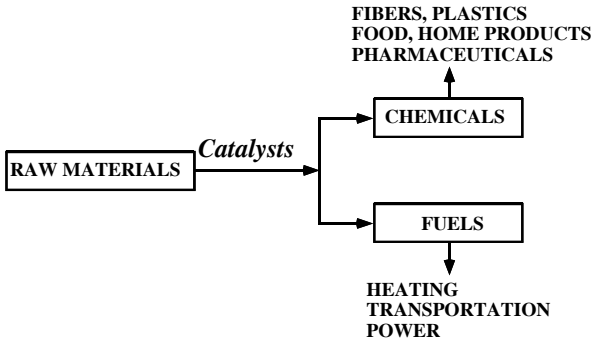

Figure 1.1 Our world economy is based on catalytic production of chemicals and fuels.

Catalysis is fundamental to life! In fact, without catalysis no form of life could exist! The life supporting reactions in our body are catalyzed by enzymes, nature's catalysts. They enable life processes such as respiration to occur rapidly at ambient temperatures and pressures, conditions under which the materials in our body can survive. Most life-related reactions in nature are enzymatic. Enzymes are marvelously efficient, complex catalysts that can manufacture on the order of 10^2 to 10^3 new molecules per second. Each enzyme contains an active site or pocket having its own peculiar geometry for binding to one specific kind of molecule. For example, the hexokinase enzyme has an active site ideal for binding and metabolizing only one molecule, glucose, and thereby catalyzes the metabolism of this simple sugar.

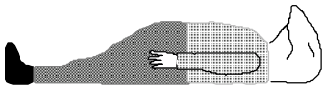

Without catalysis no form of life could exist!

Enzymes, the catalysts of life, play an important role in growth and maturation processes; however, they apparently also play a role in the growth of cancers and the AIDS virus. For example, the aspartic HIV-1 proteinase enzyme, shown schematically in Figure 1.2, has been found to play an active role in the process of HIV-1 viral replication (Keech and Lazou, 1990); it is, in fact, responsible for the cleavage of its own precursor, a gag-pol fusion polyprotein. Because the HIV-1 retrovirus has been implicated as a causal agent of AIDS, recent research has focused on developing inhibitors that would block the active site of proteinase, thereby interrupting the sequence of AIDS virus maturation.

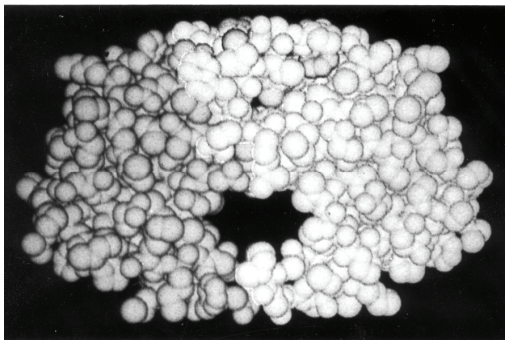

Figure 1.2 Supercomputer model of aspartic proteinase, a dimeric enzyme active in the cleavage of its own precursor, a gag-pol fusion polyprotein; this reaction is one of several steps in replication of the HIV-1 retrovirus, a possible causal agent of AIDS (Cray Channels, 1990).

1.2.2 Economic Importance of Catalyst Technology

Catalyst technology has played an increasingly key role in the economic development and the national interest of countries of the world during the 20th Century. It was Fischer-Tropsch catalyst technology that enabled the Germans to sustain their World War II effort by synthesizing gasoline fuels for their war machinery from German coals at a time when petroleum feedstocks had been cut off. On the other hand, it was superior catalyst technology that led to the crucial 1940 victory of the British Air Force over the German Luftwaffe in the Battle of Great Britain (NRC Report, 1992). While the Germans lost 1733 planes, the British lost only 915 planes because of their greater maneuverability with 50% faster bursts of acceleration from their superior 100-octane fuel compared to the Germans' 88 octane gasoline; the new high octane fuel was produced by catalytic cracking, a process developed at Universal Oil Products in 1938.

Catalytic cracking has also had a major favorable impact on the United States balance of payments by enabling more efficient use of petroleum feedstocks whose cost has increased greatly in the past two decades. In particular, the use of more efficient zeolite catalysts has benefited the United States balance of payments about $8 billion per year (400 million barrels of oil/year at about $20/barrel) since about 1972 (NRC Report, 1992).

Catalyst technology is the backbone of the chemical and petroleum industries, two of the largest global industries with worldwide sales of 1.5 and 2 trillion U.S. dollars per year, respectively. In the United States alone these two industries employ more than 1.5 million workers. In fact, of 63 major new products and 34 process innovations in the chemical industry from 1930 to 1980, 60% of these products and 90% of these processes were based on catalyst technology. Catalysis is likewise critical to the petroleum refining industry; indeed, except for distillation, more than 90% of refining processes are catalytic.

Catalyst technology can be leveraged to great advantage, because (1) catalyst cost is only 0.1% of the product value of petroleum refining and 0.22% of that from petrochemical processes and (2) commercial catalysts typically have been designed with remarkable longevity, i.e. they typically turnover (convert one molecule per site) $20–100 \times 10^6$ times before requiring regeneration or disposal. From a global economic perspective, $10 billion invested worldwide in catalyst technology leads to about $10 trillion of gross world product.

1.2.3 Catalyst Technology of the Present

Present-day catalyst technologies can be classified into three areas of important activity in the world economy, namely, petroleum refining, chemicals manufacturing, and environmental clean-up. Environmental catalysts can be further divided into technologies for control of emissions from mobile and stationary sources. Chemicals manufacture can be broadly classified according to reaction type, i.e. hydrogenations, oxidations, synthesis, polymerizations, and enzyme reactions. Detailed descriptions of these technologies are provided in Chapters 6–12, the practice section, of this book.

Most process catalysts are supplied in a highly competitive world market by several hundred firms, some of the largest of which are listed in Table 1.2. In the past decade this market has experienced a healthy growth rate of about 5% (see Table 1.3). Estimates of world catalyst sales vary over a significant range. For example, estimated sales for the year 2000 range from about $10 billion (Catalysis Letters, 2000) to $17 billion (Bartholomew, 2004), although the higher figure includes about $4 billion in noble metals (see Table 1.3), while the lower figure may not. Estimated worldwide and United States catalyst sales for 1993 to 2005 summarized in Table 1.3 (Bartholomew, 2004) are based on a careful study of pertinent literature, a comprehensive marketing study of the auto catalyst market, and calculations from actual or projected world markets. A continued overall growth rate of about 5% is predicted for the catalyst industry, although growth is likely to be lower for catalysts used in the synthesis of bulk and fine chemicals and for petroleum refining catalysts but higher for biocatalysts and environmental catalysts (not counting the auto catalyst market).

Table 1.2 Major Catalyst Producers and Their Products

	Chemical Production			Petroleum Refining					Envir.	H_2, Syngas
Company	NH_3 / methanol	Hydrog-enation	Oxida-tion	Polymer-ization	Cat cracking	Cat re-forming	Hydro-cracking	Hydro-treating	Environ-mental	Production /Conversion
Advanced Catalyst Systems										
Advanced Refining Technologies LLC										
Akzo Nobel Inc.										
Axens Procatalyse										
BASF										
Catalysts & Chemicals										
Catalyst Plant of Fushun Petrochemical										
Chevron Lummus Global LLC										
Criterion Catalyst										
Davison Catalysts, W.R. Grace & Co.										
Degussa AG										
Engelhard Corporation										
Exxon Research & Engineering Co.										
Haldor Topsøe										
Heraeus, W.C. GmbH										
Instituto Mexicano del Petroleo										
Johnson Matthey										
Kataleuna GMBH Catalysts										
Leuna-Werke AG										
Nanking Chemical										
Nikki Chemical										
Nippon Shokubai Co.										
Nissan Girdler Catalyst										
OMG										
Otsuka Chemical Co.										
Parekh Plantinum										
Shell Chemical Co.										
Süd-Chemie										
UOP										
W.R. Grace-Davison										
Zeochem										
Zeolyst International										

Table 1.3 Catalyst Sales (billions of U.S. dollars) [a] (Bartholomew, 2004)

Category	1993	1997	2000	2001	2005	Annual growth rate, %	References
Worldwide							
Auto catalysts[b]	2.18	2.65	6.75	7.09	8.61	5.0	Bartholomew, 2002
Chemicals							www.nacatsoc.org, 2002; Morbidelli *et al*., 2001
Biocatalysts (enzymes)	1.79	2.26	2.69	2.83	3.44	6.0	www.nacatsoc.org, 2002; C&EN, 1999
Bulk	1.75	1.80	1.97	2.07	2.51	3.0	Chemweek, 1999
Fine (non bio) [c]	0.41	0.45	0.49	0.52	0.63	3.0	C&EN, 2001
Polymers	0.94	1.70	2.02	2.12	2.58	5.0	Chemweek, 1999
Environmental (minus auto) [d]	0.62	0.67	0.73	1.01	1.23	10.0	www.nacatsoc.org, 2002; Chemweek, 1999; C&EN, 1999
Petroleum refining	1.80	2.10	2.00	2.32	2.82	4.0	www.nacatsoc.org, 2002; O&G, 2002; Chemweek, 1999; C&EN, 2001
Recovery of spent catalysts	0.62	0.65	0.75	0.79	0.96	5.0	Chemweek, 1993 [e]
Total	*10.1*	*12.3*	*17.4*	*18.7*	*22.8*	*5.0*	
U.S./North America							
Auto catalysts[b]	0.83	1.41	3.38	3.55	4.11	5.0	Bartholomew, 2002
Biocatalysts	0.48	0.51	0.64	0.67	0.78	6.0	Chemweek, 1993; Chemweek, 1999
Chemicals	1.20	1.26	1.42	1.49	1.72	3.0	Chemweek, 1993; Chemweek, 1999
Environmental (minus auto) [d]	0.06	0.09	0.13	0.39	0.46	10.0	Chemweek, 1993; Chemweek, 1999
Petroleum refining	0.52	0.75	0.88	0.92	1.07	4.0	Chemweek, 1993; Chemweek, 1999
Recovery of spent catalysts	0.31	0.33	0.40	0.42	0.48	5.0	Chemweek, 1993
Total	*3.4*	*4.3*	*6.8*	*7.4*	*8.6*	*4.7*	

[a] Does not include about $1.2 billion per year of catalysts produced and consumed internally by chemical and petroleum companies, nor $4.3 billion per year in process/catalyst licenses and other royalties (2001 figures).

[b] Starting in 2000, precious metals are included with automotive catalysts. If noble metal catalysts are excluded from auto catalysts, the 2001 worldwide and US totals are reduced $3.45 and 1.73 billion, respectively, to $15.2 and 6.9 billion, respectively. However, the arguments for excluding the noble metals are weak.

[c] Fine chemicals include about 75–80% pharmaceuticals and 20–25% agricultural chemicals, dyes, food and feed additives. It is assumed that biocatalysts account for 80% of fine chemicals, non-biocatalysts for 20%.

[d] Initial estimate for industrial emissions control (other than auto) is based on 1989 figures from Greek (1989). Growth rate of industrial emissions is estimated at 10% per year worldwide. An extra spurt of growth is anticipated in 2001–5 due to installation in the U.S. of SCR units on coal-fired power plants (about 0.25 billion/year). SCR catalyst replacement cost for Europe and Japan is potentially $1 billion/year; assume $0.5 billion/year because of regeneration.

[e] Assumes 50% U.S./50% Europe & Japan

1.2.4 Catalysis in Your Future

What kinds of catalyst technology will we be seeing in the next several decades and how will this impact your future? There are a number of important trends emphasizing the feather approach, with development of new materials and innovations in reactor design. These include:

- ***Milder reaction conditions*—**lower temperatures and pressures (the feather), i.e. greater application of homogeneous and enzyme catalysts.

- ***Improved selectivity for desired products***—More active, selective catalysts, lower temperatures, and fewer undesirable side reactions.
- ***New catalysts***—enantiomer-selective catalysts, multifunctional bimetallic catalysts, chemzymes, zeozymes and enzymes.
- ***The emergence of new materials***—e.g. new zeolites, new tailored supports, and catalysts designed at the nanoscale and even at the molecular level (see Chapter 2).
- ***Greater use of sophisticated tools to study and characterize catalytic materials*** (see Chapter 3).
- ***Innovations in contacting and reactor design***—e.g. microchannel and membrane reactors and more sophisticated modeling methods.

During the next 15–20 years, three important areas of emerging catalyst technology will greatly change the way in which energy, fuels, chemicals, foods, and drugs are produced and refined.

The *first* is increased production of *energy, fuels and chemicals from natural gas, coal and biomass*—As natural gas and coal gradually replace petroleum as the major sources of energy and chemicals, scientists and engineers will be involved in the design, construction, and operation of natural gas/petroleum refining complexes and biomass/coal-conversion complexes. For example, Fischer-Tropsch wax/crack technology, such as that recently developed by Shell, Exxon-Mobil, and Sasol to convert natural gas to gasoline and chemicals (see Chapter 6), will involve many new catalytic and chemical operations and will revolutionize petroleum refineries. Due to increasing emphasis on renewable energies, new catalytic processes will be developed for economically converting biomass to fuels and chemicals.

In the power sector, there will be dramatic and important developments, including catalytic combustion of fuels, fuel cells that use catalyst electrodes to convert fuels to electricity at high efficiencies, and solar-powered electrochemical cells. A shift to more distributed power production appears inevitable.

The *second* major area involving catalysis is that of *environmental engineering*—There is a growing and genuine concern about man's destruction of Earth's natural environment. Pressures are mounting on every front to minimize air, water, and solids pollution. These issues are bringing catalysis to the spotlight once again.

Some developing and promising new catalytic applications on the environmental front include advanced catalyst technologies for ultra low level auto emissions control, particulate reduction from diesel engines, selective catalytic reduction (SCR) of NO_x to elemental N_2 in effluents from power plants and turbines, and catalytic destruction of hazardous wastes such as polynuclear aromatic hydrocarbons and chlorinated biphenyls that are potent carcinogens. Some anticipated developments in auto/truck emissions control for the coming decade include rapid warm-up converters, which minimize startup emissions, NO_x reduction traps for lean-burn/diesel engines, and SCR converters for reducing NO_x in diesel truck engines. In the not-so-distant future, we can expect catalytic control of emissions in small businesses and households, e.g. catalytic control of carbon monoxide and hydrocarbon emissions from dry cleaners, paint shops, restaurants, and small engines, including lawnmowers, boats, snow blowers, and motorbikes. In the long term, there will be CO_2- and H_2-based catalytic chemistries to convert CO_2 emissions to useful fuels and chemicals and new catalytic processes to minimize hydrocarbons and CO_2 emissions.

The *third* major area involving catalysis is that of *enzymatic and homogeneous catalysis*—The rapidly growing biotech industry already involves biologists, chemists, and chemical engineers in the design and manipulation of enzymes and organometallic enzyme-mimics. It has revolutionized and will continue to revolutionize the way we produce chemicals, drugs, and food products.

Let's mention some examples. Enzymes supported on glass and ceramics are already used in the food industry to convert cellulose waste to glucose and glucose to fructose; the application of biocatalysts in production of pharmaceutical products is expanding at a brisk pace. New processes are being developed for using bacteria or cells to convert waste to useful or harmless materials.

What was just a few years ago wild speculation is now probably an inevitable development in our future, namely, *biocatalytic computers*. The nerve cell, a component of the human mind, is presently the most compact computer known to man. How does it work? What little we know indicates that it involves very complex chemical and enzymatic reactions. As computers continue to get smaller, what is the ultimate in miniaturization? Perhaps it is the coupling of DNA with enzymes at the molecular level.

1.3 Fundamental Catalytic Phenomena and Principles

1.3.1 Definitions

Having established the importance of catalysis in enabling life processes and of catalytic technology to the functioning of society, we have set the stage for discussion of the fundamentals of catalytic chemistry and physics.

Catalysts and catalysis. A *catalyst*, in simplest terms, is a material that enhances the rate and selectivity of a chemical reaction and in the process is cyclically regenerated. *Heterogeneous catalysis* is the process whereby reactants adsorb onto the surface of a solid catalyst, are activated by chemical interaction with the catalyst surface, and are rapidly and selectively transformed to adsorbed products, which desorb from the catalyst surface. Once the product is desorbed from its surface the catalyst momentarily returns to its original state until additional reactants adsorb, repeating the catalytic cycle. These interactions provide a chemical shortcut in which reactants are converted to products more rapidly and at much milder conditions than if no surface interactions occurred. A catalyst has been likened (Mills, 1994) to a mountain guide, who directs a group of people (molecules) over a highly favorable mountain pass (low activation energy path) to a selected valley (of products) and returns unchanged to guide additional groups.

The second aspect of our definition indicates that reactants can be directed down a certain chemical transformation path to generate a specific product. In this respect, the catalyst provides selectivity or specificity. It is these two important functions, enhancing rate and directing reactants to specific products, which explain catalysts' major role in the environmental, petroleum, chemical, and energy industries.

Examples of catalysis. Automobile emissions control provides an interesting example of how rate enhancement by a catalyst is put to useful practice. The internal combustion engine in automobiles combusts a gasoline/air mixture to generate heat that is converted to mechanical work in the engine. The combustion process, however, is stoichiometrically less than 100% efficient; that is, undesirable by-products such as carbon monoxide (CO) and unburned hydrocarbons (HC) are produced in addition to CO_2 and H_2O.

$$\text{Hydrocarbons} + O_2 \rightarrow CO_2 + H_2O + CO + HC + \text{Heat} \tag{1.1}$$

At the moderately high temperatures and high flow rates typical of auto exhausts there is insufficient time for CO and HC to react further in the gas phase with available O_2 to CO_2 and H_2O before they exit the tailpipe. However, placing a suitable catalyst in the exhaust manifold allows these reactions to occur within the limited residence time and at the moderate reaction conditions of the catalytic converter. Thus the catalyst provides a more rapid alternative chemical path leading to the destruction of would-be pollutants.

Another consequence of combustion processes is the generation of nitrogen oxides or NO_x (NO, NO_2 and N_2O) from either the oxidation of nitrogen compounds in the fuel or the oxidation of nitrogen in air at temperatures in excess of about 1400°C. These undesirable pollutants can be converted catalytically to N_2 in a reducing environment (e.g. automotive exhausts) by reduction with either CO or hydrocarbons or in an oxidizing environment (e.g. the flue gas of a power plant) by selective catalytic reduction with NH_3. Either process demonstrates the selectivity of the catalyst in directing the CO or HC to CO_2, and NO or NO_2 to N_2 at appreciable reaction rates under relatively mild reaction conditions.

The reactions cited above illustrate applications of catalysts in enhancing conversion of undesirable pollutants to desired products. These catalytic processes are already practiced widely on a commercial scale,

for example, in the form of automotive catalytic converters now used on most automobiles and in large emission control devices at power plants throughout the world. This topic of catalytic emissions control will be more completely developed in subsequent chapters (Chapters 10 and 11).

Effects of catalysis on activation energy and reaction rate. The concept of catalysis can be developed further by describing its effects on a simple redox reaction, the oxidation of ferrous ion with ceric ion, which occurs in the absence of a catalyst at a very slow rate.

$$Fe^{2+} + Ce^{4+} - (\text{slow}) \rightarrow Fe^{3+} + Ce^{3+} \tag{1.2}$$

When this reaction is carried out in aqueous solution, waters of coordination are attached to each ion. For reaction to occur, the Fe^{2+} must interact with the Ce^{4+} through the coordinated water molecules and transfer an electron. For simplicity, we will ignore the coordinated H_2O. During this transfer reaction, an activated state composed of a Fe^{3+} and Ce^{3+} complex exists. The dissociation of this complex leads to the final product.

It has been observed that this reaction can occur appreciably faster by adding a small amount of Mn^{4+} from a suitable water-soluble salt. The Mn^{4+} acts as a homogeneous catalyst in that it exists in the same phase as the reactants and provides a chemical shortcut for electron exchange. Instead of Fe^{2+} forming a complex intermediate with Ce^{4+} and transferring an electron, two Fe^{2+} ions transfer an electron each to the Mn^{4+} producing two Fe^{3+} and one Mn^{2+}. Subsequently, the Mn^{2+} interacts with two Ce^{4+} and donates an electron to each two Ce^{4+} producing Mn^{4+} and $2Ce^{3+}$. The net reaction can be written:

$$2\,Fe^{2+} + Mn^{4+} - (\text{fast}) \rightarrow 2\,Fe^{3+} + Mn^{2+} \tag{1.3}$$

$$Mn^{2+} + 2\,Ce^{4+} - (\text{fast}) \rightarrow Mn^{4+} + 2\,Ce^{3+} \tag{1.4}$$

Adding these reactions results in the cancellation of the Mn ions and yields reaction 1.2. Since Mn ions participate in the rapid conversion of Fe^{2+} and Ce^{4+} to their respective products while being cyclically regenerated, our simple definition of a catalyst is satisfied.

The role of a catalyst in reducing the energy barrier or *activation energy* (and thus enhancing the rate) necessary for electron exchange between the reactants and products is illustrated in the potential energy diagram in Figure 1.3; reduction of E_{act} (a purely kinetic quantity) increases rate dramatically because (as will be shown later) rate increases exponentially with decreasing E_{act}. The catalyst lowers the activation barrier by providing a surface or site for adsorption and dissociation of the reactants, in which they are more readily transformed to products. The energy difference between reactants and products (Figure 1.3) is the heat of reaction or negative ΔH_r (change in enthalpy), a purely thermodynamic quantity (which in Figure 1.3 happens to be positive since the reaction is exothermic).

It is important to recognize that both the enthalpy and free energy are unaffected by the presence of the catalyst; that is, the catalyst does not change the energetics of the initial and final states, but only increases the rate of their attainment. In other words, a catalyst cannot make a thermodynamically unfavorable reaction occur, but it does increase the rate of approach to the equilibrium state. Thus ΔH and ΔG (and consequently the equilibrium constant K) are not altered by the presence of a catalyst.

The rate of reaction has been mentioned several times. The *specific reaction rate for a stoichiometric catalytic reaction* (sometimes called ***activity***) is formally defined as

$$r = \frac{1}{\nu_i Q} \frac{dn_i}{dt} \tag{1.5}$$

where $Q = V$, W, or S, the volume, weight, or surface area of the catalyst; ν_i is the stoichiometric coefficient in the stoichiometric reaction $\Sigma_i \nu_i M_i = 0$ involving species M_i (ν_i is negative for reactants and positive for products); and n_i is the number of moles of species M_i. For example, for the ammonia synthesis, the

stoichiometric reaction can be written as $2NH_3 - N_2 - 3H_2 = 0$; thus, stoichiometric coefficients for NH_3, N_2, and H_2 are 2, –1, and –3, respectively, and the specific rate for reaction based on iron catalyst surface area in terms of hydrogen disappearance is $r = (1/\nu_i Q)(dn_i/dt)$. For a constant volume system, n_i can be couched in terms of concentration, since $C_i = n_i/V$, or for mild conditions in terms of pressure using the ideal gas law $P_i = n_i RT/V$. The number of moles of species *i* at any point in time is defined by $n_i = n_i^o + \nu_i \xi$ where n_i^o is the number moles of species *i* initially present and ξ is the extent of reaction (in moles). It can be easily shown from this definition of n_i and the definition of conversion $X_i = (n_i^o - n_i)/ n_i^o$ that conversion $X_i = -\nu_i \xi / n_i^o$.

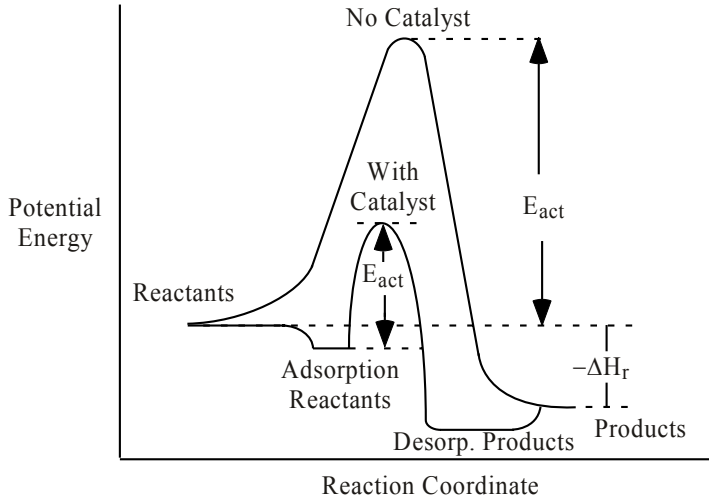

Figure 1.3 Catalytic and noncatalytic potential energies versus reaction coordinate for an elementary reaction.

The reaction rate is generally a function of both temperature and reactant concentrations. Accordingly, the rate equation is generally approximated as a product of a function of temperature and concentration:

$$r = k(T)\, f(C_i) = A\, \exp(-E_{act}/RT)\, \Pi_i (C_i)^{\alpha_i} \tag{1.6}$$

where $k(T)$ is the rate constant described by the Arrhenius law

$$k(T) = A \exp(-E_{act}/RT),$$

A is the pre-exponential or frequency factor, and E_{act} is the activation energy; the frequency factor is (from collision theory) proportional to the number of collisions, which might lead to reaction and in the case of a catalytic reaction to the concentration of catalytic sites, while the quantity $\exp(-E_{act}/RT)$ is the fraction of collisions that results in reaction. Accordingly, a catalyst increases the rate and hence the rate constant by increasing A (by providing catalytic sites) and/or decreasing the activation energy E_{act} (hence increasing the fraction of collisions resulting in reaction). Note that the Arrhenius law predicts an exponential increase in rate with increasing temperature; accordingly, the dependence of rate on temperature can possibly overwhelm other factors, particularly where E_{act} is large (i.e. greater than 30–50 kJ/mol) as is characteristic of a process in which chemical bonds are broken and/or formed such as in a catalyzed surface reaction.

The concentration function $f(C_i)$ may be expressed in its simplest form as a product summation of reactant and possibly product molecules raised to empirically determined exponents (positive or negative and generally decimal fractional), e.g. for thermal NO formation it is experimentally observed under certain conditions that $\Pi_i(C_i)^{\alpha i} = (C_{O_2})^{0.5}\ (C_{N_2})^{1.0}$. The empirically determined exponents or α_i values are the reaction orders with respect to a species M_i while their sum is the overall reaction order; accordingly, for NO formation the reaction orders are 0.5 and 1.0 with respect to O_2 and N_2, respectively, and the reaction is 1.5 order overall. Generally, reaction orders must be determined experimentally by measuring rate as a function

of reactant concentration independently for each reactant; however, in the case of elementary steps (discussed in the next section) reaction orders may be predicted. For example, for a bimolecular elementary step A + B → C, the rate is proportional to the concentration of each species A and B; hence, the reaction is first-order in each kind of molecule and overall second-order.

Elementary steps, active sites and active centers. Consider catalytic CO oxidation. Gaseous CO and O_2 interact with a solid catalyst, e.g. Pt, and rapidly convert to CO_2. This is a heterogeneous catalytic reaction since the catalyst is a solid and the reactants are gases. The overall stoichiometric reaction can be simply written as

$$CO + 1/2\ O_2 \rightarrow CO_2 \tag{1.7}$$

Mechanistically, however, the reaction can be broken down into a number of simple or ***elementary steps***, each of which occurs as written at the molecular level and which cannot be further simplified. The following is one of several possible mechanistic sequences:

$CO(g) + Pt_s$	$\leftrightarrow$	$CO\text{-}Pt_s$	(quasi-equil)	(1.8)
$O_2(g) + 2\ Pt_s$	$\leftrightarrow$	$2\ O\text{-}Pt_s$	(quasi-equil)	(1.9)
$CO\text{-}Pt_s + O\text{-}Pt_s$	$\rightarrow$	$CO_2\text{-}Pt_s + Pt_s$	(slow, irrev., rds)	(1.10)
$CO_2\text{-}Pt_s$	$\rightarrow$	$CO_2(g) + Pt_s$	(fast, irrev.)	(1.11)

where CO(g) denotes gas phase CO; Pt_s is a surface Pt atom or ***active site*** for reaction; Pt_s, Pt_s-O, Pt_s-CO, and Pt_s-CO_2 are short-lived intermediates on the catalyst surface called ***active centers***.

This sequence illustrates the complexity of the catalytic surface reactions operating in the simple conversion of CO to CO_2. First, CO is chemisorbed onto a Pt atom (or active site) rapidly, reversibly, and at near equilibrium or quasi-equilibrium (as denoted by the double arrow). This and all chemisorption reactions are exothermic, since both ΔG and ΔS are negative, that is, chemisorption occurs spontaneously and with an increase in the ordering of the phase molecules as they adsorb. Similarly, diatomic O_2 chemisorbs dissociatively, rapidly, reversibly, and in quasi-equilibrium on two Pt surface sites forming two chemisorbed O atoms. Chemisorbed CO and O ($CO\text{-}Pt_s$ and $O\text{-}Pt_s$) then react relatively slowly and essentially irreversibly (denoted by single arrow) in step 1.10 forming chemisorbed CO_2 ($CO_2\text{-}Pt_s$), which subsequently desorbs rapidly but essentially irreversibly (step 1.11) into the gas phase. Experimental studies have shown that under certain reaction conditions the slow or rate determining step (rds) is the reaction between adsorbed CO and O (step 1.10), and thus this reaction controls the overall reaction rate. In other words, the overall reaction rate involving gaseous CO and O_2 to CO_2 can be no faster than the rate of the slowest step, in this case, the reaction between adsorbed species. In the absence of a catalyst, O_2 decomposition is the rate-limiting step, and the thermal reaction becomes important at about 500°C. The presence of Pt, however, decreases the activation energy for the O_2 dissociation reaction allowing complete oxidation to occur at 200–250°C.

What has been described above is the chemical surface reactions involved in a catalytic process. Physical processes such as mass transfer define the flow of gases or liquids to the active catalytic sites and play a critical role in overall reaction kinetics. They are discussed in Section 1.3.3 below.

Finally, a catalyst influences ***selectivity***, i.e. the ratio of rates (r_1/r_2), for competing reactions by preferentially increasing the rate at which the desired rate determining step (rds) and hence the desired stoichiometric reaction proceeds relative to another rds and stoichiometric reaction. For example, selectivity is an important issue in NO reduction with CO or H_2 on noble metals in the reducing environment of automotive three-way converters, since on Rh catalysts NO is reduced to the desired product, N_2, but on Pt catalysts to another pollutant, ammonia. Hence, the selectivity to N_2 is $S_{N_2} = r_{N_2}/r_{NH_3}$. Accordingly, it is critical in many different kinds of catalytic processes that the catalyst be tailored to enhance the rate of the desired reaction.

1.3.2 The Structure of a Supported Catalyst: Model and Reality

From our definitions of a catalyst and of specific reaction rate, it should be clear that the number of reactant molecules converted to products in a given time interval is directly related to the number of catalytic sites available. It is, therefore, common practice to maximize the number of active sites available to the reactants by dispersing the catalyst species onto a support or 'carrier' surface. Furthermore, the larger the support surface the more likely that the catalytic species, whether it be a metal such as Pt, Fe, or Ni; an oxide such as CuO, PdO, or CoO; or a sulfide such as MoS_2 or NiS, will be present as tiny, discrete particles (or crystallites). The smaller the crystallite, the greater its individual surface to volume ratio and hence the greater total surface area per unit mass for a collection of small crystallites. Thus maximizing catalytic surface area per unit mass enhances the number of sites per unit mass upon which chemisorption and catalytic reaction can occur.

To accomplish this, most (but not all) commercial catalyst components are dispersed on high surface area porous oxides (carriers) such as Al_2O_3, SiO_2, or TiO_2, or on high surface area carbons. These supported catalysts are in turn fabricated into pellet forms or washcoated on monolithic substrates for use in industrial reactors. The preparation and properties of supported catalysts and the influence of supports on catalytic reactions are discussed in Chapter 2.

Supported metal systems are complex nanostructures; however, a simple 'raisin in the sponge cake' model, using Pt supported on alumina (Pt/Al_2O_3) as an example, provides some insights into the nature of this structure. Figure 1.4a shows an enlarged, idealized schematic of a porous Al_2O_3 particle composed of relatively straight interconnecting pores of two different size ranges, namely, mesopores having diameters in the range of 5–12 nm and macropores with diameters of 50–500 nm. Pt crystallites of 1–5 nm are shown to be distributed along the surface of these pores. Most of the support surface area and most Pt crystallites with their attendant active metal sites are found in the mesopores, while the macropore network provides a relatively accessible path for reactants to diffuse from the outer surface of the catalyst pellet to the mesopores and finally to the metal crystallite surfaces. The mesoporous network with its associated high surface area, tortuosity, and interaction with metal crystallites also provides a medium for preparing well-dispersed, small crystallites of metal and maintaining their high metal surface area by preventing migration and agglomeration at high reaction temperatures.

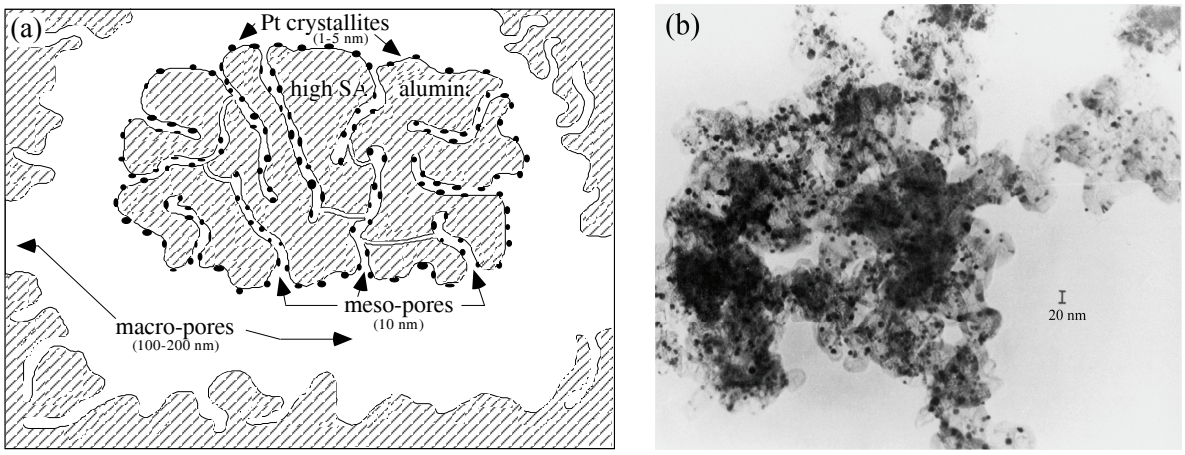

Figure 1.4 (a) Schematic model of platinum metal crystallites supported on γ-alumina. (b) Transmission electron micrograph of a real Pt/alumina catalyst (bar represents 20 nm).

The pore and crystallite dimensions mentioned here are typical of commercial $Pt/\gamma\text{-}Al_2O_3$ catalysts; however, the porous $\gamma\text{-}Al_2O_3$ in a real catalyst (Figure 1.4b) is composed of numerous interconnecting pores of less uniform diameter and greater tortuosity (curvature of the pore paths) than illustrated in Figure 1.4a. In

fact, the structure of each real supported catalyst at this scale is best described as a fractal, each catalytic phase/support combination having its own unique structure.

1.3.3 Steps in a Heterogeneous Catalytic Reaction

To maximize reaction rates on a porous catalyst, it is essential to maximize accessibility of all reactants to the active catalytic sites, which are dispersed throughout the internal pore structure of the catalyst. Imagine gas A flowing through a bed of a heterogeneous catalyst and reacting on the catalyst surface to form a gaseous species B. In order for A to convert at any appreciable rate to product B, the following physical and chemical steps (shown schematically in Figure 1.5) must occur:

1. Film mass transfer of the reactant A, i.e. bulk diffusion of A through the stagnant gas film or boundary layer surrounding the catalyst particle to the external catalyst surface.
2. Diffusion of species A (by either bulk or molecular (Knudsen) diffusion) through the porous network of the catalyst to the catalytic surface.
3. Adsorption of A onto the catalyst surface.
4. Reaction of A to B on catalytic sites on the catalyst surface.
5. Desorption of the product B molecules from the surface.
6. Diffusion of species B through the porous network to the pore mouth.
7. Film mass transfer of product B, i.e. bulk diffusion of B from the external catalyst surface through the stagnant gas film to the bulk gas stream.

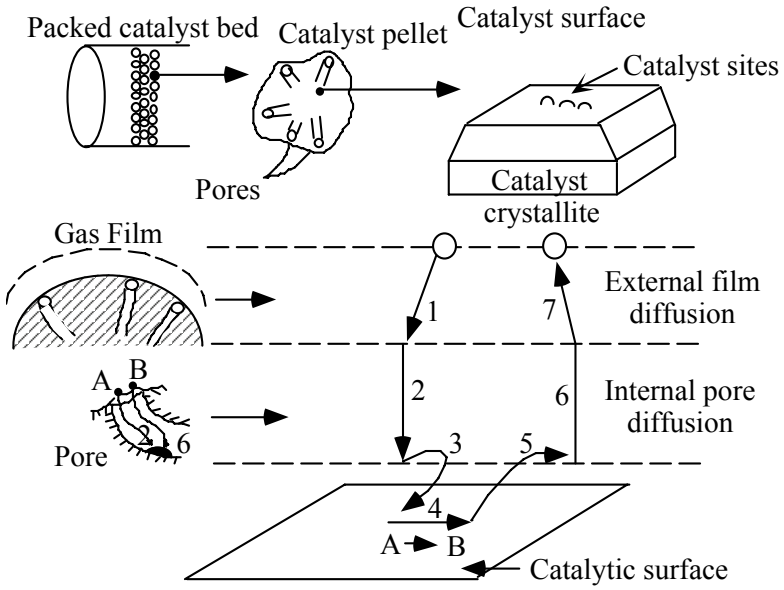

Figure 1.5 Steps in a heterogeneous catalytic reaction A → B in a porous, supported catalyst (adapted from Fogler, 1999; courtesy of Prentice Hall).

Steps 1, 2, 6, and 7 are diffusional processes having small ($T^{1/2}$ or $T^{3/2}$) dependences on temperature. Steps 3, 4, and 5, however, are chemical processes with large temperature dependences, i.e. activation energies of 20–200 kJ/mol. Any of these steps can be sufficiently slow, relative to the others, that it controls the overall rate of reaction. Given, however, that the rates of the chemical steps are exponentially dependent on temperature and have relatively large activation energies compared to the diffusional processes, they are generally the slow or rate-limiting processes at low reaction temperatures. But as the temperature is increased, the rates of chemical steps with higher activation energies increase enormously relative to diffusional processes, and hence the rate limiting process shifts from chemical to diffusional. At intermediate reaction temperatures, the combination of pore diffusion and surface reaction inside the pores is slowest, and

hence the temperature dependence is reduced to an average of the activation energies for chemical and diffusional steps. Finally, at high reaction temperatures, the chemical reaction is sufficiently rapid that reactants are converted on the exterior surfaces of the catalyst (before they can diffuse into the interior of the catalyst); in this situation, film mass transfer (diffusion) with a temperature dependence of only $T^{3/2}$ (E_{act} = 4–8 kJ/mol) becomes rate limiting. The decrease in activation energy with increasing temperature corresponding to the different limiting processes is represented in Figure 1.6 in the form of an Arrhenius plot of the apparent rate constant. Since according to the Arrhenius law, $k_{app} = A \exp(-E_{app}/RT)$, a plot of $\ln(k_{app})$ versus $1/T$ should have a slope of $-E_{app}/R$, where E_{app} is the apparent activation energy.

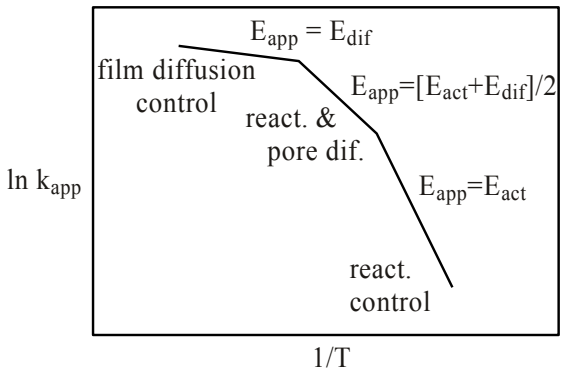

Figure 1.6 Typical temperature dependence of a catalytic reaction in the form of an Arrhenius plot for which the slope is $-E_{app}/R$ (app = apparent); rate controlling regimes are shown for low, intermediate and high reaction temperatures.

1.3.4 Adsorption and Desorption

Definition of adsorption. Adsorption of reactants and desorption of products are two necessary and sufficient chemical steps in a catalytic reaction. One of the important functions of the catalyst is to provide a surface with partially uncoordinated sites chemically suited for adsorbing reactant molecules. Thus in chemical terms, adsorption is the formation of chemical bonds between adsorbing species (the adsorbate) and an adsorbing surface (adsorbent) driven by the propensity of adsorbent surface atoms to increase their coordination numbers, (i.e. decrease their surface energy) as illustrated in Figure 1.7.

Physical and chemical adsorptions. There are two kinds of adsorptions, chemical and physical, typically referred to as chemisorption and physisorption (see Figure 1.7b, 1.7c and Table 1.4). Physisorption (Figure 1.7b) is the relatively weak, nonselective condensation of gaseous molecules on a solid at relatively low temperatures (i.e. –200 to –25°C); the attractive forces between adsorbate and adsorbent involve Van der Waals forces, atomic distances typical of a Van der Waals layer, and heats of adsorption less than about 15–20 kJ/mol. Chemisorption, by contrast, is the relatively strong, selective adsorption of chemically reactive gases on available sites of metal or metal oxide surfaces at relatively higher temperatures (i.e. 25–400°C); the adsorbate-adsorbent interaction involves formation of chemical bonds and heats of chemisorption on the order of 50–300 kJ/mol. Observed differences between these two adsorption processes are summarized in Table 1.4.

Chemisorption of a reactive diatomic or polyatomic molecule commonly occurs via the physically adsorbed precursor state shown in Figure 1.7b followed by dissociation to reactive atomic species (see Figure 1.7c). Dissociation is favorable where the energy gain due to interactions of atoms from the molecule with metal atoms exceeds the binding energy of the atoms in the molecule.

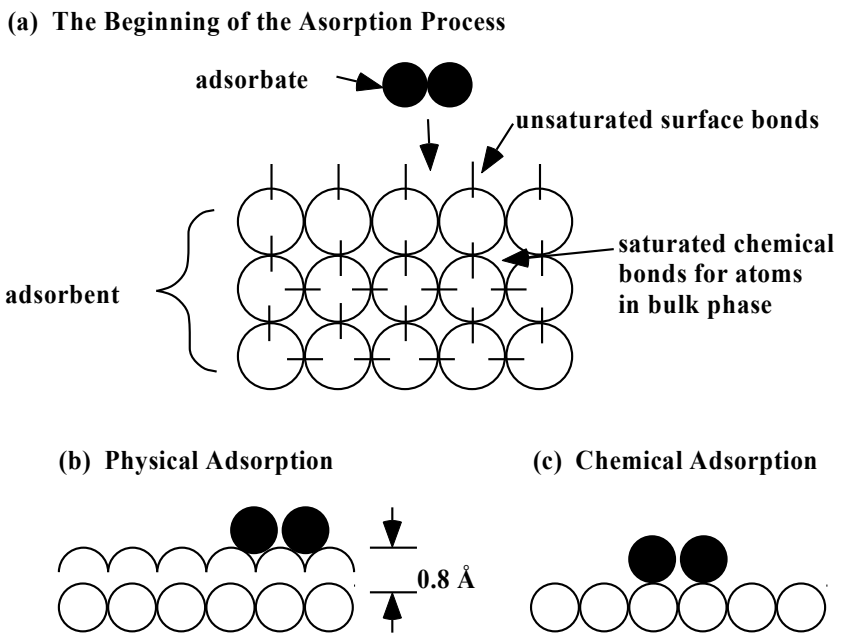

Figure 1.7 Schematic illustration of adsorption on a surface.

Table 1.4 Physical versus Chemical Adsorption

Parameter	Physical adsorption	Chemisorption
Adsorbent	all solids	some solids
Adsorbate	all gases below critical temperature	some chemically reactive gases
Temperature range	low-temperature, ≈ b.p. of adsorbate	generally high-temperature > b.p. of adsorbate
Heat of adsorption	low ($\approx -\Delta H_{condensation}$) $-\Delta H \leq 20$ kJ/mol	high: order of heat of reaction $-\Delta H \approx 50$–300 kJ/mol
Rate, activation energy	very rapid, non-activated	sometimes slow, usually activated
Function of pressure	strong	weak
Coverage	multilayer, nonspecific	monolayer, specific
Desorption	easy in vacuum or purge gas	E_{act} for desorption > 50–100 kJ/mol; occurs only at high temperatures
Reversibility	highly reversible	largely irreversible
Importance	for determination of surface area and pore size	for determination of active-surface area and description of surface-reaction kinetics

Changes in the volume of gas adsorbed due to physisorption and chemisorption with temperature are shown qualitatively in Figure 1.8. The volume of gas physically adsorbed is large at low temperatures and decreases sharply with increasing temperature, while the amount adsorbed due to activated chemisorption increases through a maximum at moderate temperatures and decreases at higher temperatures as the rate of desorption exceeds the rate of adsorption.

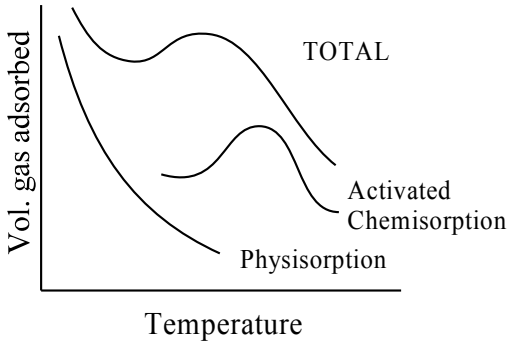

Figure 1.8 Volume of gas adsorbed during activated physisorption, chemisorption, and the total of both physisorption and chemisorption as a function of temperature.

Adsorption isotherms. The quantity of a species adsorbed is generally characterized by an isotherm, a plot of θ versus pressure at constant temperature, where θ is the fraction of surface covered with a specific adsorbed atom or molecule. Isotherms relate surface concentration (an immeasurable) to gas phase concentration (a measurable). Fractional coverage θ is defined as the volume adsorbed per volume required for monolayer coverage (V/V_m). Generally, $\theta = f(T, P)$ but $\theta = f(P)$ at constant T. The temperature dependence is related to ΔH_{ads} as will be shown later.

Langmuir isotherm. The Langmuir isotherm is the simplest and most widely used form for monolayer adsorption. It is based on the following assumptions: (1) the adsorbate is typically strongly adsorbed (chemisorbed) in a monolayer; (2) one species is adsorbed per site (this can be adjusted if the stoichiometry is not 1:1); (3) ΔH_a (enthalpy of adsorption) is independent of θ (coverage) which implies that sites are energetically uniform and there are no interactions of sites and/or adsorbates; and (4) equilibrium exists between adsorption and desorption.

The Langmuir isotherm is derived below, where

A	=	species adsorbed (adsorbate)
S	=	site on the surface (e.g. metal atom)
θ_A	=	fraction covered by A
$1 - \theta_A$	=	fraction not covered by A
P_A	=	pressure of the gas A
k_a	=	rate constant for adsorption
k_d	=	rate constant for desorption

The elementary equilibrium reaction is written

$$A + \mathbf{S} \leftrightarrow A - \mathbf{S} \tag{1.12}$$

where **S** denotes a surface site and A-**S** is adsorbed A. The overall rate of adsorption is the sum of forward and reverse rates. In terms of coverage,

$$r = k_a P_A (1 - \theta_A) - k_d \theta_A \tag{1.13}$$

since the rate of adsorption is directly proportional to the gas phase pressure of A (P_A) and the fraction of available sites ($1 - \theta_A$), while the rate of desorption is proportional to the coverage of A (θ_A). Since $r = 0$ at equilibrium, equation 1.13 can be rewritten as

$$(k_a / k_d) P_A (1 - \theta_A) = \theta_A.$$

Defining K as the equilibrium constant and writing the rate constants in terms of frequency factors and activation energies from the Arrhenius law,

$$K = (k_a / k_d) = (A_a / A_d)\, e^{-\Delta H_a / RT} \tag{1.14}$$

where $\Delta H_a = E_a - E_d$; assuming $\Delta H_a \neq f(\theta_A)$,

$$K P_A (1 - \theta_A) = \theta_A$$

Solving for θ_A

$$\theta_A = K P_A / (1 + K P_A) \tag{1.15}$$

Langmuir isotherms for weakly, moderately, and strongly adsorbed species A are plotted in Figure 1.9. At low pressure the isotherm is linear, while at high pressure the volume adsorbed approaches the monolayer volume V_m or a fractional saturation coverage of one.

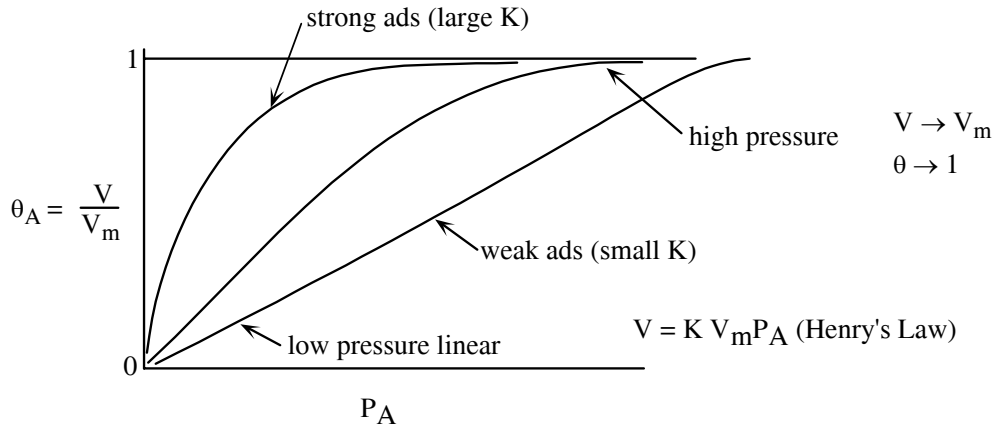

Figure 1.9 Isotherms or coverage versus pressure curves for weak, moderately strong, and strong adsorption of a species A on a surface.

Conformity to the Langmuir isotherm can be tested by plotting volume-pressure data in linear form to obtain constants. Starting with equation 1.15,

$$\theta_A = V / V_m = K P_A / (1 + K P_A)$$

the numerator and denominator on opposite sides of the equation are multiplied to obtain cross products,

$$V + V K P_A = K P_A V_m$$

which are each divided by P_A and rearranged to obtain

$$V / P_A = -K V + K V_m \tag{1.16}$$

which has the form $y = mx + b$.

The data are tested by plotting V/P_A versus V to obtain a straight line with a slope of $-K$ and intercept of KV_m. This form has the advantage of using both slope and intercept to evaluate K. Other forms, e.g. those involving $1/P_A$, should be avoided because the low pressure part of the isotherm is weighted too highly.

Few physical and chemical adsorption systems conform to the Langmuir equation over the entire range but usually conform over a restricted range of θ, i.e. most surfaces are not uniform. What causes Langmuir theory to breakdown? Probably a combination of the following phenomena:

- Surface heterogeneity, i.e. the surface consists of different exposed crystal planes and coordination sites, e.g. edge, corner and defect sites having a wide range of binding energies (sites of lower coordination, i.e. atoms bonded to fewer neighboring atoms, having the highest binding energies).
- Interaction of sites, i.e. (a) repulsion between adsorbed species and (b) donation of electrons from or capture of electrons by the surface (through adsorbate-adsorbent lattice electronic interaction).

Note that site interaction is a phenomenon highly dependent upon coverage. Evidence for heterogeneity of sites and site interaction has been provided by numerous studies showing that the heat of adsorption decreases significantly (by 50–100%) with increasing coverage (see Figure 1.10). This phenomenon is explained by the tendency for adsorption to occur first on the most energetic sites followed by adsorption on less energetic sites.

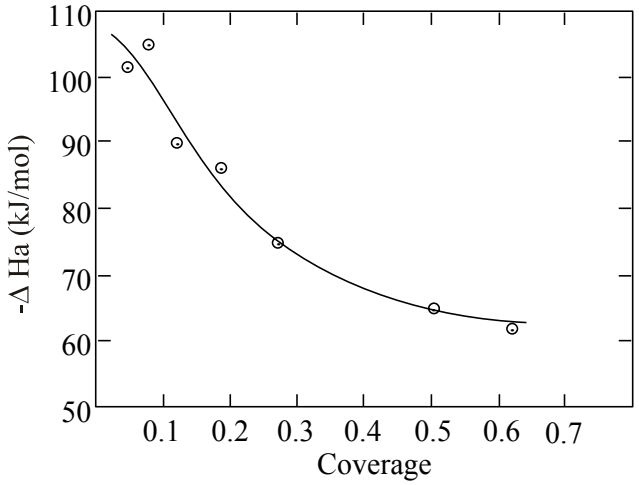

Figure 1.10 Heat of adsorption of H_2 on 10% Co/Al_2O_3 as a function of coverage from temperature programmed desorption (Zowtiak and Bartholomew, 1983; courtesy of Academic Press).

Other forms of the Langmuir isotherm—Equation 1.15 is generally applicable to the adsorption of a single molecular species. The Langmuir isotherm, however, can be adapted to adsorption with dissociation:

$$A_2 + 2\mathbf{S} \leftrightarrow 2\ A\text{-}\mathbf{S}$$

Again, equating the rates of adsorption and desorption at equilibrium ($r = 0$):

$$r = k_a P_{A_2} (1 - \theta_A)^2 - k_d \theta^2_A$$

$$(K P_{A_2})^{1/2} (1 - \theta_A) = \theta_A$$

$$\theta_A = [(K P_{A_2})^{1/2}] / [1 + (K P_{A_2})^{1/2}] \qquad (1.17)$$

By a similar treatment one can derive isotherms for simultaneous competitive (nondissociative) adsorption of A and B:

$$\theta_A = (K_A P_A) / (1 + K_A P_A + K_B P_B) \qquad \theta_B = (K_B P_B) / (1 + K_A P_A + K_B P_B) \qquad (1.18)$$

In general, the isotherm for competitive adsorption of the *i*th species with N species (including *i*) can be shown to be:

$$\theta_i = \frac{P_i K_i}{1 + \sum_{j=1}^{N} P_j K_j} \tag{1.19}$$

Multilayer isotherms and the BET isotherm model—Physical adsorption can result in multilayers. Various types and shapes of multilayer adsorption isotherms have been observed but Type IV for mesoporous solids (Figure 1.11) is most common. In principle, if an isotherm can be modeled and V_m can be measured or calculated from other measurable quantities, then total surface area of any solid can be determined.

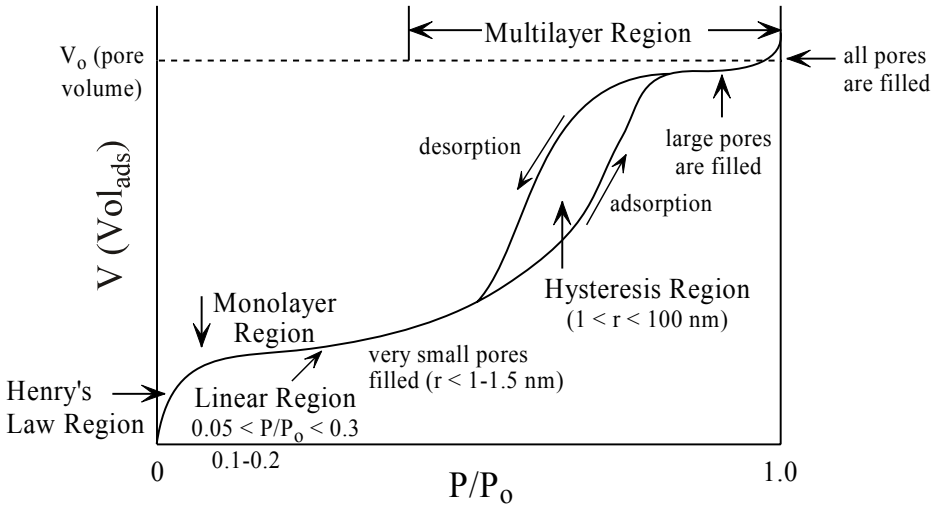

Figure 1.11 Full range Type IV adsorption isotherm with adsorption and desorption branches.

The model of Brunauer, Emmett, and Teller in 1938 was the first successful attempt to model multilayer adsorption. The important assumptions for the BET theory are: (1) the same starting assumptions as Langmuir; (2) adsorbed species in the first layer serve as sites of adsorption for the second layer; (3) the rate of adsorption (r_a) on the ith layer is equal to the rate of desorption (r_d) of the (i + 1) layer; and (4) ΔH_{ads} is the same for second and succeeding layers and equal to the heat of condensation of the gas (i.e. $\Delta H_{a_2} = \Delta H_{a_3} = \ldots \Delta H_c$). Based on these assumptions, the following isotherm can be derived:

$$\theta = \frac{V}{V_m} = \frac{cx}{(1-x)\left[1+(c-1)x\right]} \tag{1.20}$$

where $x = P/P_o$, P_o = vapor pressure of the adsorbing gas at a given temperature, V_m is the volume of gas required to provide a complete monolayer and

$$c = c_o \exp\left[\frac{\Delta H_{a_1} - \Delta H_c}{RT}\right] \tag{1.21}$$

where ΔH_{a_1} = heat of adsorption on the first layer, ΔH_c = heat of condensation of gas, and $c_o = \frac{a_1 b_2}{a_2 b_1}$

where a_1, b_1, a_2, and b_2 are the preexponentials for condensation to and evaporation from the first and second layers, respectively. Equation 1.20 can be linearized by inverting and rearranging to

$$\frac{x}{V(1-x)} = \frac{1}{cV_m} + \frac{(c-1)x}{cV_m} \tag{1.22}$$

Experimentally, isotherm data versus P/P_o in the form of volume adsorbed are collected at the boiling point of the adsorbate, usually N_2 at –196°C. The data can be tested against this equation by plotting $x/[V(1-x)]$ versus x to get a straight line with intercept $1/cV_m$ and slope $(c-1)/cV_m$. To calculate surface area, the monolayer volume is corrected to the number of moles adsorbed. Surface area is then calculated based on the following equation:

$$\hat{S} = n_m N_{Av} \alpha \tag{1.23}$$

which has units of (area/g) = (moles/g) (molecules/mole) (area/molecule) and for which N_{Av} = Avogadro's number, $\alpha = 16.2 \times 10^{-20}$ m^2/molecule for N_2. For adsorption of N_2 at liquid N_2 temperature Equation 1.23 simplifies to

$$\hat{S} = 4.35 \hat{V}_m \ (m^2/g) \tag{1.24}$$

if $\hat{V}_m$ (cm^3/g) is corrected to STP.

The full range adsorption isotherm. A full range adsorption isotherm with adsorption and desorption branches is shown in Figure 1.11. Information that may be obtained from the curves includes: (a) surface area, (b) pore volume, (c) pore size and distribution, and (d) pore structure. How this information is obtained can be inferred from Figure 1.11 and Table 1.5 and is illustrated in Chapter 3. Highly detailed, rigorous treatments of adsorption are found in books by Gregg and Sing (1982), Thomas and Thomas (1997), and Masel (1996).

Table 1.5 Information Available from Full Range Isotherm

Region	Pressure Range	Information obtained
Henry's Law Region. (Adsorption is a linear function of pressure.)	$P/P_o < 0.01$	SA can be obtained if Henry's Law constant k_H is known e.g. $k_H = V_m C \times 10^4/P_o$ based on BET
Monolayer Region. (Adsorption increases only slightly and linearly with increasing pressure.)	$0.05 < P/P_o < 0.3$	Uptake at "knee" is proportional to the SA. SA can be estimated by extrapolating linear portion to $P/P_o = 0$ or calculated from linear form of BET equation.
Multilayer Region or Capillary Condensation Region. (Adsorption uptake increases markedly as pores are filled; hysteresis occurs upon desorption due to constrictions in pores.)	$0.3 < P/P_o < 1.0$	Pore volume - determined at $P/P_o = 1$ Pore structure can be inferred from shape of hysteresis curve. Kelvin equation can be used to determine cumulative pore volume and pore size distribution—plot V versus r and take derivative to get dV/dr versus r.

1.3.5 Reaction and Diffusional Resistances for a Catalytic Reaction

Physical picture and model for reaction in a porous catalyst pellet. Most industrial catalysts are porous solids that catalyze reactions at the exterior and inside the pores of a catalyst pellet or thin catalyst layer coated on a monolithic substrate. Imagine, for example, a gaseous reaction occurring inside a reactor containing spherical pellets; gas flows into the reactor and around each of the pellets (see Figure 1.5). In order for reactant molecules to reach the catalyst surface, they must diffuse (1) through the stagnant gas film surrounding each pellet and (2) inside the pores of the catalyst (since most of the active catalytic sites are in the interior of the catalyst pores).

A section of the catalyst pellet containing a single ideal pore can be used in modeling the catalytic reaction process (see Figure 1.12). In this simple Wheeler/Levenspiel model, molecules of a reactant A

diffuse from the flowing bulk gas phase through the stagnant gas film surrounding the pellet where they can react either at the exterior of the pellet or diffuse inside the pore and react on the interior surface of the pore. As molecules of A are converted at the external surface and inside the pore, there is a drop in concentration first through the gas film and then further along the pore (see Figure 1.12).

The electrical analog of the reaction process is shown schematically in Figure 1.12. In the view of the overall reaction process, each reaction or diffusion step can be considered to be a resistance to surface reaction. The resistances for diffusion through the gas film and reaction (either at the external surface or internal surface) are in series; however, the resistances for external surface reaction and internal diffusion/reaction are in parallel. We will use this information at a later point to derive the overall rate expression for the catalytic process in terms of each of the individual resistances. First, however, it is expedient that we derive individually the rate expressions for (1) film mass transfer, (2) external surface reaction, and (3) internal surface reaction (which accounts for internal pore diffusion) assuming an irreversible, first-order reaction.

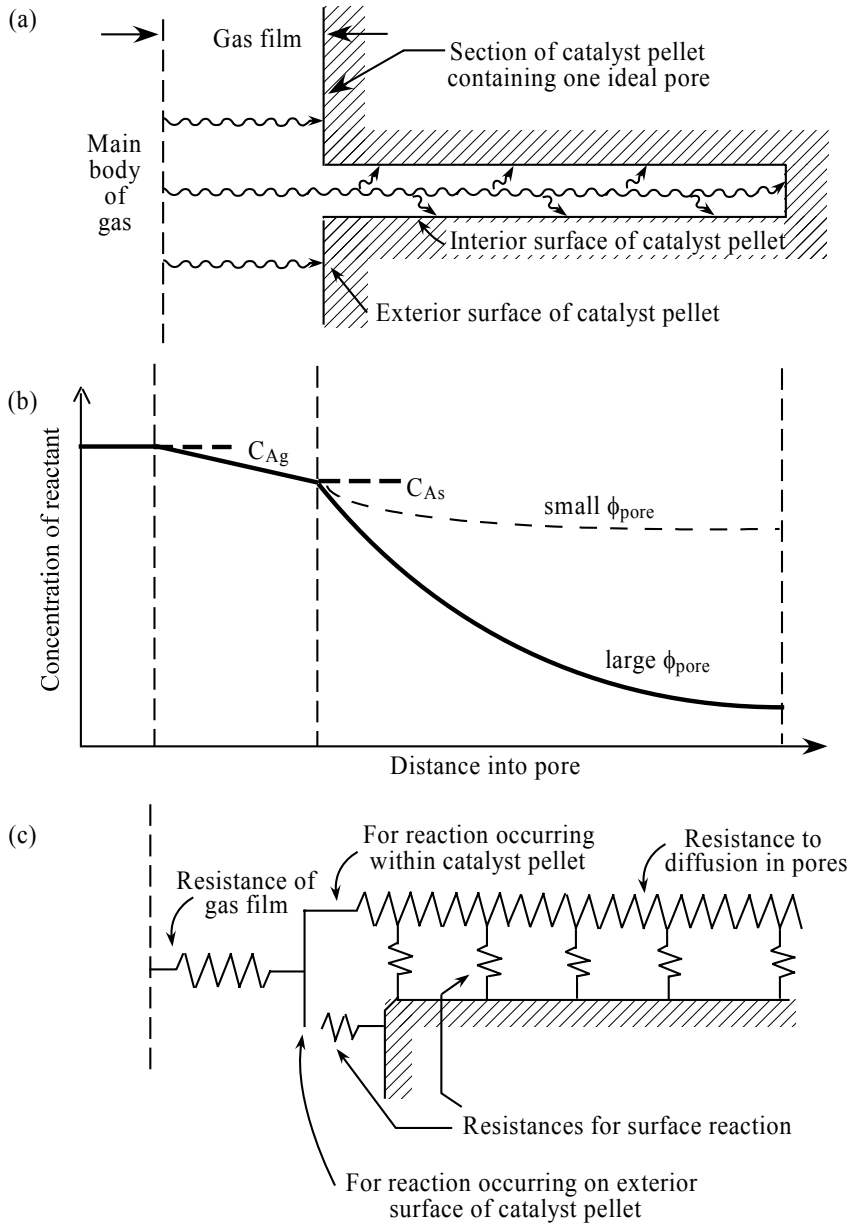

Figure 1.12 Simplified single-pore model for diffusion and catalytic reaction in a porous catalyst (adapted from Levenspiel, 1999; courtesy of John Wiley & Sons).

Individual rates for film mass transfer, external surface reaction, and internal surface reaction with pore diffusion.

Film mass transfer—From Fick's first law we can define the mass transfer flux N_A of a species A across an interface as

$$N_A = -(1/S_{ex})(dn_A/dt) = D\,(dC/dx) = k_c\,(C_b - C_s) \tag{1.25}$$

where the flux or rate of mass transfer (N_A) has units of moles/area·time, S_{ex} is the surface area of the interface (or in the case of a pellet, the external geometric surface area), n_A is the number of moles of A, C the concentration of A, C_b the concentration of A in the bulk fluid phase, C_s the concentration at the surface of the catalyst pellet, D the diffusivity of A in the fluid, and k_c the mass transfer coefficient (an effective diffusivity per unit film thickness) having units of cm^2/s. Note that the A subscripts have been omitted from C_b and C_s for convenience. Recouching the *rate of mass transfer in a pellet* r_p in terms of the moles transferred per unit mass of catalyst

$$r_p = k_c\, a_m\, (C_b - C_s) \tag{1.26}$$

for which $a_m = S_{ex}/W$, i.e. specific area/mass of the catalyst pellet in cm^2/g_{cat}.

Rate of reaction at the exterior surface—For an irreversible, first-order reaction, *the rate of disappearance of species A at the exterior surface* is simply defined as

$$-(1/S_{ex})(dn_A/dt) = kC_s \tag{1.27}$$

where k = the first-order reaction rate constant. Expressing the reaction rate in terms of the overall rate of disappearance of A at the exterior surface of the pellet per mass of catalyst gives

$$r_p = k\, a_m\, C_s. \tag{1.28}$$

Rate of reaction at the interior surface—Again, for an irreversible, first-order reaction, *the rate of disappearance of species A at the interior surface* is simply defined as

$$-(1/S_{in})(dn_A/dt) = k\, C_s\, \eta \tag{1.29}$$

where S_{in} = the interior catalytic surface area of the pores and η is the effectiveness factor (the ratio of actual reaction rate in the pellet to the rate with no drop in concentration due to pore diffusional resistance). Again, couching the reaction rate in terms of the overall rate of disappearance of A at the interior surface of the pellet per mass of catalyst based on exterior surface area

$$r_p = k\,(S_{in}/S_{ex})\, a_m\, C_s\, \eta \tag{1.30}$$

From a steady-state material balance on the single pore shown in Figure 1.12a, which takes into account diffusional fluxes and reaction on the interior surface, it can be shown (Levenspiel, 1972) that the drop in concentration through the pore is

$$\frac{C_A}{C_{A_s}} = \frac{\cosh\left[\phi_{pore}\left(1 - \frac{x}{L}\right)\right]}{\cosh\ \phi_{pore}} \tag{1.31}$$

where ϕ_{pore} is the Thiele modulus for the pore defined by $\phi_{pore} = L(k\rho_p/D_{eff})^{1/2}$ where D_{eff} is the effective diffusivity, ρ_p is the density of the catalyst pellet, and L is the length of the pore; note that the Thiele modulus is proportional to pore length (and thus pellet diameter) and is a function of the ratio of the rate constant to the diffusivity; thus it is large at high reaction temperatures for which the rate constant is large relative to the diffusivity. For small values of ϕ_{pore} (i.e. less than 0.4) the drop in concentration through the pore is small while for large ϕ_{pore} the drop is large (see Figure 1.12b).

For a first-order reaction the definition of the effectiveness factor can be simplified to $\eta = (C_A)_{ave}/C_{As}$. Evaluating this ratio from Equation 1.31 leads to the following relationship for a single pore

$$\eta = (C_A)_{ave} / C_{As} = (\tanh \phi_{pore}) / \phi_{pore} \tag{1.32}$$

which enables calculation of the effectiveness factor in terms of the Thiele modulus, which in turn can be calculated if values of L, D_{eff}, and k are known. A plot of η versus ϕ for several geometries in Figure 1.13 shows that at values of ϕ below 0.4, η is near unity, while at values of ϕ greater than about 4, $\eta = 1/\phi$ and thus η decreases rapidly with increasing ϕ; in other words, at large values of ϕ, η is inversely proportional to ϕ, to L, and thus to pellet diameter.

While the equations above for η and ϕ_{pore} were derived for the simplified case of first-order reaction and a single pore, they are in general approximately valid for other reaction orders and geometries if L is defined as V_p/S_p, the volume to surface ratio of the catalyst particle; hence $L = z/2$, $r_c/2$, and $r_s/3$, respectively, for a flat plate of thickness z, a cylinder of radius r_c, and a sphere of radius r_s; the general applicability of these relationships to different geometries is also evident from Figure 1.13.

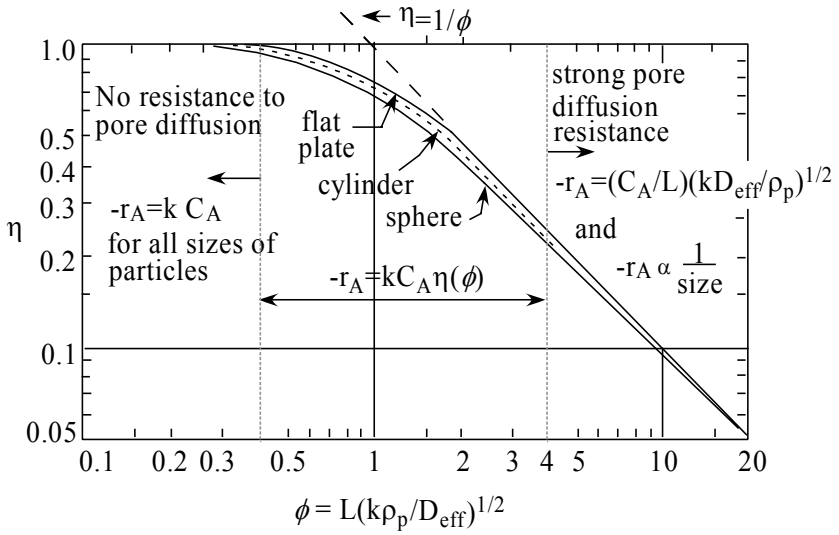

Figure 1.13 Effectiveness factor η (fraction of internal surface available for reaction) versus Thiele modulus ϕ for catalyst particles of different geometries.

Derivation of the overall reaction rate from reaction and diffusional resistances; limiting cases. Recalling from Figure 1.12c that surface reaction processes on exterior and interior surfaces occur in parallel, we can derive the *overall rate of reaction in the pellet* by adding equations 1.28 and 1.30 to get

$$r_p = k\,(S_{in}/S_{ex})\,a_m\,C_s\,\eta + k\,a_m\,C_s = k\,a_m\,C_s\,(1 + (S_{in}/S_{ex})\,\eta) \tag{1.33}$$

In order for the mass of A to be conserved, the rate of mass transfer of A to the pellet surface must be equal to the overall rate of reaction in the pellet at steady-state, i.e. film mass transfer and reaction resistances are in series (see Figure 1.12c). Accordingly, from equations 1.26 and 1.33,

$$k_c\,a_m\,(C_b - C_s) = k\,a_m\,C_s\,[1 + (S_{in}/S_{ex})\,\eta] \tag{1.34}$$

Solving Equation 1.34 for the unknown surface concentration C_s

$$C_s = (k_c\,C_b) / [k_c + k\,(1 + (S_{in}/S_{ex})\,\eta)] \tag{1.35}$$

Substituting for the value of C_s from Equation 1.35 into Equation 1.33 to eliminate C_s

$$r_p = [k\, a_m\, (1 + S_{in}/S_{ex}\ \eta)\, k_c C_b] / [k_c + k\, (1 + (S_{in}/S_{ex})\eta)] \tag{1.36}$$

and dividing top and bottom by $k\ k_c\ (1 + S_{in}/S_{ex}\ \eta)$ leads to a rate expression in terms of the known concentration C_b as well as rate constants and surface areas that can be determined experimentally

$$r_p = \frac{a_m C_b}{\dfrac{1}{k_c} + \dfrac{1}{k\left(1 + \dfrac{S_{in}}{S_{ex}}\eta\right)}} \tag{1.37}$$

in which the terms $1/k_c$ and $1/[k\ (1 + S_{in}/S_{ex}\ \eta)]$ are film mass transfer and reaction resistances, respectively. Since the interior surface area S_{in} greatly exceeds exterior surface area S_{ex} in most catalysts, Equation 1.37 can be simplified:

$$r_p = \frac{a_m C_b}{\dfrac{1}{k_c} + \dfrac{1}{k''\eta}} \tag{1.38}$$

where $k'' = k\ (S_{in}/S_{ex})$. Values of k and k_c can be obtained experimentally. Moreover, values of k_c can be calculated from mass-transfer correlations (Smith, 1984; Hines and Maddox, 1985; Fogler, 1998) (see Example 1.1).

At low reaction temperatures, the rate constant k is generally small relative to the mass transfer coefficient k_c, and thus the $1/k_c$ term in the denominator of Equation 1.38 is relatively small compared to the reaction resistance term, and Equation 1.38 simplifies to $r_p = k\ (S_{in}/S_{ex})\ a_m C_b \eta$, the rate of interior surface reaction (same as Equation 1.30 assuming $C_b = C_s$). Therefore in this case, the rate of reaction from Equation 1.38 is dominated by surface reaction terms, the surface reaction rate is the slow step, and we say that the surface reaction is controlling. Moreover, under these conditions, the Thiele modulus is small (since k is small relative to D_{eff}) and thus η is unity. In this case, the diffusion processes are fast relative to the reaction process, and the concentration profiles across the film and inside the pore are flat, i.e. the concentration is everywhere the same as in the bulk stream (equal to C_b); this case of *surface reaction rate control* is illustrated in Figure 1.14a.

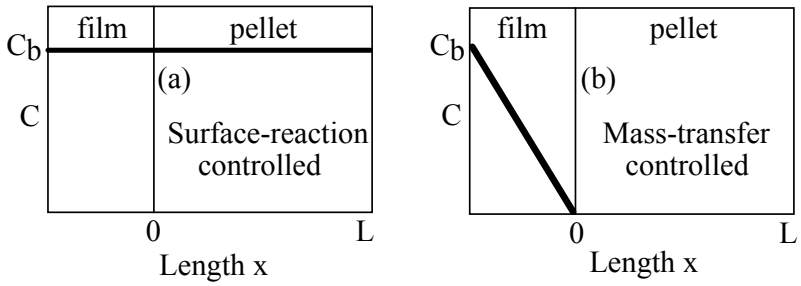

Figure 1.14 Concentration profiles across the gas film and catalyst particle for (a) surface reaction control and (b) film mass transfer control.

At high reaction temperatures, k becomes large relative to k_c because of the much higher activation energy for reaction relative to diffusion. Accordingly, the reaction resistance term in Equation 1.38 becomes small relative to $1/k_c$, and Equation 1.38 reduces to the rate of film mass transfer, i.e. $r_p = a_m\, k_c\, C_b$ (same as Equation 1.26 assuming $C_s \cong 0$); thus, film mass transfer is the rate controlling process (slow relative to reaction). In this case, the surface reaction is sufficiently fast and the Thiele modulus sufficiently large that surface reaction on the exterior surface dominates; in fact, the reaction is sufficiently rapid relative to the rate of diffusion across the film that the concentration at the surface of the catalyst solid is reduced several orders

of magnitude relative to the bulk concentration C_b (see Figure 1.14b). Thus surface reaction rate controlling and film mass transfer controlling are the limiting cases for reaction and mass transfer. The reader is cautioned that the situation of strong pore diffusional resistance (slow pore diffusion rate) coupled with rapid surface reaction in the interior of the catalyst is not a limiting but rather an intermediate case, despite some statements in the literature and even in textbooks to the contrary.

It is important in conducting experimental measurements of rate to be able to recognize which resistances (i.e. surface reaction, film mass transfer, pore diffusion, etc.) contribute to the overall rate; moreover, in the collection of specific activity and kinetic data all resistances other than the surface reaction resistance should be minimized. In calculating/modeling reaction rate it is important to include all applicable resistances in the rate expression as in Equation 1.38 (assuming isothermal reaction).

In the case of a first-order reaction we can *experimentally determine if film mass transfer is important* for a first-order reaction by comparing $1/k_c$ with $1/k''$ (Equation 1.38) as illustrated in Example 1.1 below. A more general approach (for any reaction order) is to compare the observed rate with the rate of mass transfer calculated from an appropriate correlation (Davis and Davis, 2003).

The *influence of pore diffusional resistance can be experimentally determined by*: (1) comparing the observed activation energy with that determined or reported under surface reaction controlled conditions; (2) measuring rate as a function of catalyst particle size, recalling that in the case of strong pore diffusional resistance, rate is inversely proportional to L or catalyst particle size (see Figure 1.13); (3) given a value of k, calculating the Thiele modulus $\phi = L(k\rho/D_e)^{0.5}$ and noting that $\phi < 0.4$ implies negligible pore diffusional resistance; and (4) given an experimental value of overall reaction rate, calculating the Weisz (or Weisz-Prater) modulus $r_{obs}(L^2)/(D_e C_{As})$, which for negligible pore diffusional resistance is less than $1/n$ where n is the overall reaction order.

The processes of checking for and including in the rate expression influences of pore diffusion and mass transfer on reaction rate are shown schematically in Figure 1.15 (parts a and b).

(a) Film Heat/Mass Transfer Logic Diagram

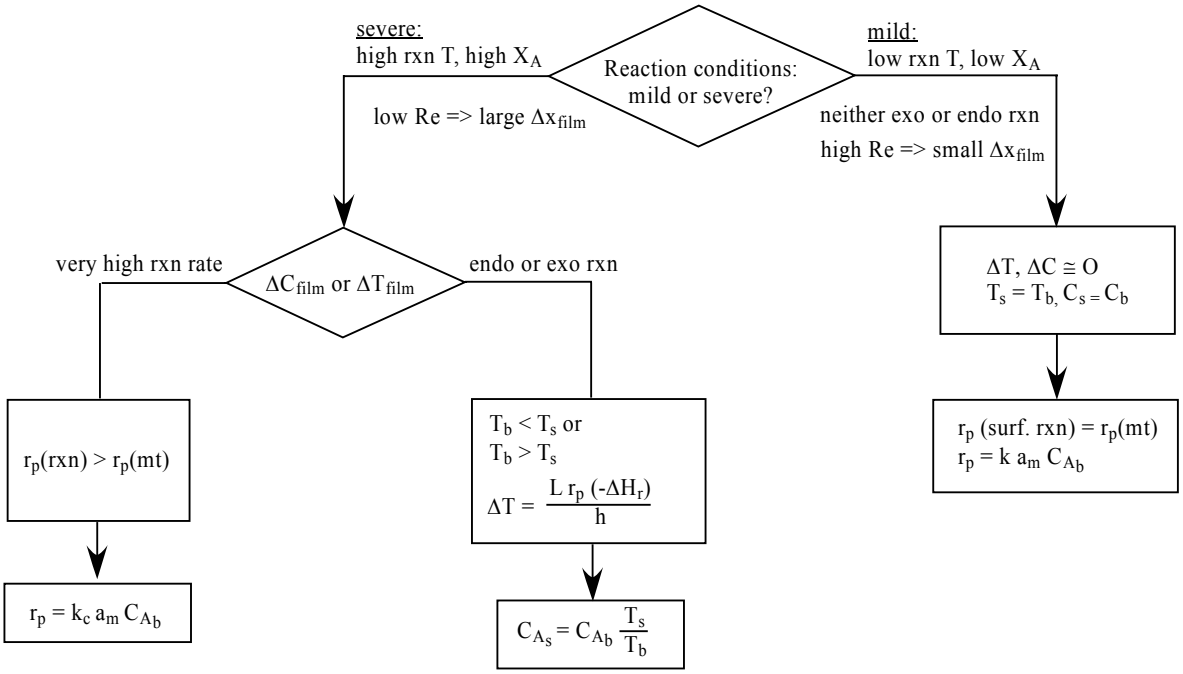

(b) Pore Diffusion Logic Diagram (adapted from Fletcher, 2003)

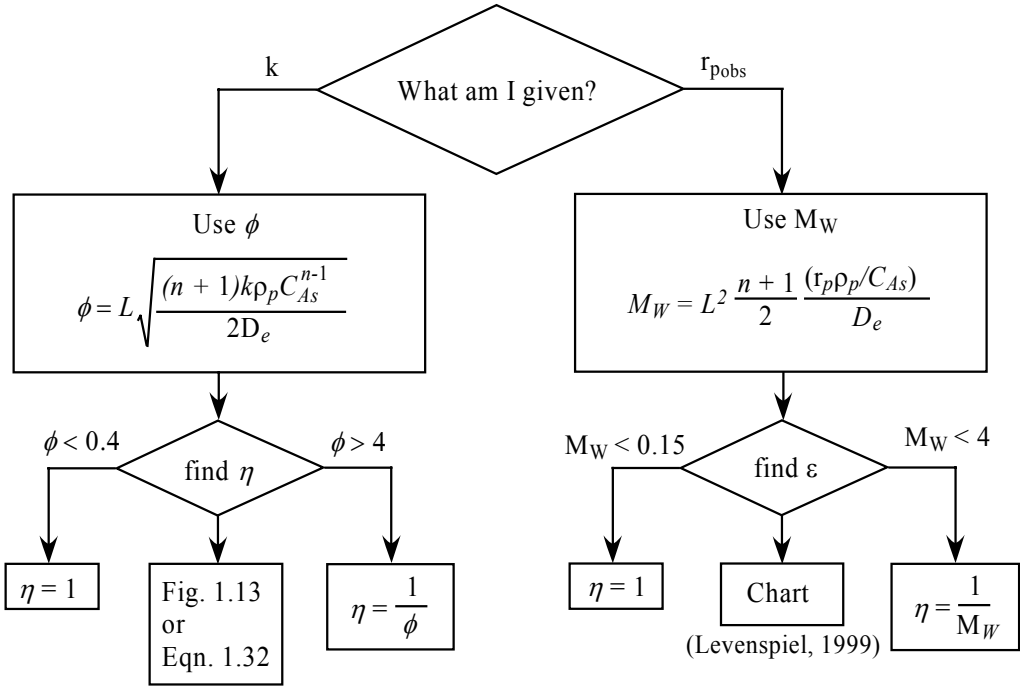

Figure 1.15 Influences of mass transfer on reaction rate (X_A = conversion of A, M_W = Wiesz modulus, Re = Reynolds number, mt = mass transfer, T_b = bulk gas temperature, T_s = surface temperature, h = heat transfer coefficient).

Finally, it should be emphasized that industrial reactions are generally run at relatively high reaction temperatures; hence some are film-mass-transfer controlled, and many are characterized by steep concentration gradients into the catalyst particle or layer, i.e. by a large pore diffusional resistance. In those involving exothermic or endothermic reactions a temperature gradient across the film is common. One of the problems in Chapter 8 treats this issue. This reality has important implications for the design of catalysts and catalyst profiles and is addressed in Chapter 2 dealing with catalyst preparation, materials, and properties.

The above treatment of film mass transfer, pore diffusional resistance, and reaction resistance is a simple introduction to the subject and adequate for guiding the reader through the remaining subjects in this book. The reader, however, should be cautioned that this simplified treatment has several limitations; for example, it is valid only for isothermal film and catalyst pellet. Indeed, the effects of temperature gradients across the film or pellet and of heat transfer on reaction rate are not treated, although heat effects are not difficult to treat since heat and mass transfer are analogous processes for which very similar equations are applicable (note the simple equation for ΔT_{film} in Figure 1.15a). Moreover, calculations of bulk diffusivity D_{AB}, combined diffusivity D (which includes bulk and Knudson diffusivities), and effective diffusivity D_{eff} are not addressed. More detailed treatments of these issues can be found in textbooks by Smith (1981), Levenspiel (1999), Fogler (1999), and Davis and Davis (2003).

Example 1.1: Role of film mass transfer in complete oxidation of benzene.

An off-gas from a chemical process contains 200 ppm benzene in air. State regulations require removal to less than 1 ppm. Given the catalyst properties, process data, and assumptions listed below, estimate by calculation:

(a) the film mass transfer coefficient k_g [defined by $r_p = k_g a_m (P_{A_b} - P_{A_s})$];
(b) the percentage resistance to film mass transfer.

Catalyst properties
Catalyst = 1% Pt/SiO_2
$\rho_p = 1.6$ g/cm^3
$\varepsilon_b = 0.42$
$d_p = 0.35$ cm (assume spherical pellets)

Catalyst has egg shell distribution of Pt and it is assumed $\eta = 1$.

Process conditions
$T = 450$ºC; $P = 1.1$ atm
F_{A_o} (molar flow rate) = 4.2 kmol/min
$d_{reactor}$ (diameter) = 20 cm
Sc = 2.04

$$\text{Re} = \frac{d_p G}{\mu} = \frac{d_p G_m (\text{M})}{\mu}$$

$\mu = \mu_{air}$ (450ºC) = 3.45×10^{-4} g/cm-s
M = molecular weight of air

(a) The following mass transfer correlation is reported for packed beds for Re = 10–10,000 (Dwivedi and Upadhyay, 1977).

$$k_g = \frac{0.455}{\varepsilon_b \, \text{Re}^{0.407}} \left[\frac{G_m}{P \, S_c^{2/3}} \right] \tag{1.39}$$

where G_m = molar flux in moles/s-cm^2; P = pressure in atm; ε_b = bulk void fraction.

$$G_m = \frac{4.2 \times 10^3 \ \dfrac{\text{mol}}{\text{min}} \left(\dfrac{1 \text{ min}}{60 \text{ s}} \right)}{\pi \ (10 \text{ cm})^2} = 0.223 \ \frac{\text{mol}}{\text{cm}^2\text{-s}}$$

$$\text{Re} = \frac{d_p G_m (\text{M})}{\mu} = \frac{(0.35 \text{ cm}) \left(0.223 \ \dfrac{\text{mol}}{\text{cm}^2\text{-s}} \right) \left(29 \ \dfrac{\text{g}}{\text{mol}} \right)}{(3.45 \times 10^{-4} \text{ g/cm-s})} = 6560$$

$$k_g = \frac{0.455}{(0.42)(6560)^{0.407}} \left[\frac{0.223 \ \dfrac{\text{mol}}{\text{cm}^2\text{-s}}}{(1.1 \text{ atm})(2.04)^{2/3}} \right] = \underline{\underline{3.82 \times 10^{-3}}} \ \frac{\text{mol}}{\text{atm-s}}$$

(b) We need to compare $1/k_g$ and $1/k$ (same units). From Bernard and Mitchell (1968) the rate expression is second-order, i.e. $r = k \, K_{O_2} \, K_B \, P_{O_2} \, P_B$ and $E_{act} = 22$ kcal/mol; however, since P_{O_2} is large and approximately constant the rate expression becomes $r = k_1 P_B$, i.e. pseudo first-order, where

$$k_1 = k \, K_{O_2} K_B P_{O_2}, \ k = 5.78 \times 10^{-5} \frac{\text{mol}}{\text{min}}, \ K_{O_2} = 1.43/\text{atm}, \ K_B = 165/\text{atm}$$

at 267°C (540 K) $k_1 = 5.78 \times 10^{-5} \ \dfrac{\text{mol}}{\text{min}} \left(\dfrac{1 \text{ min}}{60 \text{ s}} \right) \left(\dfrac{1.47}{\text{atm}} \right) \left(\dfrac{165}{\text{atm}} \right) (0.21 \text{ atm})(1.1) = 5.40 \times 10^{-5} \ \dfrac{\text{mol}}{\text{atm-s}}$

at 450°C (723 K) using the Arrhenius law, $k = Ae^{-E/RT}$, $k_1(723) = k_1(540) \ \exp\left[\dfrac{-22{,}000}{1.98} \left(\dfrac{1}{723} - \dfrac{1}{540} \right) \right]$

$$= (5.40 \times 10^{-5}) \exp\left[1.11 \times 10^4 \left(\frac{723 - 540}{723(540)} \right) \right]$$

$$= 9.8 \times 10^{-3} \ \frac{\text{mol}}{\text{atm-s}}$$

From Equation 1.38 and assuming $\eta = 1$

$$\% \text{ resistance to film mass transfer} = \frac{10^2\left(\frac{1}{k_g}\right)}{\frac{1}{k_g}+\frac{1}{k_1}}$$

$$= \frac{100\left(\frac{1}{3.82 \times 10^{-3}}\right)}{\left(\frac{1}{3.82 \times 10^{-3}} + \frac{1}{9.8 \times 10^{-3}}\right)} = \frac{100(9.8)}{(3.82 + 9.8)} = \underline{\underline{72\%}}$$

Example 1.2: Pore diffusional resistance for SCR solid monolith catalyst.

Selective catalytic reduction (SCR) of NO_x is an important, effective process for reducing NO_x emissions from electric power plants (see Ch. 11). Wong and Nobe (1984) have reported first-order reaction kinetics, i.e. $r_p = k\, C_{NO}$ for a 5% V_2O_5/TiO_2 catalyst. Nackos *et al.* (2004) have observed a first-order rate constant of 0.566 cm^3/g_{cat}-s at 226ºC (499 K) and an activation energy of 109 kJ/mole for a commercially representative 1% V_2O_5/9% WO_3/TiO_2 catalyst.

Calculate the effectiveness factor and reaction rate at the inlet to a commercial SCR unit containing an extruded cellular monolith consisting of 1% V_2O_5/9% WO_3/TiO_2 with a channel wall thickness of 1.35 mm and open frontal area of 64% under typical commercial operating inlet conditions of 400 ppm NO, 350ºC, and 1 atm. Assume catalyst in the square monolith walls can be treated as a flat plate. Additional data: $\rho_p = 1.48$; $D_e = 0.070$ cm^2/s. Also, assume film mass transfer resistance is negligible.

Equations for calculating effectiveness factor:

$$\eta = \frac{\tanh\ \phi}{\phi} \tag{1.32}$$

$$\phi = \left(\frac{V_{cat}}{S_{ex}}\right)\sqrt{\frac{k\rho_p}{D_e}} \tag{1.40}$$

$$\frac{V_{cat}}{S_{ex}} = \frac{L \times W \times T'}{2(L \times W)} = \frac{T'}{2} \qquad (T' = \text{thickness; factor of 2 accounts for each wall having 2 sides.})$$

(a) Calculation of ϕ and η:

$$k_{623} = k_{499} \exp\left\{\left[\frac{E_{act}}{R}\left(\frac{1}{623}-\frac{1}{499}\right)\right]\right\} = 106\ cm^3/g_{cat}\text{-s}$$

$$\phi = \left(\frac{T'}{2}\right)\sqrt{\left(k_{623}\frac{\rho_p}{D_e}\right)} = \underline{\underline{3.19}}$$

$$\eta = \frac{\tanh \phi}{\phi} = \underline{\underline{0.31}}$$

(b) Calculation of reaction rate:

$$r = k\, C_{NO}\, \eta$$

$$C_{NO} = \left(\frac{P\, y_{NO}}{82.1\, T} \right) = 7.82 \times 10^{-9}\ \text{mol/cm}^3$$

$$r = k\, C_{NO}\, \eta = \underline{\underline{2.58 \times 10^{-7}\ \text{mol/g}_{cat}\text{-s}}}$$

1.3.6 Kinetics of Catalytic Surface Reactions

Introduction. In a previous section (1.3.3) we introduced the seven important steps that occur in a heterogeneous, catalyzed surface reaction: (1 and 2) diffusion of reactants from the bulk gas phase through the fluid film surrounding the catalyst particle and through the pores of the catalyst to the surface, (3) adsorption of reactants on the surface, (4) reaction on the surface, (5) desorption of products from the surface, and (6 and 7) diffusion of products through the pores and gas film to the bulk gas. If now the surface chemical processes are assumed to be rate controlling (and we will assume this for the remainder of this section), the rates of the diffusional processes (Steps 1, 2, 6, and 7) will be high enough that they will not affect the rate of reaction; hence we only need to consider the rates of adsorption, reaction, and desorption processes (Steps 4, 5 and 6) to determine the overall rate. How do we do this? We will demonstrate how three kinetic tools can be used to determine an overall rate expression in terms of measurable quantities: (1) the rate determining step approximation, (2) the concept of a fixed number of active centers for a solid catalyst, and (3) the steady-state approximation.

Unimolecular surface reactions. Consider, for example, a simple unimolecular rearrangement of a gas A to gas B catalyzed by a solid catalyst, e.g. the isomerization of methylcyclopentane to cyclohexane:

$$\text{A(g)} \rightarrow \text{B(g)} \tag{1.41}$$

Is this an elementary step? No, because adsorption of A on the catalyst and desorption of B from the catalyst must occur in order for the surface reaction to take place. Thus the overall reaction consists of three elementary steps in a series, namely, adsorption of A, surface reaction of A to B, and desorption of B. The adsorption process can be represented by a reversible elementary reaction involving the formation of a chemical bond between the reactant species A and a surface site **S** (reaction 1.42). This chemisorbed species transforms reversibly on the surface to adsorbed B; these chemisorbed species are designated A-**S** and B-**S** (reaction 1.43). Desorption involves the reversible breaking of the bond between the product species B and a surface site **S** (reaction 1.44).

$$\text{A} + \mathbf{S} \leftrightarrow \text{A} - \mathbf{S} \quad \text{forward and reverse constants } k_1 \text{ and } k_{-1} \tag{1.42}$$

$$\text{A} - \mathbf{S} \leftrightarrow \text{B} - \mathbf{S} \quad \text{forward and reverse constants } k_2 \text{ and } k_{-2} \tag{1.43}$$

$$\text{B} - \mathbf{S} \leftrightarrow \text{B} + \mathbf{S} \quad \text{forward and reverse constants } k_3 \text{ and } k_{-3} \tag{1.44}$$

Since these steps occur in a series, the slowest or rate determining step (rds) will determine the overall reaction rate. Let's consider the overall form of the rate expression if the rds is (a) the surface reaction, (b) adsorption of A, and (c) desorption of B; we will also consider the general case for which all three steps are co-rate determining.

Reaction controls—For this case, reaction 1.43 is assumed to be the rate determining step (rds) and irreversible (at low conversions); hence, it is the slowest step and its rate controls the overall rate of reaction. Accordingly, the overall rate is equal to the rate of reaction 1.43, and assuming it is an elementary step, the rate of reaction is proportional to the surface coverage of A, i.e. it is first-order in the fractional coverage of A (θ_A).

$$r = r_2 = k_2\ \theta_A \tag{1.45}$$

This rate expression, however, is expressed in terms of θ_A which is not directly measurable. Accordingly, we need to find an expression which relates θ_A to measurables.

Since reactions 1.42 and 1.44 are relatively much faster than reaction 1.43, they are close to equilibrium, i.e. in near equilibrium or 'quasi-equilibrium' (note that they cannot be in true equilibrium; otherwise, the overall reaction rate would be zero; rather, the forward rate is slightly larger than the reverse rate). The kinetic definition of equilibrium states that the forward rate of reaction is equal to that for the reverse step; thus forward and reverse rates are essentially equal for both reactions 1.42 and 1.44. Thus for reaction 1.42, $k_1P_A[1-\theta_A]= k_{-1}\theta_A$ (assuming θ_B is small, generally a good assumption for low reaction rates and low conversions of A). Couching in terms of the fraction surface coverage of A or θ_A and remembering that $K_1 = k_1/k_{-1}$

$$\theta_A = \frac{K_1P_A}{1+K_1P_A} \tag{1.46}$$

Note this expression is identical to the equilibrium isotherm for adsorption of A (Equation 1.15). Substituting for θ_A from Equation 1.46 into Equation 1.45 yields the following rate expression

$$r = \frac{k_2K_1P_A}{1+K_1P_A} \tag{1.47}$$

which is a shifting-order rate equation; that is, at low P_A and/or K_1 values, the K_1P_A term in the denominator is small relative to 1 and the rate expression simplifies to $r = k_2K_1P_A$, which is first-order in A. However, at high P_A or K_1 values, the K_1P_A term in the denominator is large relative to 1 and the rate expression simplifies to $r = k_2$, which is zero-order in A. The shift in reaction order with increasing P_A is illustrated in Figure 1.16.

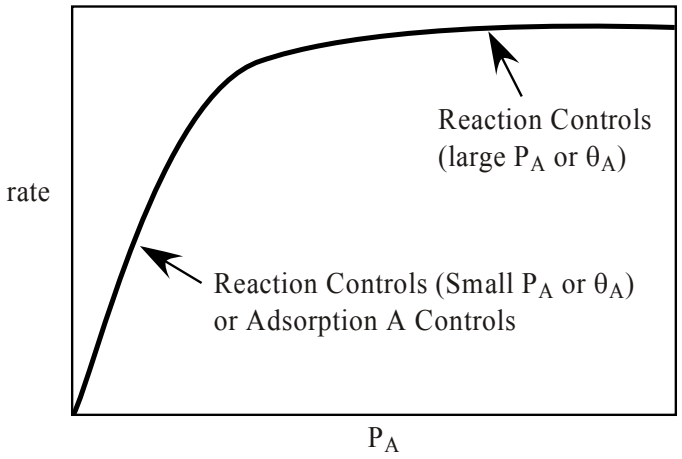

Figure 1.16 Reaction rate versus partial pressure of the reactant for a unimolecular catalyzed surface reaction.

Adsorption of A controls—If adsorption or reaction 1.42 is the rds, it will be slow and essentially irreversible (at low conversions) while reactions 1.43 and 1.44 will be relatively fast and in quasi-equilibrium. Thus

$$r = r_1 = k_1 P_A \theta_V \tag{1.48}$$

where the rate is proportional to θ_V, the coverage of vacant sites, which is not directly measurable; hence, an equation relating θ_V to measurables must be found.

To this end, we invoke the principle of constant number of active centers for a solid catalyst. An active center is an active site on the catalyst; it may be empty or occupied by adsorbed species. Hence, for the unimolecular reaction A $\rightarrow$ B taking place on a solid catalyst surface, this principle requires that the total concentration of surface sites L is the sum of the unoccupied sites and those occupied by chemisorbed A or B species, i.e. L = [**S**] + [A–**S**] + [B–**S**]. This expression can be normalized by dividing each term by L to obtain the expression

$$\theta_V + \theta_A + \theta_B = 1 \tag{1.49}$$

in which θ_V, θ_A, and θ_B are the fractional coverages of vacant sites, A, and B, respectively. From the equilibrium expressions for reactions 1.43 and 1.44, we obtain $\theta_A = \theta_B/K_2$ and $\theta_B = P_B\theta_V/K_3$. Substituting these expressions into Equation 1.49 to eliminate θ_A and θ_B and solving for θ_V we obtain the expression

$$\theta_V = \frac{1}{1+\left[\left(1+K_2\right)P_B/\left(K_2K_3\right)\right]} \tag{1.50}$$

Substituting for θ_V from Equation 1.50 into 1.48 yields a form of the rate expression, which contains either constants or measurable concentrations:

$$r = \frac{k_1 P_A}{1+\left[\left(1+K_2\right)P_B/\left(K_2K_3\right)\right]} = \frac{k_1 P_A}{1+K' P_B} \tag{1.51}$$

This rate expression is shifting-order as in the previous case of surface reaction controlling; at low conversions of A and hence low values of P_B, it simplifies to $r = k_1P_A$ which is first-order in A. At large values of K' or P_B, it becomes $r = k_1P_A/(K' P_B)$ which is first-order in A and inverse first-order in B; in other words, the rate is inhibited by B.

However, it should be pointed out that at high P_A, moderate to high conversion and hence moderate to large P_B, adsorption of A is fast and coverages of A and B are high; adsorption under these conditions closely approaches equilibrium, and hence it is unlikely that adsorption will be rate controlling at high P_A.

Desorption of B controls—If desorption of B is the rds, the overall rate of reaction is determined by the rate of the third step (reaction 1.44), and the rate expression (assuming again the rate determining step is irreversible) is

$$r = r_3 = k_3\theta_B \tag{1.52}$$

Proceeding as in the previous case, equilibrium expressions from the first and second steps are substituted into Equation 1.49 (the expression for the sum of the fraction coverages) to eliminate θ_V and θ_A; then solving in terms of θ_B we obtain the expression

$$\theta_B = \frac{K_1K_2P_A}{1+\left(K_1+k_1K_2\right)P_A} \tag{1.53}$$

Then, substituting for θ_B in Equation 1.52, we obtain the rate expression in terms of constants and measurable concentrations:

$$r = \frac{k_3 K_1 K_2 P_A}{1 + (K_1 + K_1 K_2) P_A} \tag{1.54}$$

This rate equation is essentially of the same form as Equation 1.47, obtained for the case of reaction controlling; thus, it is first-order in P_A at low values of P_A and zero-order at high P_A.

Chemical processes are co-rate determining/steady-state approximation. In the previous three subsections, we used the rate-determining step approximation to determine a rate expression for the cases of adsorption, reaction, or desorption being rate controlling. This approach greatly simplifies the derivation of a rate expression from a sequence of elementary steps, since all steps other than the rds can be assumed to be in a quasi-equilibrium—hence equilibrium constants can be used to find concentration relationships for reactants and products.

There are, however, some *pitfalls in using the rds approximation*. Indeed, which of several elementary steps is rate determining depends greatly on reaction conditions; hence, the rds may shift with changes in temperature, reactant concentrations, and conversion. Accordingly, the rds approximation is not a general but rather a specific tool and the resultant rate expression is valid only over a relatively narrow range of conditions.

A generalized rate expression having application over a wide range of conditions can be obtained through the application of the ***steady-state approximation***. The steady-state approximation is *the single most general, useful tool in treating a sequence of elementary steps to obtain a rate expression*. The principle of this approximation can be simply stated as follows: *in a closed, batch or transient system, the derivative of the concentration of an intermediate with respect to time is approximately zero, i.e.*

$$dC_I / dt \cong 0 \tag{1.55}$$

It should be emphasized that in a batch or transient system this is an approximation, although one which is generally very good, since changes in intermediate concentrations are negligible in comparison to changes in concentrations of measurable species with time. Nevertheless, because it is an approximation, Equation 1.55 cannot be integrated to obtain the result C_I = constant.

The practical implications of this approximation are as follows:

- Equation 1.55 can be used to set-up rate equations in terms of the concentrations of intermediates (active centers) and measurable species; by setting the derivatives equal to zero, these equations can be readily solved for the intermediate concentrations in terms of measurable concentrations. These relationships can in turn be substituted into the rate expression to eliminate the concentrations of intermediates.
- For a series sequence of elementary steps proceeding through common intermediates, it can be shown that $r_1 = r_2 = r_4 = ...r_i$. We will now demonstrate how these principles can be applied to derivation of a generalized rate expression for a unimolecular reaction.

Application of the steady-state approximation. From the general definition of reaction rate (Equation 1.5), it follows that the rate of a gaseous, unimolecular reaction A → B is simply

$$r = (-1)\, dP_A/dt = dP_B/dt \tag{1.56}$$

since the stoichiometric coefficients for A and B are –1 and +1, respectively. From the general sequence of elementary steps (reactions 1.42 to 1.44), we can write down the terms in the rate equation by inspection for production and disappearance of species A in equations 1.42 and 1.43 (recalling that for an elementary step the rate is simply proportional to the reactant concentration raised to their molecularity (molecularity = $|\nu_i|$)):

$$r = -dP_A / dt = k_1 P_A\, \theta_V - k_{-1} \theta_A \tag{1.57}$$

Applying the steady-state approximation to the production (and disappearance) of vacant sites to the same sequence we find that

$$\mathrm{d}\theta_V / \mathrm{d}t = -k_1 P_A \theta_V + k_{-1}\theta_A + k_3\theta_B - k_{-3} P_B \theta_V \cong 0 \tag{1.58}$$

We can write similar equations for the changes in coverage of A and B with time; these equations could be combined with Equation 1.58 and solved simultaneously to find expressions for the coverages of A and vacant sites in terms of measurables. However, the mathematical expressions are tedious and there is a better way.

From the steady-state approximation we also know that $r = r_1 = r_2 = r_3$, for which

$$r_1 = k_1 P_A \theta_V - k_{-1}\theta_A$$

$$r_2 = k_2\theta_A - k_{-2}\theta_B$$

$$r_3 = k_3\theta_B - k_{-3} P_B \theta_V.$$

This set of three equations with three unknowns can be written in matrix form:

$$\begin{bmatrix} -k_{-1} & 0 & k_1 P_A \\ k_2 & -k_{-2} & 0 \\ 0 & k_3 & -k_{-3} P_B \end{bmatrix} \begin{bmatrix} \theta_A \\ \theta_B \\ \theta_V \end{bmatrix} \tag{1.59}$$

Following the solution of Boudart (1991) for this matrix, it can be shown that the rate is

$$r = \frac{L\Delta}{\sum_{i=1}^{3} M_i} \tag{1.60}$$

where L is the total concentration of active centers that in connection with the use of surface coverages is the sum of the coverages of A, B, and vacant sites, which is unity; $\Delta = k_1 k_2 k_3 P_A - k_{-1} k_{-2} k_{-3} P_B$, and M_i is the determinant of the matrix containing values of L (in connection with coverages containing a column of ones) in the ith column; otherwise the coefficients for surface coverages of A, B, and **S** (vacant sites) appear in the first, second, and third columns, respectively. Thus the matrix M_1 is of the form

$$M_1 = \begin{vmatrix} 1 & 0 & k_1 P_A \\ 1 & -k_{-2} & 0 \\ 1 & k_3 & -k_{-3} P_B \end{vmatrix} \tag{1.61}$$

having the solution $M_1 = k_{-2} k_{-3} P_B + k_1 k_3 P_A + k_1 k_{-2} P_A$. Similar solutions are found for M_2 and M_3 ($M_2 = k_{-1} k_{-3} P_B + k_1 k_2 P_A + k_2 k_{-3} P_B$ and $M_3 = k_{-1} k_{-2} + k_2 k_3 + k_{-1} k_3$). Substituting the values of L, Δ, and M_i into Equation 1.60, the general rate law is

$$r = \frac{k_1 k_2 k_3 P_A - k_{-1} k_{-2} k_{-3} P_B}{\left(k_2 k_3 + k_{-1} k_3 + k_{-1} k_{-2}\right) + \left(k_1 k_2 + k_1 k_3 + k_1 k_{-2}\right) P_A + \left(k_{-1} k_{-3} + k_{-2} k_{-3} + k_2 k_{-3}\right) P_B} \tag{1.62}$$

Equations similar to 1.62, or sequences involving a larger number of steps, can be obtained using this general matrix notation developed by Boudart (1991). In most cases, these general forms can be further simplified by substituting equilibrium constants for ratios of rate constants where possible. For example, if it is assumed that P_B is low (true at low conversion), k_2 is small (the surface reaction is the rds), and k_{-2} is negligible (the surface reaction is essentially irreversible), and dividing by $k_{-1} k_3$ while noting that $K_1 = k_1 / k_{-1}$

and $K_3 = k_3/k_{-3}$, Equation 1.62 can be greatly simplified so that it contains only one rate constant k_2 and one equilibrium constant K_1.

$$r = \frac{k_2 K_1 P_A}{1 + K_1 P_A} \tag{1.63}$$

Note that this is the same rate expression as Equation 1.47 developed for the case of surface reaction controlling.

Bimolecular surface reactions. Since the surface reaction controlling case is generally the most important for industrial reaction conditions, our discussion of bimolecular reactions will be restricted to this case. There are two different mechanisms for bimolecular surface-catalyzed reactions: (1) the Langmuir-Hinshelwood mechanism for the reaction of two adsorbed surface species to products and (2) the Eley-Rideal mechanism for the reaction of a gas phase species with an adsorbed species to products. In both cases, the overall stoichiometric reaction is simply

$$A + B \rightarrow \text{Products} \tag{1.64}$$

Langmuir-Hinshelwood: Reaction of two adsorbed species—In this mechanism it is assumed that the adsorptions of A and B occur in quasi-equilibrium (equations 1.65 and 1.66), while the rds is the irreversible reaction of adsorbed A and B to products, thus:

$$A + \mathbf{S} \leftrightarrow A - \mathbf{S} \text{ (quasi-equilibrium)} \tag{1.65}$$
$$B + \mathbf{S} \leftrightarrow B - \mathbf{S} \text{ (quasi-equilibrium)} \tag{1.66}$$
$$A\text{-}\mathbf{S} + B\text{-}\mathbf{S} \rightarrow \text{products (rds)} \tag{1.67}$$

The rate expression for reaction 1.67 is

$$r = r_3 = k_3 \, \theta_A \, \theta_B \tag{1.68}$$

The expressions for fractional coverages of A and B in terms of partial pressures of A and equilibrium adsorption constants were given earlier (Equation 1.18, Section 1.3.4). It was assumed in their derivation that species A and B compete for adsorption on the same sites and that there is only one kind of site for adsorption and reaction. Substituting these expressions for θ_A and θ_B into Equation 1.68 gives the generalized Langmuir-Hinshelwood rate equation:

$$r = \frac{k_2 K_A K_B P_A P_B}{\left(1 + K_A P_A + K_B P_B\right)^2} \tag{1.69}$$

The reaction rate versus P_A (at constant P_B) is plotted in Figure 1.17. It is evident that the rate passes through a maximum with increasing P_A, a direct mathematical consequence of the squared terms in the denominator. It can be shown mathematically that the maximum occurs at $K_A P_A = K_B P_B$; hence, K_A/K_B can be calculated at the rate maximum. From a physical point of view, the rate decreases (becomes negative-order) at high P_A values because high P_A is a driving force for increasing coverage of A at the expense of other species including B; since the reaction rate is proportional to the product of θ_A and θ_B, rate decreases as θ_B becomes small. In addition, more strongly adsorbed species replace others on the surface, e.g. CO replaces O_2 in CO oxidation on Pt.

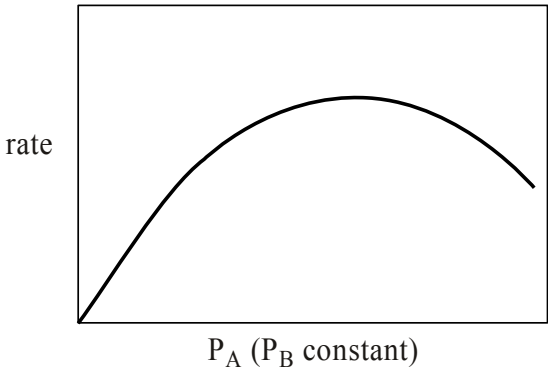

Figure 1.17 Reaction rate versus partial pressure of reactant A (partial pressure of B held constant) for a bimolecular catalyzed surface reaction (Langmuir-Hinshelwood mechanism).

Eley-Rideal: Reaction of an adsorbed species with a gas phase species—In this mechanism it is assumed that adsorption of A occurs in quasi-equilibrium (Equation 1.65), while the rds is the irreversible reaction of adsorbed A and gas phase B to products. Thus:

$$\text{A-}\mathbf{S} + \text{B(g)} \rightarrow \text{products} \tag{1.70}$$

The rate of reaction is

$$r = k\,\theta_A\,P_B \tag{1.71}$$

for which the coverage of A (assuming equilibrium between adsorption and desorption of A) is given by the expression derived earlier for the Langmuir isotherm:

$$\theta_A = \frac{K_A P_A}{1 + K_A P_A} \tag{1.72}$$

Upon substituting Equation 1.72 into 1.71, we obtain the reaction rate in terms of measurables:

$$r = \frac{kK_A P_A P_B}{1 + K_A P_A} \tag{1.73}$$

which is again a shifting-order rate expression, which at constant P_B is first-order in A at low P_A and zero order in A at high P_A or K_A (see Figure 1.18a). If, however, P_A is held constant, the reaction rate reduces to $r = k' P_B$ which predicts first-order in B (see Figure 1.18b).

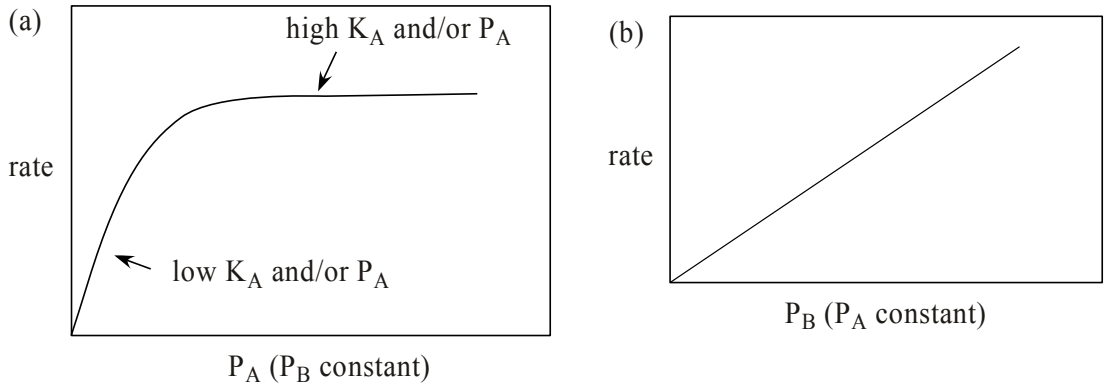

Figure 1.18 (a) Reaction rate versus partial pressure of reactant A (partial pressure of B constant) for reaction of an adsorbed A with gas phase B (Eley-Rideal mechanism); (b) reaction rate versus partial pressure of reactant B (partial pressure of A held constant) for reaction of adsorbed A with gas phase B or Eley-Rideal mechanism.

Thus if experimental rates are available as a function of concentration, and the reaction is suspected to involve either a Langmuir-Hinshelwood (LH) or Eley-Rideal (ER) bimolecular surface reaction, the rate can be plotted as a function of reactant concentration as in Figs. 1.17 and 1.18 to identify qualitatively which mechanism is most consistent with the data.

Example 1.3: Derivation of LH rate equation from a sequence of elementary steps for CO oxidation on a Pt catalyst.

We wish to develop a physically meaningful rate expression for CO oxidation on Pt that might be fitted to available kinetic data and used over a wide range of conditions for purposes of reactor design. For many catalytic reactions, including CO oxidation on Pt, it is known that under typical reaction conditions the reactants adsorb rapidly and in near equilibrium. Accordingly, the sequence of elementary steps introduced earlier for CO oxidation (reactions 1.8 through 1.11) would be applicable, at least at low conversions where only the forward half of the rate-determining step, reaction 1.10, would be important. Thus the rate determining step (rds) is the essentially irreversible reaction of chemisorbed CO molecules and oxygen atoms, and the rate is given by:

$$r = r_3 = k_3 \theta_{CO} \theta_O \tag{1.74}$$

for which k_3 is the rate constant for reaction 1.10. From equations 1.8 and 1.9, involving the near equilibrium adsorption of CO and O_2, we can express the fractional coverages of CO and O covered sites as:

$$\theta_{CO} = K_1 P_{CO} \theta_V \tag{1.75}$$

$$\theta_O = K_2^{1/2} P_{O_2}^{1/2} \theta_V \tag{1.76}$$

Recalling that the sum of the fractional coverages of filled and vacant sites is unity (Equation 1.49), we can substitute from equations 1.75 and 1.76 into 1.49 to obtain an expression for the fractional coverage of vacant sites:

$$\theta_V = \frac{1}{1 + K_1 P_{CO} + K_2^{1/2} P_{O_2}^{1/2}} \tag{1.77}$$

Now substituting from equations 1.75, 1.76, and 1.77 into 1.74 to eliminate fraction coverages, we obtain a rate expression in terms of measurable quantities and constants,

$$r = \frac{k_3 K_1 K_2^{1/2} P_{CO} P_{O_2}^{1/2}}{\left[1 + K_1 P_{CO} + K_2^{1/2} P_{O_2}^{1/2}\right]^2} \tag{1.78}$$

and which can be tested against experimental rate data as will be illustrated in Chapter 4. This rate expression (Equation 1.78) is, in fact, consistent with experimental evidence for CO oxidation. It predicts orders for CO and O_2 ranging from 1 to –1 and 1/2 to –1/2. Indeed, positive, zero, and negative orders are observed for CO.

Microkinetics, the most general approach for kinetics of surface reactions. A fully general approach to analyzing the kinetics of surface reactions has been developed relatively recently for surface reactions. This approach, based on the kinetics of elementary steps, has been practiced for almost three decades by workers in combustion to describe gas phase kinetics. Its more recent application to surface reactions was

pioneered by Dumesic and Rudd (Dumesic *et al*., 1993); it is founded on principles of the kinetics of elementary reactions set forth in the 1960s by Boudart (1991).

Microkinetics analysis is the quantitative examination of the kinetics of a catalytic reaction in terms of the kinetics of the elementary chemical reactions that occur on the catalytic surface and their relationship to each other and to the catalytic surface. It begins with the formulation of elementary steps to describe the progress of a chemical reaction. In the analysis of a sequence of elementary steps, no assumptions are made as to which step may be the rds or which species is most abundant on the surface. The kinetics may be analyzed using the steady-state approximation to obtain an overall rate expression as illustrated for a unimolecular reaction earlier in this section, although the analysis is not limited to steady-state. In the application of microkinetics, available fundamental data such as rate constants and activation energies are gathered from experimental data or estimated using sound empirical or theoretical correlations and then used to estimate the overall reaction rate as a function of concentrations and temperature. Thus application of microkinetics to a unimolecular reaction would involve finding values of the rate constants and activation energies for adsorption, surface reaction, and desorption, solving these in matrix form similar to Equation 1.61, and then using this expression to calculate rates as a function of the concentrations of species A and B and of temperature for the region of conditions in which heat and mass transport effects are not important. However, the more general application would also involve adding the equations for pore diffusion and film mass transport (see Section 1.3.5). These equations and the rate equation could then be solved numerically to obtain overall rate as a function of concentration and temperature over a wide range of conditions.

The application of microkinetics to the analysis of a number of different catalytic reactions, including ethane hydrogenolysis and ammonia synthesis on metal catalysts, methane oxidation on oxides, and selective catalytic reduction of NO on zeolites, is described in a book by Dumesic *et al*. (1993) and in a later review (Cortright and Dumesic, 2001). The microkinetics approach is an important advance that takes us well beyond the classical Langmuir-Hinshelwood kinetics; it is the kinetic paradigm of the future. In addition to the formulation of general rate models for reactor design, it provides a scientific basis for catalyst design, a topic addressed in Chapter 2.

1.3.7 Effects of Surface Structure and Support on Catalytic Activity

Introduction. For decades, scientists working in the field of catalysis have attempted to correlate the activity and selectivity of catalysts with their chemical and physical properties in the ultimate hope of being able to predict catalytic activity. Taylor and other early scientists introduced the notion of electronic and geometric factors, the former constituting a kinetic factor (e.g. activity or selectivity) influenced by the electronic properties of the solid surface (e.g. the number of d electrons) and the latter referring to a kinetic factor influenced by the geometric structure of the solid surface (e.g. number of corner, edge, or planar sites). Early attempted correlations included activity versus number of d electrons and activity versus heats of adsorption of a reactant.

In early critical reviews (Boudart, 1961; Derouane, 1971), correlations in heterogeneous catalysis were reviewed and classified with an emphasis on Type I correlations, involving the relationship of a kinetic parameter with a property of the solid catalyst or active center on the catalyst. In the same decade in which these reviews appeared, Boudart (1969) advanced the concept of structure sensitive reactions, namely, that catalytic activity of some reactions may depend upon crystallite size or morphology; this concept has since stimulated many studies of activity versus metal particle size or metal surface structure and the discovery of a number of structure sensitive reactions.

That catalyst supports or carriers may affect catalytic activity began to be recognized about a decade later. Before this discovery, catalyst supports had been considered to have little effect on the properties of supported metals, metal oxides, or sulfides. However, a significant number of studies since about 1980 have established that interactions of support with the active catalytic phase can greatly influence the activity and selectivity of the catalyst (Stevenson, 1987).

Beginning in the 1970s and 1980s, the development of sophisticated characterization methods (selective chemisorption, XRD, TEM, FTIR, Mössbauer, TPD, XPS, and other electron spectroscopies) has enabled catalytic scientists to determine important physical and chemical properties of supported metals including metal surface area, crystallite size, crystallite size distribution, surface structure, surface composition, and the nature of the support/metal interface. Efforts have been made to correlate catalyst activity with the geometric and electronic properties of the catalysts, including metal dispersion, metal crystallite size, the electronic d-band structure, electron density at the nucleus, and extent of reduction of the metal.

This section focuses on the definition of catalytic activity and structural factors, which influence catalytic activity. Influences of surface structure, crystallite size, and support on the activity/selectivity properties of supported metal crystallites in several important reactions are considered and discussed.

Definition of specific catalytic activity. Catalytic activity is an important measure of catalyst performance and is most generally defined as the rate of a specified catalytic reaction under specified conditions in the presence of a specified catalyst. Specific catalytic activity is the same as specific rate (see Equation 1.5 in Section 1.3.1), i.e. $r = (1/\nu_i Q)\, dn_i/dt$ where Q = mass, volume, or surface area. For a supported metal, metal oxide, or metal sulfide, the most meaningful form of activity, which enables valid comparison for different catalysts of the same type, is that based on metal, metal oxide, or metal sulfide surface area, i.e. the surface area of the active phase. Although activities or specific rates are often reported in the literature on a mass or volume basis, this is not nearly as meaningful because:

1. The extensive rate rQ is proportional to the number of catalytic sites which is in turn proportional to the active catalytic surface area S. Thus in principle, $r = (1/\nu_i S)\, dn_i/dt$ should be a constant for a given catalyst type, for a given reaction and set of reaction conditions. For example, all nickel catalysts (regardless of preparation, support, metal loading, and nickel surface area) should in principle have and indeed are observed to have the same specific activity for methanation of CO at 225°C, 1 atm, 10% conversion, and H_2:CO = 3:1.
2. Active catalytic surface area for a given catalyst type may vary over an order of magnitude, e.g. Ni surface areas of commercial Ni/Al_2O_3 catalysts range from 5 to 50 m^2/g catalyst. Hence, rates based on the mass of catalyst could vary by as much as a factor of 10 for the same nickel catalyst type, reaction, and reaction conditions. Thus comparison of rates on a per mass basis, while having utility in industrial applications, is invalid in the fundamental, scientific setting.

Turnover frequency. The turnover frequency (TOF) is a specific reaction rate based on number of active sites. It is the most fundamental definition of reaction rate, since it is the frequency at which molecules react on an active site. Turnover frequencies must be defined at specified conditions of temperature, concentration of reactants, and conversion. To be valid, TOFs must be measured in the absence of heat and mass transport limitations and pore diffusional restrictions (generally low reaction temperature and low conversion). They must be measured in the absence of deactivation effects, e.g. poisoning, coking, and sintering. Guidelines for measurement and comparison of specific activities are discussed in Chapter 4.

Turnover frequencies have units of molecules/site-second or s^{-1}. Values of TOF for commercial catalysts are typically in the range of about 10^{-3} to 10 s^{-1}, while TOF values for enzymes are in the range of 10^2 to 10^4 s^{-1}.

In principle, the TOF is a constant for a given metal, metal oxide, or metal sulfide in a given reaction at specified reaction conditions. For example, the TOF for CO methanation on unsupported Ni, 10–20% Ni/SiO_2, and 10–20% Ni/Al_2O_3 catalysts is about 4×10^{-3} at 525°C, H_2:CO = 3, P_{CO} = 1 kPa, and a conversion of 1–10% (Bartholomew *et al*., 1982). In practice, however, TOF may differ significantly (factors of 2–1,000) among catalysts of the same type because of (1) differences in surface structure in a structure sensitive reaction, (2) varying degrees of metal-support or metal-promoter effects and (3) differences in surface composition in a series of bimetallic or multimetallic catalysts. Differences in surface structure, surface composition, and metal-support or metal-promoter interaction from one catalyst to another may

depend upon the catalyst preparation, thermal pretreatment history, reducing or oxidizing atmosphere, and crystallite size.

Effects of surface structure on specific activity. According to Boudart (1984), catalytic reactions are of two types: (1) structure sensitive or demanding reactions and (2) structure insensitive or facile reactions. In structure sensitive reactions specific activity or TOF depends on surface structure, i.e. is a function of the geometric distribution of sites of different coordination or ensembles (collections of sites). In other words, structure sensitive reactions require special sites. The distribution of these special sites may vary with metal loading, crystallite size, dispersion (fraction exposed), and/or preparation method.

The variation in atomic coordination number C_i (i = number of nearest neighbors) for different atoms at the surface of a metal crystallite is illustrated in Figure 1.19, a ball model of a close-packed imperfect surface. Several different kinds of atomic coordination are evident: planar (P) or face sites having coordination number 9 (C_9; note that hcp bulk atoms have C_{12} coordination—6 in the same plane, 3 above, and 3 below); edge (E) atoms having C_7 coordination; corner (C) sites having C_6 coordination; edge adatoms (A_E) with C_5 coordination; and terrace adatoms (A_T) having C_3 coordination. It is logically anticipated that surface atoms of lower coordination (i.e. having a greater fraction of their bonding capacity unsatisfied) would adsorb atoms more strongly than surface atoms of higher coordination. Thus one might expect terrace and edge adatoms, corner atoms, and edge atoms to be the most active sites at least initially, and by the same token, possibly the ones to be poisoned most rapidly by feed impurities or coke. If the fraction of low coordination sites at a crystallite surface is a function of crystallite diameter, a variation in activity with metal dispersion is predicted. Indeed, the fraction of corner and edge atoms of low coordination is predicted to be large for crystallites of diameter smaller than about 10–20 nm and is likewise predicted to decrease with increasing crystallite diameter (see Figure 1.20). Moreover, changes in activity with dispersion (in some cases increases and in some cases decreases) are observed for a number of catalytic reactions. These observations are generally thought to provide evidence of structure sensitivity.

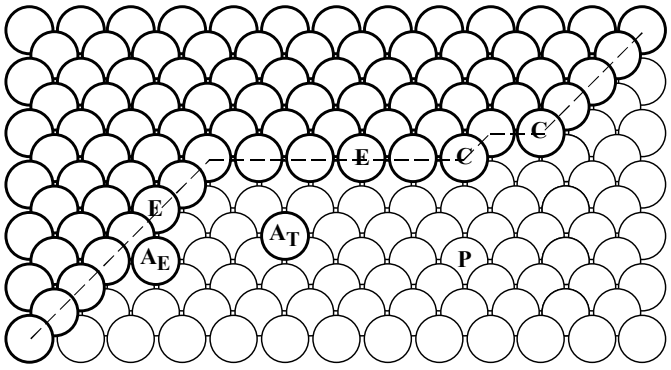

Figure 1.19 Model of close-packed imperfect surface; atoms of differing coordination are designated as planar (P), edge (E), corner (C), edge adatom (A_E), and terrace adatom (A_T).

There are two kinds of structure sensitivity: (1) primary structure sensitivity due to geometric effects and (2) secondary or 'apparent' structure sensitivity due to preferential poisoning of sites of a given geometry or coordination, e.g. due to preferential poisoning of edge or corner sites. It is not easy to experimentally discriminate between these two. Moreover, an observation of increasing activity with increasing crystallite diameter may in some cases be the result of metal-support effects, which may be more important for small crystallites. Accordingly, the observation of changes in activity with changes in dispersion does not constitute proof of primary or secondary structure sensitivity; it does, however, suggest that possibility.

According to Boudart (1984), there are several distinguishing features of a structure sensitive reaction: (1) it typically occurs on large, multiple-atom sites, (2) it typically involves activation of C-C and N-N bonds, and (3) effects of alloying and poisoning on reaction rate are large. Thus hydrogenolysis reactions

involving the rupture of C-C bonds and ammonia synthesis involving the rupture of N-N bonds might be expected to be structure sensitive.

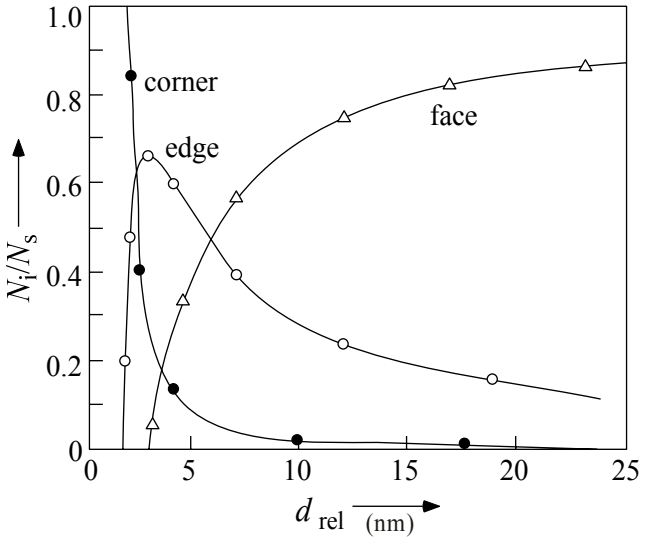

Figure 1.20 Distribution of corner, edge, and planar atoms for a crystallite of octahedron geometry (adapted from van Hardefeld and Hartog, 1969; courtesy of Elsevier).

Reactions that on the basis of reasonably solid experimental evidence are thought to be structure insensitive are listed in Table 1.6, while reactions thought to be structure-sensitive are listed in Table 1.7. A number of hydrogenation reactions listed in Table 1.6, e.g. hydrogenation of ethylene, benzene, cyclopentane, cyclohexane, and CO, have been shown to have the same TOF on both supported metals and single crystal surfaces. The hydrogenation of CO has been shown to be structure-insensitive on Co, Fe, Ni, Rh, and Ru catalysts. As expected on the basis of their chemistries, structure sensitive reactions (Table 1.7) include neopentane isomerization, ammonia synthesis, and ethane hydrogenolysis. On the other hand, the observation that hexane hydrogenolysis is structure-insensitive on Pt catalysts (Table 1.6) is somewhat contrary to expectation and emphasizes the difficulty in predicting such behavior.

The structure sensitivity of ethane hydrogenolysis on Pt and Ni catalysts has been well-documented (Goodman, 1982; Goodman, 1992; Ribeiro, 1997). Hence, it serves as a good example for probing the causes of structure-sensitivity. Data from Goodman (1982) show that methane formation rate is significantly higher at any temperature on the Ni(100) surface relative to the Ni(111) (see Figure 1.21). Upon examining the arrangement of atoms on the two surfaces, it is evident that the distance between four-fold sites on the Ni(100) surface is larger than that between three-fold sites of the Ni(111) surface; moreover, this distance between the fourfold sites in Ni(100) is possibly ideal for cleaving the C-C bond of ethane.

Table 1.6 Reactions that have been shown to be Structure-Insensitive

Metal	Reaction	Large Single Crystals	Supported Metallic Clusters
Pt	*n*-C_3H_6 hydrogenation	Kahn *et al*. (1974)	Boudart *et al*. (1966) Wong *et al*. (1980)
Ni	C_2H_4 hydrogenation C_6H_6 hydrogenation	Dalmai-Imelik and Massardier (1977)	Dalmai-Imelik and Massardier (1977)
Co, Fe Ni, Ru Rh	CO hydrogenation	Goodman *et al*. (1980); Somorjai *et al*. (1980); Johnson *et al*. (1991)	Vannice (1976); Rameswaren and Bartholomew (1989); Johnson *et al.* (1991)
Pt	*n* - C_6H_{10} hydrogenation	Davis and Somorjai (1980)	Segal *et al*. (1978)
Pd	CO oxidation	Engel and Ertl (1979); Xu *et al.* (1994)	Ladas *et al*. (1981)
Pt	*n* - C_6H_{14} hydrogenolysis	—	Ribeiro *et al*. (1997)

Table 1.7 Reactions that have been shown to be Structure-Sensitive

Metal	Reaction	Reference
Pt	neopentane isomerization	Boudart and Ptak (1970)
Fe	NH_3 synthesis	Boudart *et al*. (1975); Ertl (1981); Spencer *et al*. (1982)
Pt, Ni	ethane hydrogenolysis	Sinfelt *et al*. (1972); Goodman (1982); Ribeiro *et al*. (1997)
Pt	H_2 oxidation	Hanson and Boudart (1978)
Pd, Rh	CO + NO	Rainer *et al.* (1997); Oh and Eickel (1991)

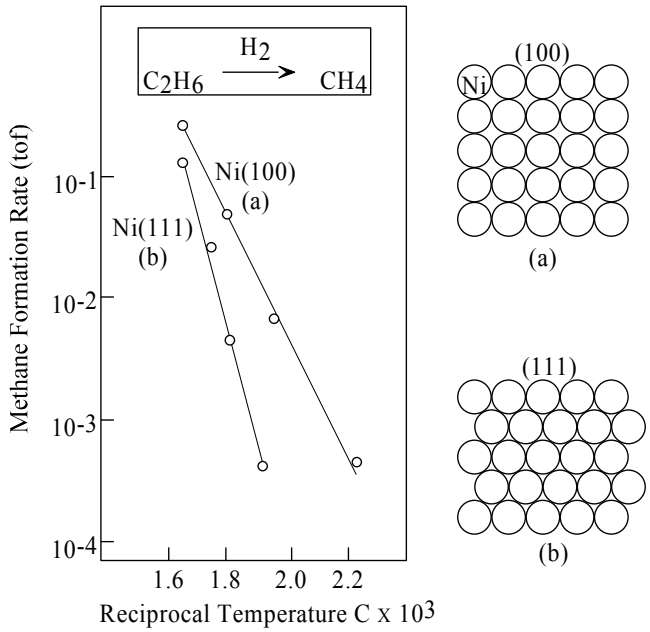

Figure 1.21 Rates in the form of turnover frequency (TOF) of methane formation during ethane hydrogenolysis on nickel single crystals (adapted from Goodman, 1982; courtesy of Elsevier).

Effects of support on catalytic activity and selectivity. Several different kinds of catalytic phase-support interactions can affect specific catalytic activity. We define here a support effect as an interaction of the support or carrier with the active catalytic phase, which causes a measurable change in TOF. According to Boudart (1984), metal-support interactions can be classified into at least six different types: (1) strong interaction of unreduced metal oxide with an oxide support leading to incomplete reduction of the metal, e.g. strong interaction of base metal oxides with alumina, silica, or zeolite supports; (2) support-induced size and morphology, e.g. pore-limited crystallite diameter, epitaxial growth of metal layers on carbon and silica, and two-dimensional raft-like structures of metals; (3) contamination of the metal by support material either during preparation or during reduction of the catalyst; (4) bifunctional catalysis, i.e. reactions on both metal and support; (5) spillover of species from the metal to the support and vice-versa; and (6) a change in the electronic properties of small crystallites ($d_{\text{crystallite}} < 2$ nm) due to intimate contact with the support, sometimes called the Schwab Effect of the second kind.

These different classes of metal-support interactions and examples of each are summarized in Table 1.8. It should be emphasized that the examples are clearly not exhaustive, that is, there are a number of documented examples of each different type of support effect (Boudart and Djega-Mariadassou, 1984; Stevenson *et al*., 1987). It should also be mentioned that Effect No. 3, contamination or 'decoration' of the metal by support material, is sometimes erroneously referred to as a 'strong metal-support interaction' or SMSI. This is largely a misnomer, since strengths of interactions between support and metal are probably most typically on the order of Van der Waals interactions. Interactions of metal oxides with oxide supports,

on the other hand, can be very strong and typically involve strong chemical bonds; for example, in the preparation of a Ni/Al_2O_3 catalyst NiO can interact chemically with γ-Al_2O_3 during calcination at 300–400ºC to form a stable $NiAl_2O_4$ surface spinel (at higher calcination temperatures a bulk spinel is formed). Although typically weak, metal-support interactions can nevertheless have a marked effect on the properties of the metal atoms in the vicinity of the metal-support interface, e.g. increases in the adsorption strength of H_2 on Ni due to decoration by reduced TiO_x species and changes in the electronic properties of metal clusters inside the pores of zeolites due to a partial electron transfer.

Table 1.8 Classes and Examples of Metal-Support Effects

Metal-support effect	Metal	Support	Reaction/phenomenon	Effects on activity/ selectivity	Reference
Unreduced metal, i.e. strong metal oxide-support interaction	Co, Fe, Ni Fe Co, Ni, Fe	Al_2O_3, MgO, zeolites	CO hydrogenation/ extent of reduction (EOR)	activity increase with increasing EOR[a] independent of metal loading; reduction to the metal is extremely difficult	Rameswaren and Bartholomew (1989); Johnson *et al.* (1989); Boudart and Djega-Mariadassou (1984)
Support-induced morphology and size	Co, Fe	Al_2O_3, C zeolites	CO hydrogenation/ preparation of 1–2 nm	decreases in CO hydrogenation activity	Fujimoto and Boudart (1979); Bartholomew *et al.* (1993); Stevenson *et al.* (1987); Goodman (2003)
	Pt, Fe, Ni	TiO_2	Co, Fe clusters, metal films, rafts		
	Au	TiO_2	2D clusters (2 nm)	enhanced CO oxidation activity	
Contamination or decoration of metal with support	Co, Ni, Pd Pt, Rh	TiO_2, Al_2O_3	H_2, CO adsorptions CO hydrogenation ethane hydrogenolysis	adsorption is suppressed; activated adsorption; CO hydrogenation activity is increased; ethane hydrogenolysis activity is decreased	Stevenson *et al.* (1987); Bartholomew (1990)
Bifunctional catalysis	Pt Co, Ni, Pt	Al_2O_3 Al_2O_3	naphtha reforming, CO hydrogenation	reaction on metal and support; e.g. isomerization on acid sites of Al_2O_3, dehydrogenation on Pt metal sites	Boudart and Djega-Mariadassou (1984); Sen and Falconer (1989); Lee and Bartholomew (1989)
Spillover	Pt, Pd	Al_2O_3 Carbon	ethylene hydrogenation pentane dehydrogenation	in EH[b] H_2 is activated on metal and moves to support; in PD[c] hydrogen atoms diffuse to the metal surface	Boudart and Djega-Mariadassou (1984); Carter *et al.* (1965); Fujimoto and Toyoshi (1981)
Electron transfer (Schwab II effect)	Pt Co, Fe	Y-zeolite Al_2O_3, C	hydrogenation and isomerization/electron-deficient clusters due to interaction with support;	large increase in activity for isomerization and hydrogenation; decrease in activity for CO hydrogenation;	Boudart and Djega-Mariadassou (1984); Bartholomew *et al.* (1993)
	Au	TiO_2	increased surface potential of Au cluster adlayer due to charge polarization at Au/TiO_2 interface	increased CO oxidation activity	Goodman (2003)

[a] Extent of reduction
[b] Ethylene hydrogenation
[c] Pentane dehydrogenation

The examples in Table 1.8 cover a wide range of different chemical and physical phenomena; the nature of these phenomena can be illustrated more vividly by considering five of these examples in more depth, namely: (1) effect of extent of reduction on CO hydrogenation activity of Co/Al_2O_3, (2) decoration of nickel crystallites by support materials and its effects on CO hydrogenation activity and selectivity, (3) bifunctional catalysis during naphtha reforming, (4) enhanced isomerization activity of electron-deficient Pt in Ca-Y-zeolite, and (5) enhanced CO oxidation activity of Au/TiO_2 due to cluster size- and support-induced changes in geometry and electronic structure.

Effects of extent of reduction—In an investigation of CO hydrogenation on Co/Al_2O_3 catalysts prepared by decomposition of cobalt carbonyls on γ-Al_2O_3 dehydroxylated at 923–1223 K, Johnson *et al*. (1991) found that the specific activity in the form of CO turnover frequency (N_{CO}) is independent of percentage dispersion from about 10–40% for catalysts having high extents of reduction to cobalt metal. Catalysts having lower extents of reduction were found to have 5–10 times lower activity; in fact, a good correlation of increasing TOF with increasing percentage reduction was found (see Figure 1.22).

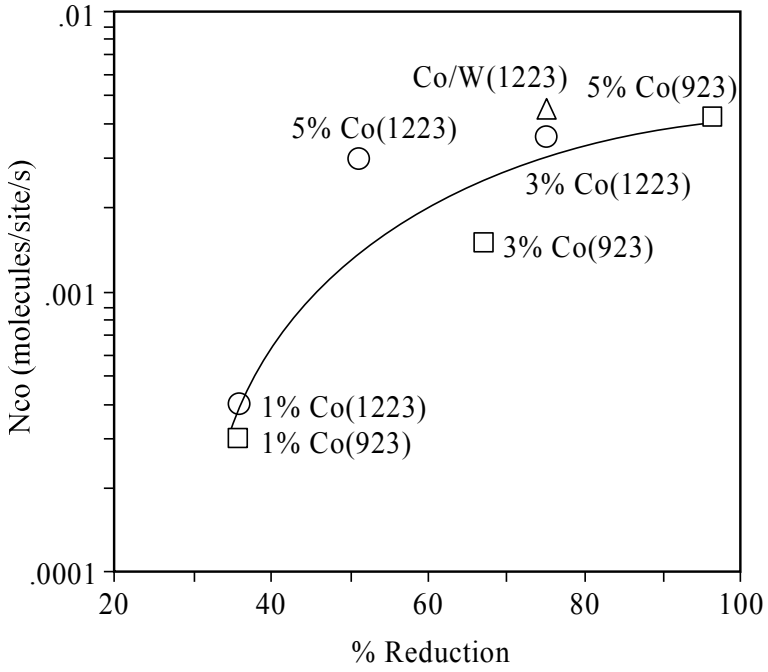

Figure 1.22 Carbon monoxide turnover frequency for CO hydrogenation on Co/Al_2O_3 catalysts at 485 K, 1 atm, $H_2/CO = 2$; catalysts were prepared by decomposition of cobalt carbonyl on the support dehydroxylated at the temperature shown in parenthesis (Johnson *et al.*, 1991; courtesy of Academic Press).

Effects of decoration of the metal surface by the support—Bartholomew *et al*. (1982) investigated the effects of preparation and support on specific activity of nickel for CO hydrogenation. Their data (Figure 1.23) indicate that silica has little effect on either activity or selectivity; alumina and titania, however, appear to increase CO conversion activity and selectivity for C_{2+} hydrocarbons, especially in those catalysts prepared by a controlled-pH precipitation. In a later review paper (Bartholomew, 1990) the increases in activity for the Ni/Al_2O_3 and Ni/TiO_2 catalysts were linked through fundamental TPD studies of Raupp and Dumesic (1985) to support moieties on the nickel surface. It was speculated that in the case of Ni/TiO_2, reduced TiO_x ($x \cong 1$) species formed during reduction of the catalyst migrate to the surface of nickel crystallites. In the case of Ni/Al_2O_3, it was proposed that alumina sols formed during aqueous impregnation or precipitation are deposited on the surface of nickel oxide particles during drying and/or calcination and remain there during reduction.

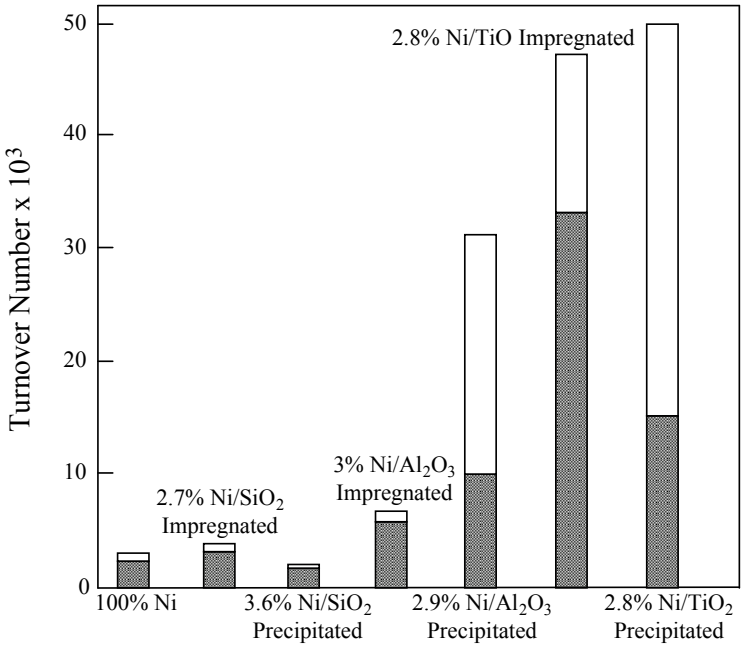

Figure 1.23 Effects of support and preparation on methane turnover frequency of nickel at 525 K; shaded bar is proportional to the CH_4 turnover frequency; unshaded bar denotes the C_{2+} hydrocarbon turnover frequency; total bar length is CO turnover frequency (Bartholomew *et al*., 1980; courtesy of Academic Press).

Bifunctional catalysis—Catalysis by both metal and support is a widely-acknowledged phenomenon. It plays an important role, for example, in dehydrogenation and isomerization reactions occurring in the catalytic reforming of naphtha. One of the important reactions in naphtha reforming is the dehydroisomerization of alkylcyclopentanes such as methylcyclopentane (Parera and Figoli, 1995). A possible mechanism for this reaction is shown in Figure 1.24. Methylcyclopentane is first dehydrogenated on a metal site to methylcyclopentene and then on a similar metal site to methylcyclopentadiene; the adsorbed diolefin migrates to an acid site (A) on the support where it undergoes isomerization to cyclohexadiene, which in turn migrates to a metal site where it is finally dehydrogenated to benzene. Generally, in these types of reactions, the metal provides metal sites for hydrogenation or dehydrogenation, while the support provides acid sites for cracking and isomerization.

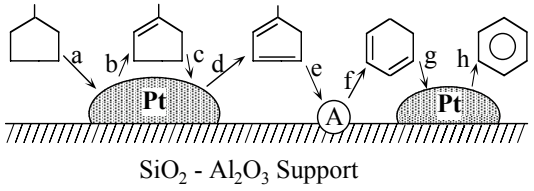

Figure 1.24 Dehydroisomerization of methylcyclopentane on Pt/SiO_2-Al_2O_3, an example of bifunctional catalysis; A = acid site (Parera and Figoli, 1995; courtesy of Marcel Dekker).

Metal-support electron transfer—One of the classical examples of a direct metal-support interaction, causing electronic modifications in metal clusters and thereby affecting their catalytic activity, was reported over three decades ago by Dalla Betta and Boudart (1973). Their paper describes the successful preparation of Pt metal clusters in Y-zeolite having about six atoms per cluster. The acidic forms of this catalyst, Pt/CaY and Pt/MgY, were found to be 50 times more active than Pt/Al_2O_3 for neopentane isomerization and 5 times more active than basic catalysts such as Pt/NaY and Pt/SiO_2 for ethylene hydrogenation (see Figure 1.25). It was speculated and later confirmed that strong electrostatic field gradients in the acidic zeolite cages polarize the Pt clusters causing them to be electron deficient (Boudart and Djega-Mariadassou, 1984).

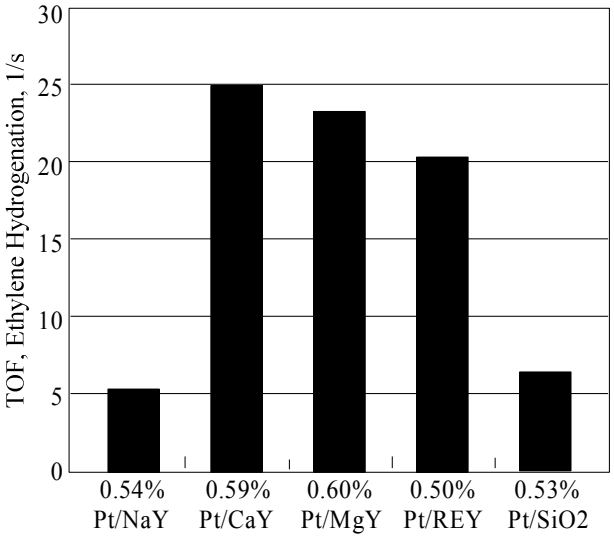

Figure 1.25 Turnover frequencies for ethylene hydrogenation on Pt/SiO_2 and Pt/Y-zeolites at 189 K and 1 atm: 23 torr C_2H_4, 152 torr H_2, and 585 torr He (Dalla Betta and Boudart, 1973; courtesy of North Holland).

Enhanced activity of Au/TiO_2 due to cluster size- and support-induced changes in geometry and electronic structure—It should be emphasized that while a number of studies provide compelling evidence of electronic interactions between metal nanoclusters of less than 2–3 nm and support, there is also clear evidence that electronic properties of metal nanoclusters are intrinsically much different than the bulk metals (Goodman, 2003). Effects of decreasing cluster size include discrete electronic structure and alterations in morphology and chemical reactivity. Separating effects of cluster size and cluster-support interactions on electronic structure is a challenging problem. Nevertheless, the application of sophisticated surface science spectroscopies (see Chapter 2) and computational methods to study and model supported metal systems, e.g. those prepared by vacuum deposition of metals on thin support films, is providing new understanding of these effects (Gunter *et al.*, 1997; Campbell, 1997; Santra and Goodman, 2002; Goodman, 2003).

For example, comprehensive studies of model Au/TiO_2 and Au/SiO_2 catalysts by TPD, STM, STS, and *in situ* activity measurements have provided new insights into the effects of cluster size and support on adsorption, morphological, electronic, and catalytic properties of Au (Goodman, 2003).

Effects of Au cluster size on band gap were studied by STS. Cluster band gap was found to increase with decreasing cluster size (Figure 1.26); a large increase in band gap, indicating the onset of nonmetallic behavior, is evident at a diameter of 3.5 nm and a height of 1.0 nm, corresponding to about 300 atoms per cluster. Moreover, cluster morphology changes from 3D for diameters larger than 4 nm to 2D (1 monolayer) at a diameter of 2 nm (see Figure 1.26). Consistent with these observed changes in electronic structure and morphology, both the heat of CO adsorption on and CO oxidation activity of Au/TiO_2 clusters increase with decreasing cluster size reaching a maximum value at 2 nm (see Figure 1.27).

To what extent could these remarkable changes in adsorption, catalytic, electronic, and morphological properties be attributed to effects of nanocluster size versus effects of support? This issue was addressed by Chusuei *et al.* (2001) through measurements of core level binding energies as a function of cluster size and of metal-metal bond strengths by Au TPD for model Au/SiO_2 and Au/TiO_2 catalysts. Core level measurements show that Au d-bands in Au/TiO_2 are much closer to the Fermi level (than for Au/SiO_2) due to a charge polarization in the interfacial region, indicating an increase in the potential of the Au adlayer. In other words, the interaction of Au clusters with the titania support creates substantial changes in their electronic properties from bulk Au.

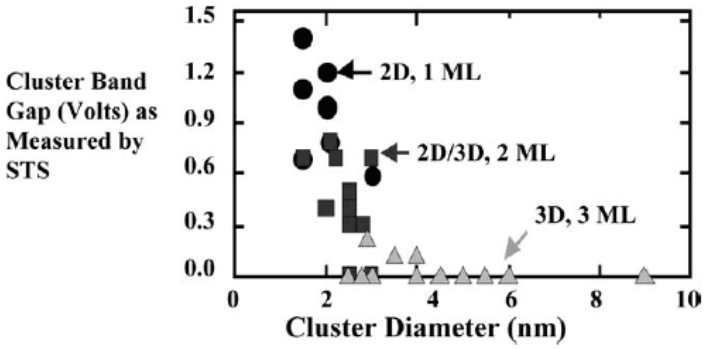

Figure 1.26 Cluster band gaps measured by STS as a function of Au cluster size supported on TiO_2(110)-(1 × 1). The band gaps were obtained while the corresponding topographic scan was acquired on various Au coverages ranging from 0.2 to 4.0 ML. (●) 2D clusters; (■) 3D clusters, 2-atom layers in height; (▲) 3D clusters, 3-atom layers or greater in height (Goodman, 2003; courtesy of Academic Press).

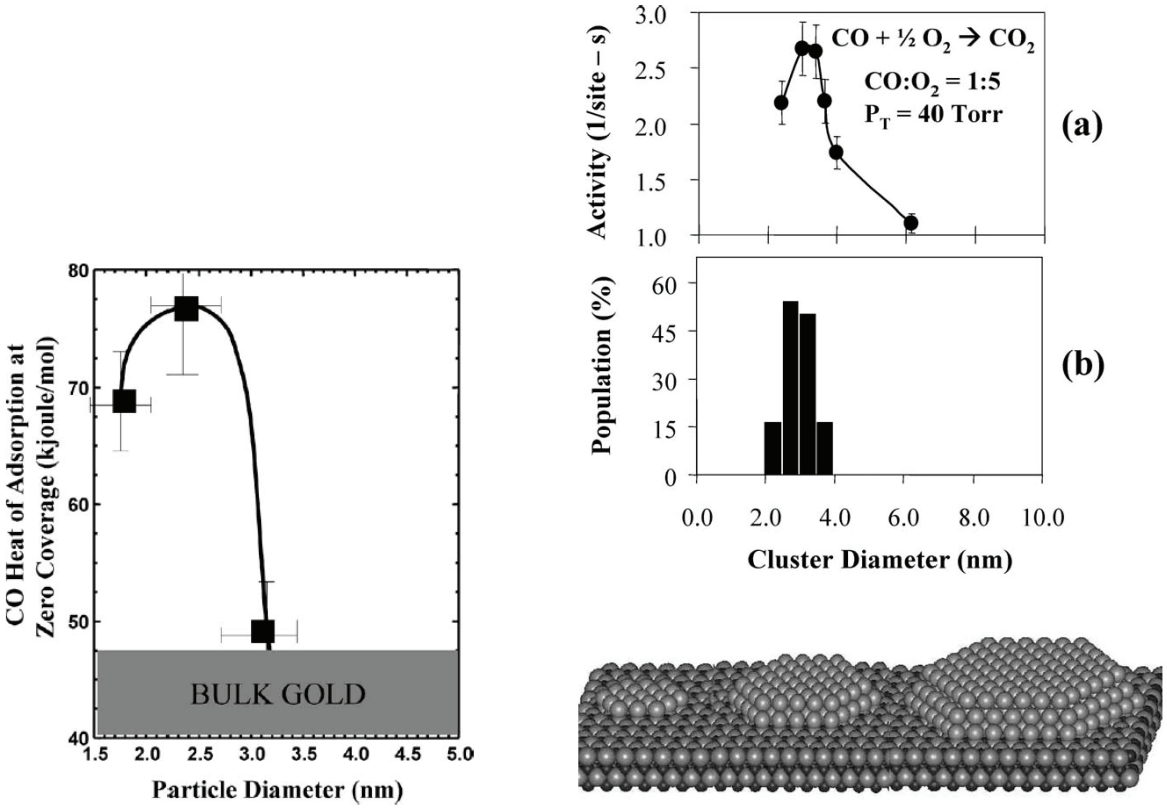

Figure 1.27 *Left:* CO heats of adsorption determined by the Clausius-Clapeyron method at a CO coverage of < 10% of saturation as a function of Au cluster size on a TiO_2(110) support. *Right:* (a) The activity for CO oxidation at 350 K as a function of Au cluster size supported on TiO_2(110)-(1 × 1) thin films grown on Mo(100); activity = (product molecules)/(total Au atoms-s); (b) a histogram of the distribution of cluster sizes. The schematic at *bottom right* shows the evolution of cluster morphologies within the 0–10 nm range. The predominant morphology for the structures corresponding to those of the histogram is the indicated bilayer structure (Goodman, 2003; courtesy of Academic Press).

Temperature programmed desorption (TPD) is a useful tool for studying the energetics of adsorbate-adsorbent and adsorbate-adsorbate interactions; for example, high-temperature TPD can be applied to the study of metal-support and metal-metal bond strengths. TPD spectra of Au from Au/SiO_2, measured as a function of Au coverage (Goodman, 2003), reveal that the sublimation energy of Au is abnormally low for small 2D clusters present at 0.2 monolayers (ML) or less, but increases from a low value of 50 kJ/mol to the

value for bulk Au of 90 kJ/mol as Au coverage increases from 0.2 to 1 mL, thereafter remaining constant to 5 mL. The abnormally low value for low Au coverage (and small 2D clusters) is explained by easy desorption of atoms of low coordination (bonded to fewer neighboring atoms and hence having fewer bonds to break) located on the edges of small clusters. On the other hand, the sublimation energy for Au/TiO_2 is constant at 50 kJ with increasing Au coverage up to 2 mL. This can be attributed to a stronger interaction of Au with titania (relative to silica) causing greater wetting of the support.

Our changing view of the surface; dynamic surface structure—In this last section of Chapter 1 we have focused on surface structure and support effects and how they influence catalytic activity and selectivity. In our discussions thus far we have assumed, rather simplistically, that while coverages of adsorbing, reacting, and desorbing species may change with time, the structure of a catalyst surface is constant with time.

Our view of catalytic surfaces has evolved considerably over the past 100 years—from that of a *smooth, homogeneous surface* (1910 to 1960) to a rough surface composed of intersections of planes or of metal atoms of varying coordination, i.e. a *rigid lattice model* (1960–1990) to a *dynamic, restructuring surface* (1990–present) (Somorjai, 2002).

In the period from 1960 to 1990, the development of sophisticated tools for studying surface structure led to the concept that rough surfaces, e.g. edge and corner sites, may be largely responsible for catalyzing surface reactions. Recently developed *in situ* methods such as scanning tunneling microscopy (STM), which enable us to study surface structure during reaction, have made it possible to observe surface dynamics. Consistent with these latest observations we are finding that:

1. Catalytic surfaces are dynamic systems that undergo restructuring during adsorption and reaction. Indeed, as molecules adsorb, neighboring surface atoms optimize their coordination causing 'relaxation' or displacement of atoms in the first layer. Moreover, different structures are favored in the presence of different adsorbates.
2. In addition to diffusion across surfaces and site-hopping of reacting intermediates, atoms and molecules from the first catalyst layer may also be mobile or at least partially displaced as molecules adsorb and desorb, especially at high temperatures. Clusters of catalytic material may be diffusing and increasing or decreasing in size, while their surfaces may undergo roughening or transition to a smooth surface (Goodman, 2003).

Complementary to these experimental observations are new insights into the chemistries of adsorption and catalytic reaction provided by computational chemistry, involving the use of developing, sophisticated theoretical models and methods, including density functional theory and *ab initio* calculations (Ziegler, 1997; Greeley *et al*., 2002). These methods enable quantitative calculations of activation energies and the identification of favorable energy paths for reaction. These theories support the notion of a dynamic catalyst surface. They are leading to breakthroughs in our understanding. For example, DFT calculations have been used to establish a universal correlation between adsorption energies and catalytic activity for a class of catalytic reactions (Norskov *et al*., 2002); this correlation provides a basis for predicting the best catalyst and/or improving catalysts for a given reaction.

Observations and insights based on these new experimental and theoretical methods are a sizable wave in the future of catalysis. They enlarge our perspective of catalytic reactions and should ultimately provide a basis for design of catalysts at the molecular level.

1.4 Summary of Important Principles

In the first part of this chapter we traced the development of catalytic science and technology from its beginning in the early 1800s to its present state of vital importance in our economy, its critical role in cleaning our environment, and its established function in enabling life processes.

This chapter focused on definitions of important fundamental catalytic phenomena, including catalysis, elementary steps, active sites, catalytic activity, structure sensitivity, and support effects. Our discussion also included important processes in catalytic reactions including adsorption, various kinds of surface reactions, pore diffusion, and film mass transfer as well as fundamental reaction parameters such as rate constant, mass transfer coefficient, Thiele modulus, and effectiveness factor.

Some of the important principles emphasized in Chapter 1 include the following:

- A catalyst is a material that enhances the rate and selectivity of a chemical reaction and in the process is cyclically regenerated. It is like a mountain guide who directs people (molecules) over a highly favorable mountain pass (low activation energy path) to a selected valley (of products) and returns unchanged to guide additional groups.
- A typical heterogeneous gas-phase catalytic reaction involves seven physical and chemical steps: (1) diffusion of reactants from the bulk gas stream through the stagnant gas film surrounding the catalyst particle to the particle surface, (2) diffusion of reactants through the porous network of the catalyst to the catalytic crystallite surface, (3) adsorption of reactants on active sites of the crystallite surface, (4) reaction on the surface of adsorbed reactant intermediates to adsorbed product species, (5) desorption of products from the surface, (6) diffusion of products out of the porous network to the pore mouth, and (7) diffusion of products from the external catalyst particle surface through the stagnant gas film to the bulk gas stream.
- Adsorption is the formation of chemical or physical bonds between an adsorbing species (the adsorbate) and an adsorbing surface (adsorbent) driven by the propensity of adsorbent surface atoms to increase their surface coordination numbers (i.e. decrease their surface free energy). Chemical adsorption (chemisorption) involves the formation of strong chemical bonds between adsorbate and adsorbent with a high heat of reaction (i.e. generally > 50–300 kJ/mol); it generally occurs at relatively high temperatures and is monolayer specific. Physical adsorption (physisorption) involves the condensation of adsorbate molecules on the adsorbent at relatively low temperatures; it generally involves Van der Waals forces and low heats of adsorption (< 15–20 kJ/mol), and it occurs in multilayers on the surface.
- Langmuir theory is a simple, useful model for relating surface coverage to gas-phase pressure during monolayer adsorption. Although it does not account for observed changes in the heat of adsorption with coverage, it nevertheless models adsorption behavior well for many adsorbate-adsorbent systems over a significant (typically intermediate) range of fractional coverage.
- BET theory, an extension of Langmuir theory, is the basis of a useful model for relating surface coverage to gas phase pressure for multilayer, physical adsorption. BET analysis of low-temperature N_2 adsorption data is a widely accepted method for measuring the total internal surface area of a porous solid.
- The complete reaction rate expression for a typical heterogeneous catalytic reaction includes terms for surface reaction, pore diffusion, and film mass transfer resistances. At mild reaction conditions the surface reaction limits reaction rate, while at severe (high-temperature) reaction conditions film mass transfer limits reaction rate causing reactant concentrations to drop markedly across the gas film surrounding a catalyst particle. Pore diffusional resistance becomes important at moderately severe conditions, causing reactant concentrations to drop through catalyst pores.
- The Thiele modulus indicates the degree to which pore diffusional resistance causes a drop in reactant concentration through catalyst pores with a subsequent overall decrease in reaction rate. A large Thiele modulus is indicative of a sharp drop in reactant concentration and hence rate throughout the pore. Thiele modulus increases with increasing pellet size and increasing reaction rate. The fractional drop in rate due to pore diffusional resistance, or the effectiveness factor, can be calculated from a hyperbolic function of the Thiele modulus.

- The rate of a chemically-controlled surface reaction may be limited by the rate of adsorption, surface reaction, or desorption. The form of the rate expression is very different for each of these three cases but can be determined by a kinetic analysis of the elementary steps for each of these cases.
- The most general kinetic tool for analyzing kinetics of elementary steps is the steady-state approximation, which states that the derivative of the concentration with time of an active center (short-lived reaction intermediate) is approximately equal to zero, i.e. $d[I]/dt \approx 0$. A consequence of this approximation is that the net rates of elementary steps in a sequence are equal (i.e. $r_1 = r_2 = r_3$....). These two relationships can be used in a kinetic analysis of a sequence of proposed elementary steps to eliminate the unknown intermediate concentrations and thus derive a rate expression in terms of measurable concentrations.
- Catalytic activity is most generally defined as the rate of a specified catalytic reaction under specified conditions in the presence of a specific catalyst. Specific catalytic activity is the same as specific rate, i.e. $r = (1/\nu_i Q)\, dn_i/dt$ where Q = mass, volume, or surface area. Turnover frequency (TOF) is a specific reaction rate per active catalytic site, i.e. it is the frequency (s^{-1}) at which molecules react on an active site defined at specified conditions of temperature, concentration of reactants, and conversion.
- While in principle TOF is an invariant for a given catalytic material and reaction at specified reaction conditions independent of catalyst preparation or metal loading, in practice it may vary with surface structure and metal dispersion. If so, the reaction is said to be structure sensitive. There are several distinguishing features of a structure sensitive reaction: (1) it typically occurs on large, multiple-atom sites, (2) it typically involves activation of C-C and N-N bonds, and (3) effects of alloying and poisoning on reaction rate are large. Thus hydrocarbon hydrogenolysis reactions, such as ethane hydrogenolysis, involving the rupture of C-C bonds and ammonia synthesis involving the rupture of N-N bonds might be expected to be structure sensitive and indeed they are.
- Support effects are defined as interactions between the catalytic phase and its carrier or support, which affect specific activity. Observed support effects include: (1) a strong interaction of an unreduced metal oxide with an oxide support preventing complete reduction of the metal, e.g. strong interaction of base metal oxides with alumina, silica, or zeolite supports; (2) support-induced size and morphology, e.g. pore-limited crystallite diameter, epitaxial growth of metal layers on carbon and silica, and two-dimensional raft-like structures of metals; (3) contamination of the metal by support material either during preparation or during reduction of the catalyst; (4) bifunctional catalysis, i.e. reactions on both the metal and support; (5) spillover of species from the metal to the support and vice-versa; and (6) a change in the electronic properties of small clusters ($d_{cluster} < 2$–3 nm) due to electronic polarization by the support. The electronic properties of these small metal clusters are inherently different than those of the bulk metal as there are a discrete number of atoms in the cluster. Accordingly, it is difficult to separate size from support effects in nanoclusters.
- Increasingly sophisticated surface spectroscopies and powerful computational methods based on fundamental theory are leading to a better understanding of the complex surface chemistries involved in adsorption and catalytic reaction processes. For example, they reveal that (a) rough surfaces, e.g. edge and corner sites, may be largely responsible for catalyzing surface reactions; and (b) catalytic surfaces are dynamic systems, which undergo restructuring during adsorption and reaction, e.g. as molecules adsorb, neighboring surface atoms optimize their coordination and first layer 'relaxation' or displacement of atoms in the first layer occurs. They are leading to breakthroughs in our understanding, which provide a basis for catalyst design at the molecular level. These methods are a sizable wave in the future of catalysis.

1.5 Recommended Sources for Further Study

Armor, J.N., 1996. Global Overview of Catalysis United States of America. *Applied Catalysis A: General*, 139: 217–228.
Boudart, M., 1991. *Kinetics of Chemical Processes*. Butterworth-Heinemann, Maine.
Davis, M.E. and Davis, R.J., 2003. *Fundamentals of Chemical Reaction Engineering*. McGraw Hill, NY.
Dumesic, J., Rudd, D.F., Aparicio, L.M., Rekoske, J.E., Treviño, A.A., 1993. *The Microkinetics of Heterogeneous Catalysis*. ACS, Washington, D.C.
Fogler, H.S., 1999. *Elements of Chemical Reaction Engineering*, 3rd edn. Prentice Hall, New Jersey.
Goodman, D.W., 2003. Model Catalysts: From Imagining to Imaging a Working Surface, *J. Catal*., 216: 213–222.
Greeley, J., Norskov, J.K. and Mavrikakis, M., 2002. Electronic Structure and Catalysis on Metal Surfaces, *Annual Review of Physical Chemistry*, 53: 319–348.
Gregg, S.J. and Sing, K.S.W., 1982. *Adsorption, Surface Area and Porosity*, 2nd edn. Academic Press, London.
Gunter, P.L.J., Niemantsverdriet, J.W., Ribeiro, F.H. and Somorjai, G.A., 1997. Surface Science Approach to Modeling Supported Catalysts*, Catal. Rev.-Sci. and Eng*., 39: 77–168.
Laidler, K.J., 1987. *Chemical Kinetics*, 3rd edn. Harper & Row, New York.
Levenspiel, O., 1999. *Chemical Reaction Engineering,* 3rd edn. John Wiley & Sons, New York.
Ribeiro, F.H., Schach von Wittenau, A.E., Bartholomew, C.H. and Somorjai, G.A., 1997. Reproducibility of Turnover Rates in Heterogeneous Metal Catalysis: Compilation of Data and Guidelines for Data Analysis, *Catal. Rev.-Sci. Eng*., 39: 49–76.
Smith, J.M., 1981. *Chemical Engineering Kinetics*, 3rd edn. McGraw-Hill Book Company, New York.
Somorjai, G.A., 1994. *Introduction to Surface Chemistry and Catalysis*. John Wiley & Sons, New York.
Somorjai, G.A., 2002. The Evolution of Surface Chemistry. A Personal View of Building the Future on Past and Present Accomplishments, *J. Phys. Chem. B*, 106: 9201–9213.
Thomas, J.M. and Thomas, W.J., 1997. *Principles and Practice of Heterogeneous Catalysis.* VCH, Weinheim.
van Santen, R.A. and Niemantsverdriet, J.W., 1994. *Chemical Kinetics and Catalysis*. Plenum Press.

1.6 Exercises

1.1 Who were four or five great pioneers of catalytic science and technology and what did they contribute?

1.2 What was in your view the greatest development in catalytic technology in the 20th century and why?

1.3 Congratulations, you have been promoted and transferred to the planning division of Cal's Catalyst Corp. Your first assignment is to make recommendations to the President (Cal) regarding the company's investment in R&D during the next 10 years. Specifically the President wants you to give him a one-page summary, which addresses the following questions:

a) Is the field of catalysis a mature technology area? Is there potential for breakthroughs, and if so in what process areas? How rapidly will the sales of catalysts grow in the next 10 years? Should the company expand its R&D? If so, how rapidly? Assume the company devotes about $10/million per year or about 2% of its annual sales to R&D.

b) What kinds of new catalyst and reactor technologies could the company expect to research and develop in the next 10 years? What are the most promising areas of new catalyst technology? Reactor technology? On what areas should the company focus its long term efforts?

1.4 For a given reaction and set of conditions does the use of a catalyst change the equilibrium constant or heat of reaction compared to the situation in which no catalyst is used? Explain.

1.5 The noncatalytic oxidation of a hydrocarbon occurs at 650°C and has an activation energy (E_a) of 167 kJ/mol. By using a catalyst the activation energy (E_a) can be reduced to 84 kJ/mol.

a) What would be the temperature for the catalytic reaction in order to achieve the same conversion assuming preexponential factors, concentration dependencies, and reactant concentrations are the same?

b) Assuming we know the equilibrium constant, enthalpy (ΔH), and free-energy (ΔG) for the noncatalytic reaction at 650ºC, how would these quantities be changed in the catalytic reaction at the new temperature?

1.6 Kinetic analogies illustrate the general applicability of kinetic principles to other aspects of life (many of which are activated rate processes). For example, the increase in salary with time of a university student is zero-order, i.e. d(pay)/dt = k where k is a small constant; radioactive decay is a first-order process, i.e. $-dC_A/dt = k\,C_A$; and bacterial growth is a second-order process, i.e. $dC_B/dt = kC_BC_N$, where C_B = the concentration of

bacteria and C_N the concentration of nutrient. Diffusion and viscosity are processes activated by temperature; learning and writing reports are highly activated processes. Think of your own analogy to a zero, first or second-order rate process; also think of your own analogy to an activated process.

1.7 (a) Search the 'popular' scientific literature (e.g. Chem and Eng. News, Chemical Week, CEP, Chemical Engineering, etc.) and find an article that relates to catalysis or kinetics. Give the reference and write a one paragraph summary. (b) Search the catalysis and/or kinetics literature (e.g. J. Catalysis, Applied Catalysis, Catalysis Reviews, etc.) and find an article on a subject of interest to you. Give the reference and write a one paragraph summary. (c) List the names of 10 periodicals found in (b).

1.8 The reaction of oxygen and hydrogen to form water, $2H_2 + O_2 = 2H_2O$, occurs explosively if a gaseous mixture of the reactants is ignited by a spark or flame or if it is heated to its ignition temperature. However, in the absence of a spark, the mixture is indefinitely stable at room temperature.

a) What will happen if a small amount of Pt catalyst (no spark) is added to the gaseous mixture? Explain from a kinetic point of view.

b) Is this relatively simple reaction an elementary step? Why or why not?

1.9 Which would you expect to be the more stable, useful catalyst for high-temperature oxidation of CO, unsupported Pt (Pt black), or Pt supported on high-surface area alumina? Explain. What kind of support effects might you expect with Pt/Al_2O_3 for this reaction?

1.10 What kind of process limits the rate of a heterogeneous catalytic reaction at mild (low-temperature) reaction conditions? At high-temperature reaction conditions? What are the approximate ranges of activation energy for these two conditions?

1.11 Explain how you might experimentally determine if adsorption of N_2 on iron is chemical or physical? Under what conditions would you expect physisorption? Chemisorption?

1.12 H_2 gas adsorbs on the active sites W_s of a tungsten surface according to the reaction:

$$H_2 + 2W_S \underset{k_d}{\overset{k_a}{\rightleftharpoons}} 2H\text{-}W_S \; (2H_{ads})$$

Express the surface coverage of H_{ads} in terms of the equilibrium constant for adsorption and the concentration of H_2 gas and draw a sketch of the surface coverage against P_{H_2} (or $P_{H_2}^{1/2}$) for the cases of $k_a >> k_d$, $k_a \approx k_d$, and $k_a << k_d$.

1.13 Derive the Langmuir adsorption isotherm for the following cases: (a) molecular adsorption of NO; (b) dissociative adsorption of NO; (c) competitive adsorption of molecularly adsorbed NO and dissociatively adsorbed H_2 without further reaction.

1.14 Data for the adsorption of nitrogen on silica gel (high pore-volume type) at –196°C are given in the following table in which $x = P/P_o$ = relative pressure and V = volume adsorbed, cc (STP)/g. Plot the isotherm and calculate the surface area. List all the information that can be obtained about the catalyst from the total isotherm.

Adsorption				Desorption	
x	V	x	V	x	V
0.052	106.3	0.804	322.1	0.888	661.2
0.085	115.9	0.878	409.8	0.878	594.4
0.142	129.8	0.908	482.3	0.830	394.9
0.225	148.7	0.918	515.6	0.775	302.0
0.246	150.6	0.930	558.3		
0.306	163.4	0.942	594.0		
0.347	169.5	0.959	669.4		
0.410	180.1	0.970	678.9		
0.548	210.4	0.983	679.6		
0.580	219.9	0.995	680.0		
0.688	252.0				
0.709	262.6				

1.15 Draw reactant/product concentration and temperature profiles as a function of distance across a gas film and into the center of a catalyst pellet for an exothermic reaction R → P: (a) controlled by chemical reaction; (b) controlled by film mass transfer; (c) influenced by pore diffusional resistance.

1.16 An unsaturated polymer is to be hydrogenated in a fixed bed reactor utilizing a particulate Ru/Al_2O_3 catalyst. Indicate how the reaction rate would change for each mode of reaction control: (a) film mass transfer control; (b) chemical reaction control; (c) high pore diffusional resistance. Consider the effects for each case above of increasing: (i) linear velocity; (ii) temperature; (iii) particle size; (iv) dispersion of Ru; (v) concentration of Ru in the outer shell of the catalyst particle; (vi) concentration of Ru in the catalyst particle.

1.17 Jarvi and co-workers (G.A. Jarvi, K.B. Mayo, and C.H. Bartholomew, *Chem. Eng. Commun*., **4**, 325–341 (1980)) report an experimental first-order rate constant k_{obs} for methanation of CO on a 3% Ni/Al_2O_3 catalyst in the form of 0.32 cm pellets at 400°C and 1 atm of 24.5 cm^3/g_{cat}-s. They also report a mass transfer coefficient of 14 cm_{gas}^3/cm_{cat}^2-s calculated from mass transfer correlations. The catalyst has a bulk density of 0.98 g/cm^3 and a specific geometrical surface area of 8.0 cm^2/cm^3 bed. (a) Calculate the fraction of the overall resistance provided by film resistance (note that reaction resistance is $1/k''\eta$ and film resistance is $1/k_m$). (b) Is the reaction film-diffusion controlled? Could we expect a high or low pore diffusional resistance under these conditions? Explain. (c) What would the rate of reaction be in the absence of film diffusion resistance?

1.18 In the cracking of *n*-propylbenzene over a new experimental catalyst in crushed-powder form (d_p = 0.01 cm) the first-order rate constant is observed to be 43.8 cm^3/g-s at 427°C. The activation energy is 167 kJ/mol. (a) Determine if the observed rate constant at 427°C for the crushed catalyst is intrinsic, i.e. unaffected by pore diffusional resistance. Assume $D_e = 9.7 \times 10^{-4}$ cm^2/s. (b) What would be the observed rate constant of this reaction at 527°C for a commercial packed bed containing pelleted catalyst and fluid with the properties listed below? Neglect film mass transfer resistance. (c) What might be done to the catalyst to increase its effectiveness?

Catalyst properties	*Gas properties in the reactor*
d_p (sphere diameter) = 0.35 cm	pressure = 1 atm
pore volume = 0.42 cm^3/g	temperature = 527°C
ρ_p (particle density) = 1.42 g/cm^3	fluid = *n*-propylbenzene in benzene
$D_{eff} = 9.7 \times 10^{-4}$ cm^2/s (427°C)	

1.19 What is the most general theoretical kinetic tool for analyzing a sequence of elementary steps? What is the mathematical statement of this theoretical approximation? What does this approximation reveal about the relative overall rates of elementary steps in a series sequence?

1.20 NO decomposition at high temperatures on Cu-ZSM-5 is thought to occur by the following mechanism where **S** is a surface site.

$$NO + 2\,\mathbf{S} \leftrightarrow N\text{-}\mathbf{S} + O\text{-}\mathbf{S} \qquad (1)$$
$$2\,N\text{-}\mathbf{S} \rightarrow N_2 + 2\,\mathbf{S} \qquad (2)$$
$$2\,O\text{-}\mathbf{S} \rightarrow O_2 + 2\,\mathbf{S} \qquad (3)$$

Derive a rate expression in terms of measurable concentrations and rate/equilibrium constants for the disappearance of NO based on the above sequence. (a) Do not assume quasi-equilibrium for (1); (b) do assume quasi-equilibrium for (1).

1.21 For the CO oxidation reaction assuming mechanistic steps 1.8 to 1.11 (re-label as steps 1–4), derive a rate expression for CO_2 formation: (a) given step 3 is the rate limiting step; (b) given step 1 is the rate limiting step. Do your answers in (a) and (b) agree with the results from Example 1.3? Why or why not?

1.22 In Example 1.3 it was demonstrated how a rate expression could be derived from a sequence of elementary steps (reactions 1.8 through 1.11) involving atomic oxygen. In this case the rate expression predicts a maximum of half order in oxygen. However, for some catalysts, e.g. $Pt\text{-}Rh/Al_2O_3$ catalysts, the rate is observed to be first-order in oxygen. What must happen to the sequence of elementary steps to enable prediction of first-order? Derive the rate expression for this case. What are the implications regarding the ability of such a catalyst to dissociate oxygen?

***1.23** In the selective oxidation of isobutylene to dimethyl ketone using a $MoO_3/U_3O_8/SiO_2$ catalyst it is thought that each reactant utilizes different catalytic sites. The reaction rate is controlled by surface reaction between the two adsorbed species. Postulate a sequence of elementary steps and derive the LH rate equation; sketch the rate versus pressure of isobutylene curve assuming the O_2 pressure is large. Compare this plot to the case where both reactants compete for the same sites.

1.24 (a) Derive the rate expression for the water-gas shift reaction on a solid catalyst surface if it follows the sequence of elementary (or simple) steps below with step 3 rate determining and steps 1 and 2 in quasi-equilibrium; **S**, CO-**S**, and O-**S** are active centers where **S** is a surface site.

$$H_2O + \mathbf{S} \leftrightarrow \text{O-}\mathbf{S} + H_2 \quad (1)$$
$$CO + \mathbf{S} \leftrightarrow \text{CO-}\mathbf{S} \quad (2)$$
$$\text{O-}\mathbf{S} + \text{CO-}\mathbf{S} \rightarrow CO_2 + 2\mathbf{S} \quad (3)$$

(b) Comment briefly on the validity of the above mechanism. Is it reasonable? Are the steps truly elementary? Is it likely that H_2O and CO would adsorb on the same sites? Explain your response to this last point.

1.25 For the isomerization of neopentane (A) to isobutane (B) over a Pt catalyst, a surface site of which is represented by σ, derive the rate of expression based upon the following mechanism; assume step 2 is the rds and that A-σ is the most abundant surface intermediate (i.e. $\theta_A > \theta_B$).

$$\sigma + A \leftrightarrow A\text{-}\sigma \quad (1)$$
$$A\text{-}\sigma \rightarrow B\text{-}\sigma \quad (2)$$
$$B\text{-}\sigma \leftrightarrow B + \sigma \quad (3)$$

1.26 Given the following sequence for reduction of NO with CO on ruthenium, derive the simplest rate expression in terms of measurables. Do not assume a rate-determining step; do assume that CO coverage is very small.

$$NO + Ru_s \leftrightarrow NO\text{-}Ru_s \quad (1) \text{ fast (quasi-equilibrium)}$$
$$CO + Ru_s \leftrightarrow CO\text{-}Ru_s \quad (2) \text{ fast (quasi-equilibrium)}$$
$$NO\text{-}Ru_s + Ru_s \rightarrow N\text{-}Ru_s + O\text{-}Ru_s \quad (3)$$
$$2N\text{-}Ru_s \rightarrow N_2 + 2\,Ru_s \quad (4)$$
$$CO\text{-}Ru_s + O\text{-}Ru_s \rightarrow CO_2 + 2\,Ru_s \quad (5)$$

***1.27** Read the paper by Hecker and Bell, *J. Catal*. 84:200 (1983). (a) List assumptions and simplifications used to derive Equation 7 in the article. (b) Derive a rate expression assuming NO adsorption is the rds. How does this agree with the experimental data? (c) Some workers are of the opinion that removal of adsorbed O atoms from the surface via $CO_s + O_s \rightarrow CO_2 + 2\mathbf{s}$ is the rds. Do you agree? (d) Propose a mechanism for formation of N_2O from NO and CO in which the rds is an Eley-Rideal reaction between adsorbed NO and gas phase CO and which goes through an intermediate NCO-**S**. Derive the predicted rate expression and tell how it agrees with experimental data.

1.28 What are the characteristics of a structure sensitive reaction? Since CO hydrogenation on Co and hydrogenolysis of n-C_6H_{14} on Pt involve the breaking of C-O and C-C bonds, how can one explain the structure insensitivity of these reactions on these catalysts?

* Relatively difficult problems

1.7 References

Armor, J.N., 1996. Global Overview of Catalysis United States of America. *Applied Catalysis A: General*, 139: 217–228.

Auerbach, M., Carrado, K.A. and Dutta, P.K. (eds.), 2003. *Handbook of Zeolite Science and Technology*. Dekker, New York.

Bartholomew, C.H., 2002. Auto Catalyst Market, 2001 to 2005, unpublished study.

Bartholomew, C.H., 2004. Catalyst Market, Present and Future, in preparation.

Bartholomew, C.H., 1991. Recent Developments in Fischer-Tropsch Catalysis, in *New Trends in CO Activation, Stud. Surf. Sci. 64,* ed. L. Guczi. Elsevier, Chapter 5.

Bartholomew, C.H., 1990. Hydrogen Adsorption on Supported Cobalt, Iron, and Nickel, *Catalysis Letters,* 7: 27–52.

Bartholomew, C.H., Neubauer, L.R. and Smith, P.A., 1993. *Proc. 10th Intl. Cong. Catalysis*, ed. L. Guczi, *et al*. Elsevier, p. 821.

Bartholomew, C.H., Pannell, R.B. and Butler, J.L., 1980. Support and Crystallite Size Effects in CO Hydrogenation on Nickel, *J. Catal.,* 65: 335.
Bernard, J.A. and Mitchell, D.S., 1968. *J. Catal*., 12: 376 and 386.
Bhatia, S., 1990. *Zeolite Catalysis: Principles and Applications*. CRC Press, Boca Raton, FL.
Boudart, M., 1961. *Chem. Eng. Prog.,* 57: 33.
Boudart, M., 1969. *Adv. Catal.,* 20: 153.
Boudart, M., 1991. *Kinetics of Chemical Processes*. Butterworth-Heinemann.
Boudart, M., Aldag, A., Benson, J.E., Dougharty, N.A. and Harkins, C.G., 1966. *J. Catal.,* 6: 92.
Boudart, M. and Djega-Mariadassou, G., 1984. *Kinetics of Heterogeneous Catalytic Reactions*. Princeton University Press, Princeton, New Jersey.
Boudart, M., Delbouille, A., Dumesic, J.A., Khammouma, S. and Topsoe, H., 1975. *J. Catal.,* 37: 486.
Boudart, M. and Ptak, L.D., 1970. *J. Catal.,*16: 90.
Burwell, R.L., Jr. 1983. Heterogeneous Catalysis, Selected American Histories, in *ACS Symposium Series, 222*, eds. B.H. Davis and W.P. Hettinger, Jr. American Chemical Society, p. 3–12.
Carter, J.L., Lucchesi, P.J., Sinfelt, J.H. and Yates, D.J.C., 1965. *Proc. 3rd Intl. Cong. Catalysis,* ed. W.M.H. Sachtler, G.C.A. Schuit and P. Zwietering. North Holland, Amsterdam, p. 664.
Catalysis Letters, 2000. Industrial Developments (1950–1999), 67 (1): 65–70.
Chemical Week, 1993. June 16, p. 36.
Chemical Week, 2002. Catalysts Enjoy Regulation Growth. March 13, p. 3.
Chemical Week, 2001. Catalysts for Growth. September 12, p. 3.
Chemical Week Today's Refinery, 1999. The Catalyst Industry: Dynamic Technology in Rapidly Changing Industries. Sept, p. 3.
Chen, N.Y., Garwood, W.E. and Dwyer, F.G., 1989. *Shape Selective Catalysis in Industrial Applications*. Marcel Dekker, NY.
Chon, H., Woo, S.I. and Park, S.-E. (eds.), 1996. *Recent Advances and New Horizons in Zeolite Science and Technology*. Elsevier, New York.
Christmann, K.R., 1988. Hydrogen Adsorption on Pure Metal Surfaces, in *Hydrogen Effects in Catalysis*, eds. Z. Paal and P.G. Menon. Dekker, pp. 3–56.
Chusuei, C.C., Lai, X., Luo, K. and Goodman, D.W., 2001. *Top. Catal*., 14: 71.
Dalla Betta, R.A. and Boudart, M., 1973. In *Proceedings 5th International Congress Catalysis*, ed. J.W. Hightower. North Holland, Amsterdam, p. 1329.
Dalmai-Imelik, G. and Massardier, J., 1977. *Proc. 6th Intl. Cong. Catalysis,* eds. G.C. Bond, P.B. Wells and F.C. Tompkins. The Chemical Society, London, p. 90.
Davis, B., 1999. The Asian Catalyst Market. *Chemical Week Today's Refinery*, September, p. 6.
Davis, M.E. and Davis, R.J., 2003. *Fundamentals of Chemical Reaction Engineering*. McGraw Hill, NY.
Davis, B.H. and Hettinger, W.P., Jr., 1983. Heterogeneous Catalysis, Selected American Histories, in *ACS Symposium Series, 222*. American Chemical Society.
Davis, S.M. and Somorjai, G.A., 1980. *J. Catal,* 65: 78.
Derouane, E.G., 1971. *Ind. Chim. Belg.,* 36: 359–374.
Dumesic, J.A., Rudd, D.F., Aparicio, L.M., Rekoske, J.E. and Trevino, A.A., 1993. *The Microkinetics of Heterogeneous Catalysis*. ACS.
Dwivedi, P.N. and Upadhyay, S.N., 1977. *Ind. Eng. Chem. Process Des. Dev*., 16: 157.
Engel, T. and Ertl, G., 1979. *Advan. Catal. Relat. Subj,* 28: 1.
Ertl, G., 1981. *Proc. 7th Intl. Cong. Catalysis,* ed. T. Seiyama and K. Tanabe. Kodansha, Tokyo, p. 21.
Fogler, H.S., 1999. *Elements of Chemical Reaction Engineering*, 3rd edn. Prentice Hall, New Jersey.
Fujimoto, K. and Boudart, M., 1979. *Journal de Physique,* 40: C2–81.
Fujimoto, K. and Toyoshi, S., 1981. *Proc. 7th Intl. Cong. Catalysis*. ed. T. Seiyama and K. Tanabe. 235. Tokyo. Kodansha.
Goodman, D.W., 2003. Model Catalysts: From Imagining to Imaging a Working Surface, *J. Catal*., 216: 213–222.
Goodman, D.W., 1992. *Catal. Today,* 12: 189.
Goodman, D.W., 1982. *Surf. Sci.,* 123: L679.
Goodman, D.W., Kelley, R.D., Madey, T.E. and Yates, J.T., Jr., 1980. *J. Catal,* 63: 226.
Greek, B.F., 1989. Process Catalysts Enjoy Surging Market, *Chem. & Eng. News,* p. 29–56.
Greeley, J., Norskov, J.K. and Mavrikakis, M., 2002. Electronic Structure and Catalysis on Metal Surfaces, *Annual Review of Physical Chemistry*, 53: 319–348.
Gregg, S.J. and Sing, K.S.W., 1982. *Adsorption, Surface Area and Porosity*, 2nd edn. Academic Press, London.
Guisnet, M. and Gilson, J.P. (eds.), 2002. *Zeolites for Cleaner Technologies*. Imperial College Press, London.
Gunter, P.L.J., Niemantsverdriet, J.W., Ribeiro, F.H. and Somorjai, G.A., 1997. Surface Science Approach to Modeling Supported Catalysts*, Catal. Rev.-Sci. and Eng*., 39: 77–168.
Hanson, V. and Boudart, M. 1978. *J. Catal,* 53: 56.

Heinemann, H., 1981. A Brief History of Industrial Catalysis. In *Catalysis, Science and Technology.* Eds. J.R. Anderson and M. Boudart. Springer -Verlag. Vol. 1, p. 1–41.

Hines, A.L. and Maddox, R.N., 1985. *Mass Transfer, Fundamentals and Applications*. Prentice-Hall, New Jersey.

Johnson, B.G., Bartholomew, C.H. and Goodman, D.W., 1991. The Role of Surface Structure and Dispersion on CO Hydrogenation on Cobalt, *J. Catal.*, 128: 231–247.

Kahn, D.R., Petersen, E.E. and Somorjai, G.A., 1974. *J. Catal.*, 34: 294.

Keech, M. and Lazou, C., 1990. Supercomputing in the U.K. Initiatives for Academic and Industrial Collaboration. In *Cray Channels,* Summer 1990, p. 6–8.

Ladas, S., Poppa, H. and Boudart, M., 1981. *Surf. Sci.,* 102: 151.

Laidler, K.J., 1987. *Chemical Kinetics,* 3rd edn. Harper and Row, New York.

Lee, W.H. and Bartholomew, C.H., 1989. Multiple Reaction States in CO Hydrogenation on Alumina-Supported Cobalt Catalysts. *J. Catal.,* 120: 256.

Levenspiel, O., 1999. *Chemical Reaction Engineering,* 3rd edn. John Wiley & Sons, New York.

Masel, R.I., 1996. *Principles of Adsorption and Reaction on Solid Surfaces*. John Wiley & Sons, New York.

Mills, G.A., 1994. Advanced Heterogeneous Catalysts for Energy Applications; Catalysts: Key to Clean Efficient Energy. A Research Assessment, Report to DOE/ER-30201-H1, p. 1–21.

Morbidelli, M., Gavriilidis, A., and Varma, A., 2001. *Catalyst Design.* Cambridge University Press, NewYork.

Nackos, A., Guo, X., Bartholomew, C.H., Baxter, L.L. and Hecker, W.C., 2004. Paper in preparation.

Norskov, J.K., Bligaard, T., Logadottir, A., Bahn, S., Hansen, L.B., Bollinger, M., Bengaard, H., Hammer, B., Sljivancanin, Z., Mavrikakis, M., Xu, Y., Dahl, S., and Jacobsen, C.J.H., 2002. Universality in Heterogeneous Catalysis, *J. Catal*., 209: 275–278.

Oh, S.H. and Eickel, C.C., 1991. *J. Catal*., 128: 526.

Parera, J.M. and Figoli, 1995. Chemistry and Processing of Petroleum and Reactors in the Commercial Reformer, in *Catalytic Naphtha Reforming*, eds. G.J. Antos, A.M. Aiteni and J.M. Parera. Marcel Dekker.

Rainer, D.R., Vesecky, S.M., Koranne, M., Oh, W.S. and Goodman, D.W., 1997. *J. Catal.,* 167: 234.

Rameswaren, M., and Bartholomew, C.H., 1988. Effects of Preparation, Dispersion and Extent of Reduction on Activity/ Selectivity Properties of Iron/Alumina CO Hydrogenation Catalysts, *J. Catal.,* 117: 218–236.

Raupp, G.B. and Dumesic, J.A., 1985. *J. Catal*., 95: 587.

Ribeiro, F.H., Schach von Wittenau, A.E., Bartholomew, C.H. and Somorjai, G.A., 1997. Reproducibility of Turnover Rates in Heterogeneous Metal Catalysis: Compilation of Data and Guidelines for Data Analysis, *Catal. Rev.-Sci. Eng*., 39: 49–76.

Satterfield, C.N., 1991. *Heterogeneous Catalysis in Practice,* 2nd edn. McGraw-Hill, New York.

Segal, E., Madon, R.J. and Boudart, M., 1978. *J. Catal.,* 52: 45.

Sen, B. and Falconer, J.L., 1989. *J. Catal.,* 117: 404.

Sinfelt, J. H., Carter, H.L. and Yates, D.J.C., 1972. *J. Catal.,* 24: 283.

Smith, J.M., 1981. *Chemical Engineering Kinetics,* 3rd edn. McGraw-Hill, New York.

Smith, J.M., 1968. *Chem. Eng. Prog.,* 64: 78.

Somorjai, G.A., 2002. The Evolution of Surface Chemistry. A Personal View of Building the Future on Past and Present Accomplishments, *J. Phys. Chem. B*, 106: 9201–9213.

Somorjai, G.A., Castner, D.G. and Blackadar, R.L., 1980. *J. Catal.,* 66: 257.

Spencer, N.D., Schoonmaker, R.C. and Somorjai, G.A., 1982. *J. Catal.,* 74: 129.

Stevenson, S.A., Dumesic, J.A., Baker, R.T.K. and Ruckenstein, E., 1987. *Metal-Support Interactions in Catalysis, Sintering, and Redispersion.* Van Nostrand Reinhold.

Thayer, A.M., 1994. Catalyst Industry Stresses Need for Partners as Key to Future Success. *Chem. & Eng. News*, July 11: 19–20.

Thomas, J.M. and Thomas, W.J., 1997. *Principles and Practice of Heterogeneous Catalysis.* VCH, Weinheim.

Vannice, M.A. 1976. *J. Catal.,* 44: 152.

van Santen, R.A. and Niemantsverdriet, J.W., 1994. *Chemical Kinetics and Catalysis*. Plenum Press.

Weisz, P.B. and Frilette, V.J., 1960. Intracrystalline and Molecular-Shape-Selective Catalysis by Zeolites, *J. Phys. Chem.,* 64: 382.

Wong, S.S., Otero-Schipper, P.H., Wachter, W.A., Inoue, Y., Kobayashi, M., Butt, J.B., Burwell, R.L., Jr. and Cohen, J.B., 1980. *J. Catal.,* 64: 84.

Wong, W.C. and Nobe, K., 1984. *Ind. Eng. Chem. Prod. Res. Dev*., 23: 564.

Xu, X.P., Szanyi, J., Xu, Q. and Goodman, D.W., 1994. *Catal. Today*, 21: 57.

Ziegler, T., 1997. Density-Functional Theory as a Practical Tool in Studies of Transition Metal Chemistry and Catalysis, in *Density-Functional Methods in Chemistry and Materials Science*, p. 69–103.

Zowtiak, J.M. and Bartholomew, C.H., 1983. The Kinetics of H_2 Adsorption on and Desorption from Cobalt and the Effects of Support Thereon, *J. Catal*., 83: 107–120.